Carbonaceous Nanomaterials as Flame Retardant Coating on Fabric

by

Takayuki Nosaka

A Dissertation Presented in Partial Fulfillment
of the Requirements for the Degree
Doctor of Philosophy

Approved May 2018 by the
Graduate Supervisory Committee:

Pierre Herckes, Chair
Paul Westerhoff
Qing Hua Wang

ARIZONA STATE UNIVERSITY

August 2018

ABSTRACT

Flame retardants (FRs) are applied to variety of consumer products such as textiles and polymers for fire prevention and fire safety. Substantial research is ongoing to replace traditional FRs with alternative materials that are less toxic, present higher flame retardancy and result in lower overall exposure as there are potential health concerns in case of exposure to popular FRs. Carbonaceous nanomaterials (CNMs) such as carbon nanotubes (CNTs) and graphene oxide (GO) have been studied and applied to polymer composites and electronics extensively due to their remarkable properties. Hence CNMs are considered as potential alternative materials that present high flame retardancy. In this research, different kinds of CNMs coatings on polyester fabric are produced and evaluated for their use as flame retardants. To monitor the mass loading of CNMs coated on the fabric, a two-step analytical method for quantifying CNMs embedded in polymer composites was developed. This method consisted of polymer dissolution process using organic solvents followed by subsequent programmed thermal analysis (PTA). This quantification technique was applicable to CNTs with and without high metal impurities in a broad range of polymers. Various types of CNMs were coated on polyester fabric and the efficacy of coatings as flame retardant was evaluated. The oxygen content of CNMs emerged as a critical parameter impacting flame retardancy with higher oxygen content resulting in less FR efficacy. The most performant nanomaterials, multi-walled carbon nanotubes (MWCNTs) and amine functionalized multi-walled carbon nantoubes (NH_2-MWCNT) showed similar FR properties to current flame retardants with low mass loading (0.18 g/m^2) and hence are promising alternatives that warrant further investigation. Chemical/physical modification of MWCNTs was

conducted to produce well-dispersed MWCNT solutions without involving oxygen for uniform FR coating. The MWCNTs coating was studied to evaluate the durability of the coating and the impact on the efficacy during use phase by conducting mechanical abrasion and washing test. Approximately 50% and 40% of MWCNTs were released from 1 set of mechanical abrasion and washing test respectively. The losses during simulated usage impacted the flame retardancy negatively.

ACKNOWLEDGMENTS

First, I would like to express my very great appreciation to my adviser Dr. Pierre Herckes, whose provided me support and guidance on research projects. His mentorship always helped me learn and accomplish my goals. I would also like to acknowledge my supervisory committee members, Dr. Paul Westerhoff and Dr. Qing Hua Wang for all of their advice and assistance with my dissertation projects.

I would like to thank all the researchers involved in collaboration projects with me, especially Dr. Howard Fairbrother and Ronald Lankone at Johns Hopkins University.

I also would like to acknowledge everyone in Herckes group and Westerhoff group at ASU: Sarah Frey, Youliang Wang, Aurelie Marcotte, Jinwei Zhang, Jershon Eager, Christy Rose, Denise Napolitano, Alysa Shelly, Samantha Donovan, Kyle Doudrick, Yu Yang, Yuqiang Bi, Onur Apul.

Finally, I would like to acknowledge all the help and support from my friends at ASU and my family.

TABLE OF CONTENTS

Page

CHAPTER Page

CHAPTER Page

CHAPTER Page

CHAPTER Page

LIST OF TABLES

LIST OF FIGURES

Figure Page

Figure Page

Figure Page

Figure Page

CHAPTER 1

INTRODUCTION

1.1 Traditional flame retardants

1.1.1 The mechanism of organic compound combustion and flame retardant use

Flame retardants (FRs) are a group of chemicals that are intended to slow or prevent fire ignition or growth by physical/chemical mechanisms and they play an important role in fire prevention and safety. They are commonly applied to fabrics and polymers such as carpets, mattresses and baby clothes as either embedded chemicals or as surface coating. In California, flammability requirements for upholstered furniture paddings are set by Technical Bulletin 117 (TB 117) [1]. Outside of the United States, the United Kingdom established The Furniture and Furnishings (Fire Safety) Regulations [2] in 1988 that ensures upholstery products for furniture meet specific ignition resistance. Although TB117 is applicable only to the state of California, a large number of consumer products are made by following TB 117 since California represents a big market for furniture. As a consequence, there has been a large amount of FRs applied to variety of indoor consumer products such as upholstery, carpeting and draperies.

There are mainly 4 types of FRs, halogenated organic FRs, inorganic FRs, organophosphorus FRs and nitrogen-containing FRs. Each type has a distinct FR mechanism. Halogenated organic FRs, for example, are classified as gas phase radical quenching FR as they reduce heat in the gas phase from combustion by scavenging reactive free radicals [3].

Combustion of organic products is a thermal radical oxidation process caused by the heat from the ignition source. Volatile/flammable products produced by the process play

a role as fuel to proceed the combustion by reacting with oxygen then creating hydroxyl radicals.

$$R\cdot + O_2 \rightarrow ROO\cdot \quad (1)$$

$$ROO\cdot + RH \rightarrow ROOH + R\cdot \quad (2)$$

$$ROOH \rightarrow RO\cdot + \cdot OH \quad (3)$$

This reaction is followed by the exothermic reaction of CO to CO_2.

$$OH\cdot + CO \rightarrow CO_2 + H\cdot \quad (4)$$

The combustion continues until the source of the exothermic reactions such as the volatile gas produced by thermal decomposition of the organic product and oxygen are depleted, meaning the heat is not sufficient to maintain the combustion. Figure 1.1 shows a diagram[4] of the general combustion process of organic materials such as polymers and fabric. There are mainly two ways to disrupt the combustion process, (1) restraining the amount of volatile gas and/or oxygen available and (2) eliminating the heat from the products.

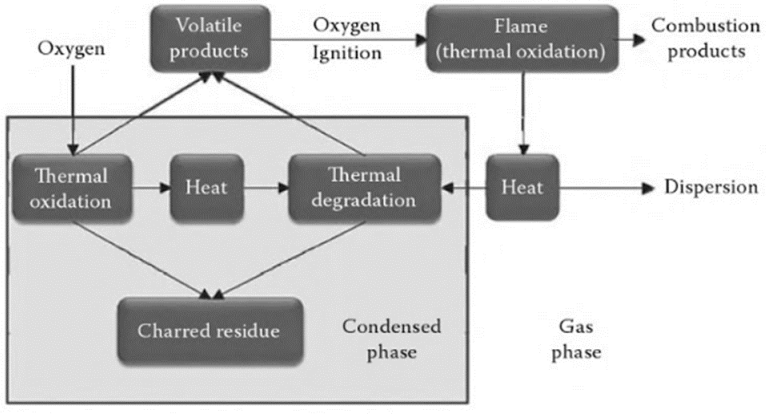

Figure 1.1 Self-sustained organic products combustion cycle[4]

1.1.2 Halogenated FRs

Among those 4 types of FRs listed in Chapter 1.1.1, halogenated FRs such as chlorinated FRs and brominated FRs have been extensively used over the years as they have a high compatibility with commercial polymers and show very low chemical reactivity in addition to resulting in low cost because of their high flame retardant efficacy [5]. Examples of halogenated FRs are shown in Figure 1.2. Halogenated FRs perform through disrupting process (1) described in Chapter 1.1.1. Under thermal stress, halogenated FRs release hydrogen halide (HX). This HX reacts with radical species like H· and OH· that are critical for flame propagation [4].

$$H\cdot + HX \rightarrow H_2 + X\cdot \quad (5)$$

$$OH\cdot + HX \rightarrow H_2O + X\cdot \quad (6)$$

The halogen radicals (X·) are much less reactive compared to H· and OH·, leading to decelerate the heat releasing reactions.

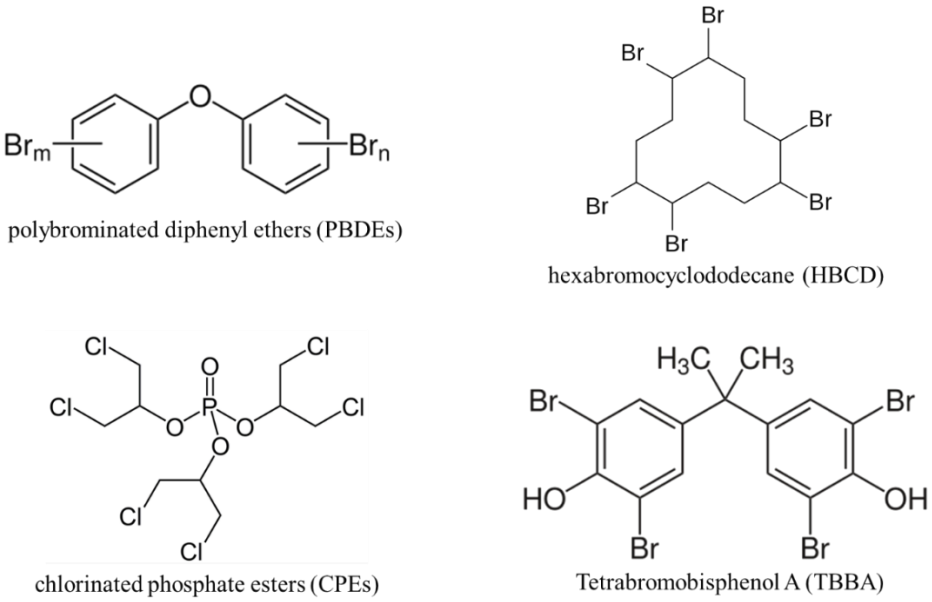

polybrominated diphenyl ethers (PBDEs)

hexabromocyclododecane (HBCD)

chlorinated phosphate esters (CPEs)

Tetrabromobisphenol A (TBBA)

Figure 1.2 Examples of halogenated flame retardants

In recent years however, many studies have emerged showing potential health risks because of the persistence and accumulation of halogenated FRs in the environment and in the human body [6, 7]. Among many kinds of FRs, polybrominated diphenyl ethers (PBDEs), hexabromocyclododecane (HBCD), and chlorinated phosphate esters (CPEs) in textiles, plastics, wire insulation, and automobiles received particularly attention as potential toxic chemicals and the potential of environmental impact and the toxicity are investigated by the U.S. Environmental Protection Agency (EPA) [8, 9]. The potential health risks that are apprehended are cancer risk [10, 11], endocrine disruption [12, 13], neurological impairments [14] and infertility [15]. Consequently, some chemicals were restricted to use for manufacturing by regulations established such as Toxic Substances Control Act (TSCA) and Federal Facilities [16]. A number of states such as New York [17] and Oregon [18] banned Polybrominated Diphenyl Ethers (PBDE) including pentaBDE, octaBDE since 2003. Similarly, Some CPEs including tris(2-chloroethyl) phosphate (TCEP) and tris(1,3-dichloro-2-propyl) phosphate TDCPP were banned in a few states like Maryland [19].

1.1.3 Inorganic FRs

The demand of non-halogenated FRs use such as inorganic FR, nitrogen FR and phosphorus FR has increased due to the restrictions on halogenated FR use.
Inorganic FRs such as aluminum hydroxide hydrate and magnesium hydroxide achieve flame retardancy through decomposition with the release of water and/or non-flammable gases which work as resistant layer over the product's surface in contrast to flame inhibiting mechanism following the radical trap theory [20]. For example, aluminum

hydroxide ($Al(OH)_3$) decomposes endothermically at high temperature by absorbing heat and releasing water vapor.

$$2Al(OH)_3 \rightarrow Al_2O_3 + 3H_2O \quad (7)$$

Although it is easy to incorporate inorganic FRs into polymers and the chemicals themselves are inexpensive, a high concentration (approximately 20 wt% to 60 wt%) of inorganic FRs is required to meet comparable flame retardancy to halogenated FRs, which leads to large loading mass [21, 22]. Therefore, it can be challenging to replace halogenated FRs with inorganic FRs as such a high loading potentially affects the physical property of the material.

1.1.4 Phosphorus FRs

Phosphorus FRs are another alternative material that has been used. It prevents the flame from sustaining the combustion process in a similar manner to halogenated FR[23]. Ammonium polyphosphate, for instance, undergoes thermal decomposition and releases phosphorus oxide radical (PO·)[24, 25]. This radical competes with H· and OH·, leading to a deceleration of the combustion process.

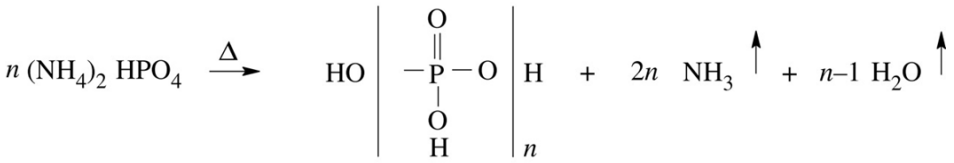

(8)

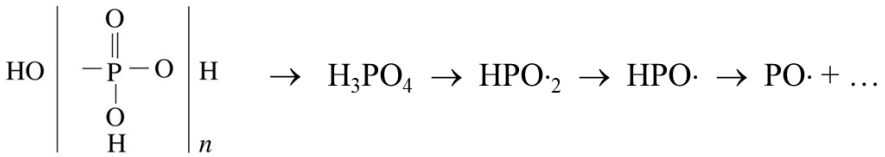

(9)

$$PO\cdot + H\cdot \rightarrow HPO \quad (10)$$

$$PO\cdot + OH\cdot \rightarrow HPO_2 \quad (11)$$

$$HPO + H\cdot \rightarrow H_2 + PO\cdot \quad (12)$$

$$OH\cdot + H_2 + PO\cdot \rightarrow H_2O + HPO \quad (13)$$

$$HPO_2\cdot + H\cdot \rightarrow H_2O + PO \quad (14)$$

$$HPO_2\cdot + H\cdot \rightarrow H_2 + PO_2 \quad (15)$$

$$HPO_2\cdot + OH\cdot \rightarrow H_2O + PO_2 \quad (16)$$

Phosphorus FRs are also categorized as intumescent FRs that form char layers on the surface of the burning material and prevent further flame propagation (Figure 1.3). Compared to halogenated FRs, the phosphorous containing alternatives have the advantage of not producing toxic chemicals while presenting a high efficacy compared to inorganic FRs, resulting in only a small dosage needed. However, in general, phosphorus FRs lack durability resulting in volatilization and leaching [26, 27]. They are not suited for certain common applications such as clothing as they can be washed off by the existence of water.

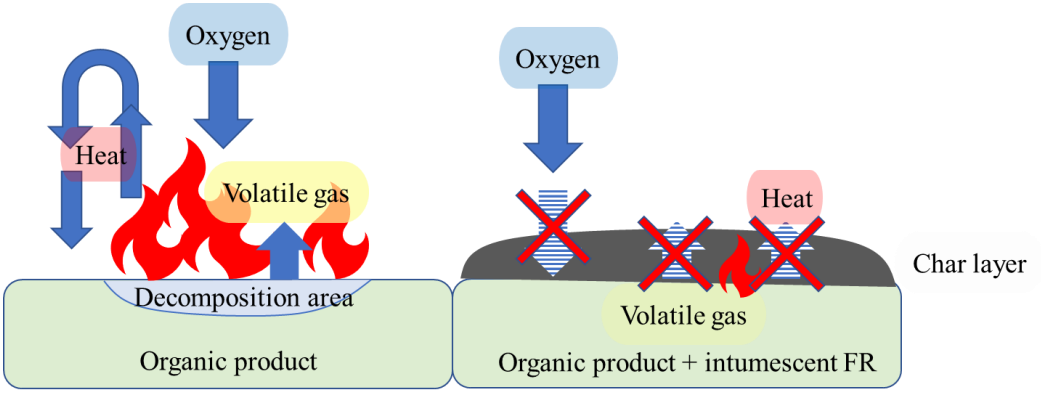

Figure 1.3 Intumescent flame retardant mechanism, adapted from an infographic by FLAMERETARDANTS-ONLINE (https://www.flameretardants-online.com/flame-retardants/intumescence)

1.2 Nanomaterials as potential alternative FR

There is no alternative material that can substitute halogenated FRs without compromising the performance, as each existing FR has different challenges. Therefore, other types of materials are being investigated to obtain a desirable FR material that has equivalent or higher flame retardant efficacy to halogenated FR, is not toxic nor generates toxic species and presents high durability. Recently, various types of nanoparticles have been explored as potential FR materials. Some researchers developed silica nanoparticles coated on cotton and showed high flame retardancy [28, 29].

CNMs such as fullerenes, carbon nanotubes (CNTs) and graphene are another family of nanomaterials that are considered to have potential to act as flame retardant. Figure 1.4 shows the structure of each CNM. Fullerene is a hollow sphere-shaped molecules composed of carbon. The most known fullerene is called C_{60}, discovered in 1985[30]. CNTs were discovered in 1991[31] as a nanomaterial made of carbon with cylindrical shape. In 2004, graphene which is single layer of carbon atoms arranged in a hexagonal lattice structure was successfully isolated from graphite layers[32]. These CNMs are reported to have unique properties and have been explored for variety of applications in different fields since they were discovered. Their high heat conductivity [33, 34] and thermal stability [35] are some of the features and CNMs could be good candidates as new FR material as CNMs are believed to perform as a protective layer that hinders transferal of thermally decomposed sample without disintegrating themselves. Additionally, some studies[36, 37] proposed CNT's radical scavenging potential. This is a promising feature as diminishing highly reactive radicals is a critical part of flame retardancy as mentioned in halogenated FRs mechanism (Chapter 1.1.2).

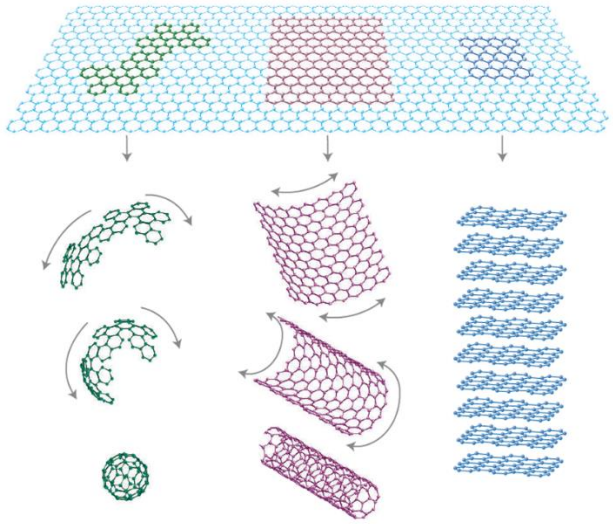

Figure 1.4 Structure of carbonaceous nanomaterials. Single layer of graphite (graphene, top and right) can be wrapped up to form fullerene (left), rolled into carbon nanotube (center)[38].

1.3 Goals and objectives

There are two core goals in this research, the development of CNMs coating as flame retardant and the assessment of the efficacy and potential release to the environment in the use phase such as abrasion and laundry washing. This work includes the development of a CNMs quantification method in polymer composites (Chapter 2). This method was extended for quantifying other types of carbonaceous materials in different matrices and summarized in Chapter 6. The CNMs quantification method was applied in Chapter 3 to evaluate the flame retardancy of different CNMs coatings by determining the mass loadings along with the burning test results. The technique was also used for release study in Chapter 5 by monitoring the mass of CNTs leached from washing and released by mechanical abrasion. Chapter 4 focused on improving coating quality without compromising the flame retardancy based on the findings in Chapter 3.

In Chapter 2, a technique to quantify CNMs in polymer composites was developed as it was essential to be able to detect/quantify CNMs for evaluating the flame retardant efficacy and life cycle assessment. Detecting and quantifying CNMs in different matrices is challenging as they require differentiation from other forms of carbon and low detection limit since the concentration of CNMs in products and environment is expected to be low. One study predicted the concentration of CNTs in the air and soil to be 1.5 x 10^{-3} µg/m^3 and 1 x 10^{-2} µg/kg respectively [39, 40]. Programmed thermal analysis (PTA) has been studied and shown as a promising CNMs quantification analysis method in different matrices such as biological tissues and biomass [41, 42]. In the earlier work [41, 43] as collaborative research, it was found that a major issue to quantify CNMs was developing a method to isolate them from other carbon sources in the matrix. Polymer samples like fabrics are especially difficult to manage to obtain reliable outcome without being interfered by other forms of carbon due to its difficulty to separate CNMs from the matrix. The hypothesis is that a standard PTA is amenable to the quantification of CNMs in polymeric matrices after the right pre-treatment. As a pre-treatment for PTA, dissolution process with organic solvent was applied.

In Chapter 3, various types of CNMs were coated on polyester fabric and their flame retardancy was evaluated. The principal hypothesis is that CNMs can perform as FR due to their high thermal stability stems from the crystal structure. CNTs and graphene oxide were chosen as coating materials among CNMs listed in section 1.2 as fullerenes have generally lower thermal stability compared to other CNMs[44]. A further hypothesis is that differences in flame retardancy might be related to differences in CNM

functionalization and/or coating process. The observations on the differences in terms of flame retardancy and mass loading among CNMs are discussed.

Subsequently, developing optimal FR coating with CNM was pursued based on the findings in Chapter 3. This Chapter 4 was focused on modifying MWCNTs and obtaining adequately dispersed MWCNTs solution for FR coating without compromising the FR property. One of the common challenges with CNMs is that they do not get dispersed in any type of solvent easily unless they are functionalized, or surfactant is added. It is essential to obtain well dispersed solution to produce uniform coating for surface application and embedding into polymer. A common solution to overcome the issue is oxidization by acid treatment [45]. However, oxidizing CNMs contradicts to the hypothesis "CNMs with less oxygen contents have better potential as FR". Amine group, among different functional groups, assists the hydrophilicity of materials, and it does not involve oxygen. However, commercially available amine functionalized CNTs often contain oxygen as bi-products. Many reaction processes take multiple steps and typically oxygen is involved at one point such as formation of amide. In this research, functionalization of amine group on CNTs was attempted to append hydrophilicity to CNTs. As another approach, dispersion of short duration obtained by bath sonication in dimethylformamide (DMF), or in water with ammonium polyphosphate (APP) was introduced. The solution was coated by spray coating method and the applicability of forming FR coating was evaluated.

Followed by the development of FR coating with CNMs in the Chapter 4, the release study of the coating was investigated in Chapter 5. The main hypothesis of this chapter is that severe abrasion (mechanical abrasion and washing process) removes

significant amount of CNMs coatings and diminish the efficacy as FR. Release study of the materials to evaluate the potential exposure is necessary as new materials are developed for consumer products. Considering the perspective of efficacy of the coating as FR, release study is also essential as the efficacy is directly associated with the durability of the coating. Many of the consumer products that contain FRs are made for indoor applications such as draperies and furniture upholstery. Consequently, health concerns arise when these FRs are released by friction and get accumulated in environments with limited ventilation and dust accumulation. One study shows the average estimated cumulative exposure to organophosphate flame retardants from house dust for children and adults are calculated to be about 1600 ng/day and 325 ng/day respectively [46].

It is important to track how much CNMs are released to the environment and where they are going during use phase although FRs are regulated under Toxic Substances Control Act (TSCA) as CNMs are relatively new materials and there are questions that are not fully understood such as how they influence the environment and if they transform to another form of material under certain condition. Chapter 5 involves release study of CNMs to the environment by mechanical abrasion and washing test in use phase. This abrasion study monitored the efficacy of FR coatings under different conditions by coupling with flame retardancy test along with the amount of CNMs potentially released/accumulated in the air or wastewater.

Physically contacting the objects with FR coating is expected to be the main source of CNM release during use phase. An abrader can simulate the friction that is caused in the situation the coated products are located in regular household. The physical

abrasion test was conducted on CNM coated fabric, subsequently the amount of CNM mass released by the abrasion test was detected with 2-step PTA method developed in Chapter 2.

Washing test is another potential route CNM could be released from the coated product. The test was conducted in a rotating mixer, then quantification of CNM mass released by PTA the same way as mechanical abrasion afterwards. The hypothesis is that the washing process which imitates water contacts such as water spill and cleaning leads to CNM release with reduced efficacy as FR. Overall, the potential of CNMs as FR coating was investigated with perspectives of mass loading, flame retardancy, dispersibility of coating solution and durability/release of the coating by mechanical abrasion and washing process.

Finally, various projects using PTA on carbonaceous materials outside of the CNTs flame retardant study was summarized in Chapter 6. In addition to the quantification technique using PTA developed in Chapter 2 for polymer composites, multiple methods modified for other types of CNMs like GO and activated carbon in different matrices were developed. The applicability of PTA to wide range of materials in various matrices was discussed.

In brief, the main research questions addressed in each Chapter are shown below.

Chapter 2: Are CNMs in polymers amenable to quantification using Programmed Thermal Analysis (PTA)?

Chapter 3: Do CNM coatings show flame retardancy comparable to existing FR coatings?

Chapter 4:

1. Can amine functionalization of CNT add hydrophilicity to CNTs and achieve stable coating dispersions?
2. Can dispersions of short duration be used in conjunction with spray coating as a viable alternative to generate homogeneous coatings?

Chapter 5: Are spray coated CNM FR coatings durable, maintain their efficacy and do not release CNMS in the environment?

Chapter 6: Can PTA be applied to other carbonaceous materials in various matrices?

CHAPTER 2

QUANTIFICATION OF CARBON NANOTUBES IN POLYMER COMPOSITES

2.1 Introduction

Carbonaceous nanomaterials (CNMs) such as carbon nanotubes (CNTs), graphene and graphene oxide (GO) proposed for use in polymers and fabrics due to their unique properties[47, 48]. CNTs are embedded in polymer matrices[49] and bulletproof fabrics[50] for mechanical reinforcement because of their high tensile strength but lower mass compared to alternative reinforcement agents. CNTs are also used in thermal packaging for electronic applications, where their high thermal conductivity facilitates heat transfer when incorporated in polymers[33, 34]. With the increase in CNM usage and production, it is critical to develop methods to quantify CNMs in these products, both for industrial quality control as well as tracking their environmental fate. The change in CNT concentration within polymers due to sun, rain, mechanical or chemical exposure is important to be quantified[51]. The type of CNT (single SWCNT or multi walled MWCNT) used in composite polymer materials depends on the application because each has different properties such as dispersion[52] and chemical resistance. However, both types were reported to enhance mechanical strength and thermal stability[53, 54].

Different analytical techniques have been proposed for CNM detection such as spectroscopy[55-58], electron microscopy[59], thermal analysis[60] and microwave induced heating method[61, 62]. Many of these techniques are qualitative or semi-quantitative, and only a few approaches allow for the CNM quantification[63-66]. Electron microscopy is widely used because it can provide visual images that are useful for morphology studies, but it only gives structure/morphology information. Optical (UV-Vis) spectroscopy is

widely available and can be used quantitatively with little sample preparation; however, it requires well dispersed solutions, and the detection limits are rather high (0.1–0.5 mg L^{-1})[51]. These optical techniques are also susceptible to interferences by other components in complex matrices such as environmental or biological samples. Near infrared fluorescence (NIRF), for instance, is capable of identifying and quantifying single-walled carbon nanotubes (SWCNTs) with specific length/chirality, but it is limited to only non-functionalized, semi-conducting SWCNTs that are dispersed without aggregation[51].

PTA (programmed thermal analysis) is a quantification method for elemental carbon that allows differentiation of refractory (elemental) carbon from organic carbon[67, 68]. CNT samples are analyzed by combusting the carbon portion at high temperature and transforming the evolved gases to carbon dioxide in an oxidizing oven. The carbon dioxide converts to methane by a methanator that is set beside the oxidizing oven, and the carbon mass is determined with a flame ionization detector (FID) signal detected with methane standard. It can quantify elemental carbon in amounts as low as 0.2 µg per sample[69]. This method has been demonstrated to quantify single and multi-walled carbon nanotubes, graphene and graphene oxide with a range of properties such as length, diameter and purity[41, 43, 67]. Using different sample preparation techniques, the methodology was applied to biological matrices and biomass[41, 70].

While CNMs are used in polymer and fabric products[71], PTA cannot be applied to CNT polymer composites directly. The high organic carbon content of these matrices requires separating the CNTs from polymer before introducing the sample to the instrument. Therefore, a pre-treatment is needed that dissolves the polymer and separates the CNTs.

This study presents a two-step extraction/detection method to determine CNTs, both SWCNTs and MWCNTs, in polymer materials. First, the polymer is dissolved, and then CNTs are quantified by PTA. Optimization of solvents and validation of the process is provided.

2.2 Experimental materials and methods

2.2.1 Materials

SWCNTs (Carbon Solutions, Inc, Riverside, USA) and MWCNTs (bundled, >95% carbon basis, O.D. x I.D. x L 7–15 nm x 3–6 nm x 0.5–200 mm, Sigma Aldrich, St. Louis, USA) were used. The polymer dissolution solvents included chloroform (>99.5%) and hexafluoroisopropanol (HFIP, CovaChem, Loves Park, USA). Tetrahydrofuran (THF, >99.9%), chloroform (>99.5%), ortho-dichlorobenzene (o-DCB, >99%) and ethyl cellulose were used to prepare polymer samples. Polymer and fabric samples included polyester fabric (Asics, Kobe, Japan), polycaprolactone (PCL, number average molecular weight Mn = 45 000), polystyrene (PS, molecular weight Mw ~ 280 000 (by Gel Permeation Chromatography)), chitosan (low molecular weight), poly(bisphenol A carbonate) (PC-BPA, Mw = 28 200 & Mn = 17 000). Unless noted otherwise, all polymers and solvents were purchased from Sigma Aldrich (St. Louis, USA).

2.2.2 Polymer composite preparation

PCL samples were prepared with different SWCNT and MWCNT concentrations[72]. The mass corresponding to the target weight percent of CNTs was added to 21 mL of THF and 21 mL of chloroform in a sealed 50 mL Erlenmeyer flask. 31.5 mg of ethyl cellulose were added to achieve a stable dispersion. The resulting

mixture was sonicated using a sonicator (Branson 1800, Danbury, USA) for 3 hours. 420 mg of PCL were then added and sonicated for another hour. The final suspension was poured at 6 mL per aluminum dish, covered and dried overnight at room temperature.

2.2.3 PTA sample preparation

CNT-containing polymer samples were weighed to 10 mg and placed in a beaker. 10 mL chloroform and 5 mL HFIP were added to the beaker using an approach previously described to dissolve polymer material[73]. The beaker was covered and let sit for 5 min. The solid residue, which was mostly CNTs, was collected by syringe filtration onto a 1 x 1.5 cm quartz fiber filter (WhatmanTMQM-A, Fisher Scientific, Hampton, USA) once the polymer was completely dissolved. The majority of polymer components was removed by this filtration process as they stay in solution. The initial CNT concentration embedded within the polymer samples ranged from 0.1 wt% to 5 wt% (0.1, 0.5, 1, 3 and 5 wt%) for MWCNTs and 0.05 wt% to 5 wt% (0.05, 0.1, 0.25, 0.5, 1, 1.5, 2, 3 and 5 wt%) for SWCNTs. Triplicate samples of 1 wt% polymer-CNT composites were prepared for evaluating the reproducibility of the analysis.

2.2.4 Programmed thermal analysis (PTA)

PTA was performed using an organic carbon/elemental carbon analyzer (Sunset Laboratory, Inc., Tigard, OR). This technique differentiates organic carbon and elemental carbon including CNTs and graphene based on the thermal stability of carbon materials. PTA was used to quantify the CNMs loaded in polymers. The temperature program and operational parameters for this technique were created based on previous CNT thermal studies[68, 74, 75].

2.2.5 Characterization of SWCNTs with metal catalysts

SWCNTs with metal catalysis were characterized using electron microscopy and a CHN elemental analyzer. A transmission electron microscope (TEM, Philips CN 300 FEGTEM) was used to image the SWCNT morphology and catalyst location following a reported procedure[76]. The carbon mass percentage in the SWCNT material was determined by CHN elemental analyzer (PE2400, PerkinElmer), and the percentage of impurity was estimated by difference form the SWCNT mass.

2.2.6 Inductively coupled plasma mass spectrometry (ICP-MS)

As a complementary quantification technique, ICP-MS was used to determine SWCNTs based on their metal impurities following a method outlined in Reed et al[64]. In brief, the SWCNT mass was determined based on the concentration of metal catalysts contained in SWCNT. Yttrium was chosen as the target metal because the previous study showed this SWCNT contains Ni and Y as catalyst[64], and Y has low risk of contamination. First, a 5-point standard curve was created with different masses (1, 1.5, 2, 2.5 and 3 mg) of neat SWCNT. Neat SWCNTs were added to 10 mL 70% nitric acid solution (Omnitrace Grade, EMD Chemicals, Darmstadt, Germany) in Teflon vessels, then the solutions were loaded in a microwave digestion system (MARS 5, CEM Corporation, Matthews, USA) and operated 3 times (800 W, ramp time: 20 min, hold time: 20 min, target temperature: 210 °C). The digested samples were diluted with Milli-Q water to adjust the acid concentration to 2% and analyzed by ICP-MS. Ten mg of PCL-SWCNT samples with varying concentrations (0, 0.1, 0.5, 1, 2 and 3 wt%) were prepared for analysis in the same way as neat SWCNT. The SWCNT mass was determined based on yttrium concentration and the standard curve.

2.3. Results and discussion

2.3.1 MWCNT quantification without polymers

PTA consists of a two-step combustion process (Figure 2.1); the first step is under inert conditions (helium atmosphere; shaded area in Figure 2.1), and the second step is under oxidizing condition (90% He/10% O_2 atmosphere). PTA thermograms show the evolved carbon as a function of time. Figure 2.1 shows the PTA results of a neat PCL polymer sample (Neat PCL) and raw MWCNT. The combusted carbon is shown as FID signal, and the accumulated area beneath the curves relates to the mass of carbon detected. Organic carbon is typically combusted under inert condition (helium, shaded area in Figure 2.1) while more refractory carbonaceous material is combusted under oxidizing condition with helium/O_2 mixture. In this latter process, the elemental carbon composing MWCNTs combusts. MWCNTs generally start combusting around 500 °C under oxidizing condition, although it can vary depending on attached functional groups that affect thermal stability[67]. PTA quantification for raw MWCNTs with different mass loadings is shown in Figure 2.2.

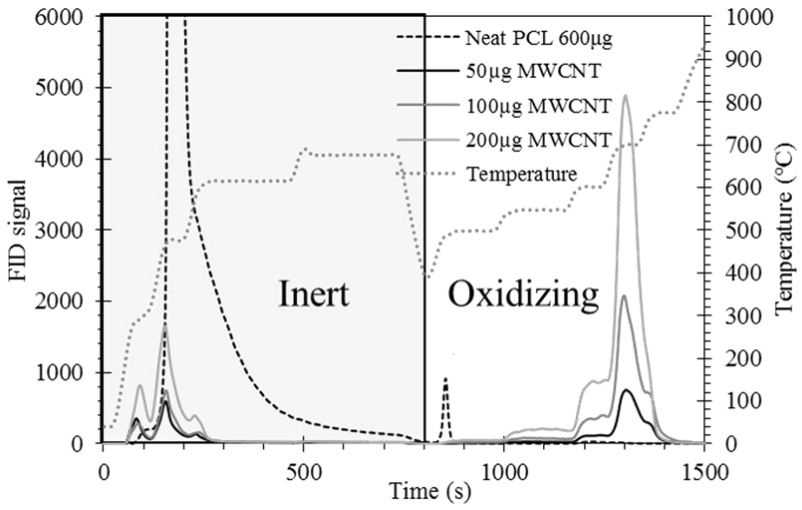

Figure. 2.1 Thermogram showing carbon FID response over time for different temperatures for different masses of MWCNT alone (no polymer) and polymer alone (no CNT, no dissolution).

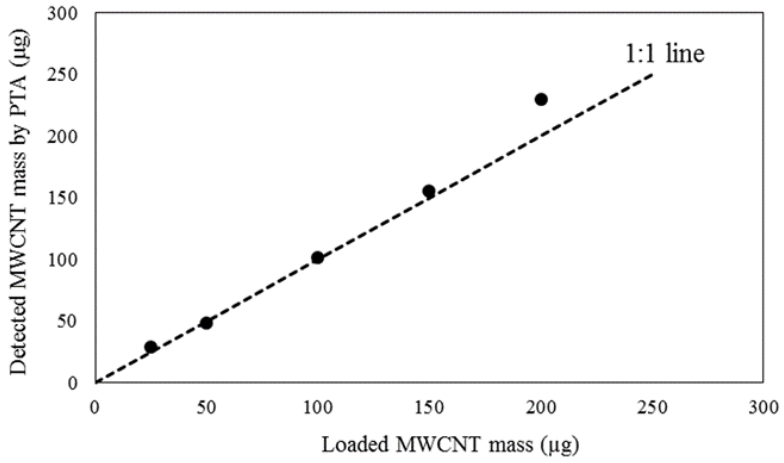

Figure 2.2 Quantification results by PTA with different mass loadings of raw MWCNTs.

For a neat polymer (e.g., PCL only), a small portion of organic carbon might evolve only at high temperature (~500 °C) under oxidizing condition. It is the result of charring, i.e., the formation of pyrolytical carbon[77] from organic carbon in the polymer[67, 78], that has similar thermal stability to CNTs. The pyrolytical carbon resulting from the sample matrix can lead to a substantial artifact (pyrolytical carbon mistaken for CNM carbon) in CNT quantification by PTA. In our case (Figure 2.2), neat PCL has a very large peak under inert condition and some smaller peaks under oxidizing condition. The peak from organic carbon under inert condition is extremely large and interferes with the peaks resulting from MWCNTs. The interference from organic carbon and the formation of char are the main two factors that make it difficult for PTA to quantify MWCNTs in complex organic matrices such as polymers.

2.3.2 Solvent dissolution potential

We evaluated a pre-treatment/polymer dissolution step on different polymers to decrease or eliminate matrix effects. Several polymers (polycaprolactone, polyester, polystyrene, nylon 6, polyethylenimine (PEI), acrylonitrile butadiene styrene (ABS), poly(bisphenol A carbonate), polysulfone, polyvinyl pyrrolidone (PVP), chitosan and polypropylene (PP)) were evaluated with two solvents (HFIP/chloroform mixture, chloroform only). Table 2.1 shows that all polymers, except chitosan and PP, dissolved in the solvent HFIP/chloroform mixture. Complete dissolution occurred within 10 min without heating or sonicating. Some polymers such as polyester and nylon 6, which have high chemical compatibility with chloroform, were effectively dissolved by the HFIP/chloroform mixture because HFIP is a strong solvent for polar polymers. This indicates the applicability of the dissolution step to a wide variety of polymers.

For the remainder of tests described in this paper, HFIP/ chloroform was used as the solvent because of its robust ability to non-selectively dissolve polymers. One polymer (PCL) was selected as target material for the method optimization because PCL is known as a biodegradable polymer[79], and its biocompatibility is a promising feature for biomedical applications. Weaknesses of PCL, however, are its poor mechanical properties, which make it a prime candidate for CNT addition; some studies suggest blending CNTs into PCL for mechanical strength improvement[80-83].

Table 2.1 Dissolution test results on various polymers in chloroform & HFIP mixture

Polymer	Chloroform	Chloroform+HFIP
Acrylonitrile butadiene styrene	✓	✓
Polystyrene	✓	✓
Poly(Bisphenol A carbonate)	✓	✓
Polycaprolactone	✓	✓
Polysulfone	✓	✓
Polyvinylpyrrolidone	✓	✓
Polyester		✓
Nylon6		✓
Polyethylenimine		✓
Chitosan		
Polypropylene		

2.3.3 Evaluation of the 2-step process: dissolution then PTA

Figure 2.3 shows the PTA results of neat PCL, a PCL sample after the dissolution process (dissolved PCL) and a PCL-MWCNT composite after the dissolution process (dissolved PCL + MWCNT). Figure 2.3 confirms that PTA was a viable technique for polymer-MWCNT samples once a dissolution pretreatment process occurred. Peak Ⓐ for

neat PCL represents residual organic carbon, and it can potentially interfere with the quantification by overlapping with the CNM peak. Dissolved PCL + MWCNT showed only peak Ⓑ, which originates from MWCNT, and no peak was observed in oxidizing condition from dissolved PCL. As such, the dissolution substantially reduced the organic matter signal and hence reduced the risk of interference. Also, the samples from the dissolved polymer did not generate any pyrolytical carbon and associated interfering signal, thereby eliminating the positive artefact formation by generating a signal overlapping or close to the CNT.

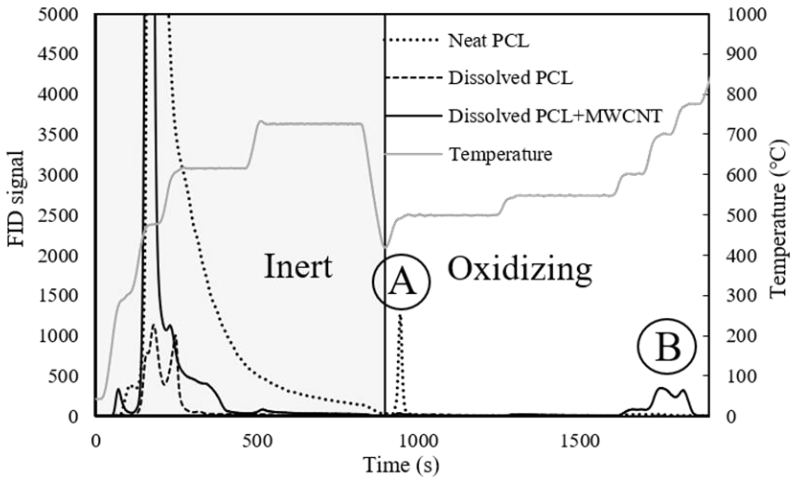

Figure 2.3 Thermogram of neat polycaprolactone (PCL), PCL after dissolution process (dissolved PCL) and PCL-MWCNT after dissolution process (dissolved PCL + MWCNT). Ⓐ represents remaining organic carbon, Ⓑ is MWCNT released from CNT-polymer composite.

2.3.4 Quantitative accuracy

In order to confirm the accuracy of the two-step technique for CNT quantification, PCL samples with varying MWCNT concentrations (based on added

mass) were analyzed. Figure 2.4 shows the MWCNT mass in each sample. The dotted line illustrates the expected MWCNT mass (shown as theoretical line, 10 mg x (sample concentration in %) x 0.01) based on the concentrations used in manufacture, and the dots show the MWCNT mass in 10 mg of PCL-MWCNT sample as determined by PTA. The measured results agreed with the expected values and demonstrated a linear response with increasing MWCNT concentrations. Triplicate analysis of 1% PCL-MWCNT samples showed a 16% relative standard deviation. The minimum carbon mass detectable by the instrument is 0.2 μg[69]; therefore the detection limit is roughly 0.2 ppm (by mass) for a 1 g sample (i.e., 0.0002 wt%) as the detection limit of this technique depends on the sample mass. Lower detection limits can be achieved if a larger sample mass is used for analysis.

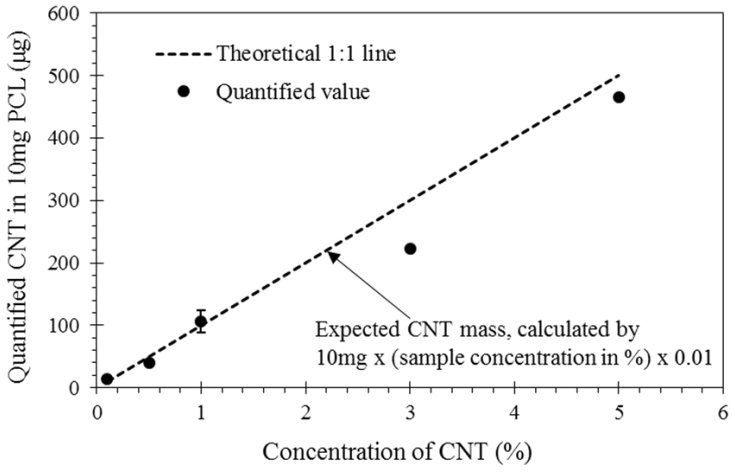

Figure 2.4 Quantified CNT mass in 10 mg PCL-MWCNT composites with different CNT concentration. Dashed line indicates expected value based on the concentration, and dots are the actual data by PTA. The bar at 1% CNT shows one standard deviation for triplicate samples.

2.3.5 SWCNT quantification

Previous research showed that SWCNTs have a lower thermal stability compared to MWCNTs because they have a smaller diameter and a higher fraction of surface atoms[67]. In this previous study[67], SWCNTs were classified as thermally "weak" CNTs. A purified SWCNT sample in the study started combusting below 500 °C under oxidizing condition. Figure 2.5 shows the thermogram for an unpurified commercial SWCNT. The sample shows a peak at 500 °C under oxidizing condition (shown as "Ⓐ" in the figure) even though SWCNTs normally do not combust at such a low temperature[67]. The presence of metals such as nickel in substantial quantities reduces CNT thermal stability[63]. A majority of commercial CNTs contain metal impurities such as cobalt, nickel, molybdenum and yttrium because they are used as catalysts during CNT synthesis[84, 85]. The SWCNTs used in Figure 2.5 contain nickel and yttrium primarily as catalyst for SWCNT synthesis as determined by ICP-MS in a different study. CHN analysis provided the mass percentage of carbon, hydrogen and nitrogen in the material as 68.4, 0.1 and 0.7% respectively. This indicates that approximately 30% of the CNT powder is composed of metal impurities. The TEM image in Figure 2.6 supports the CHN analysis by showing a significant amount of metals appearing as small dots on SWCNTs. The catalytic effect of metals can amplify the already lower thermal stability of SWCNTs, resulting in lower temperature combustion in PTA. The resulting peaks may overlap with peaks that stem from other/matrix components, so this interference will impact the quantification accuracy.

While it is possible to remove metal impurities from SWCNTs, it is unlikely that commercial large-scale applications will perform this step. Hence the unpurified metal-containing SWCNTs are the most realistic target species in regard to the challenges they pose for quantification. Figure 2.7 shows the CNT mass in PCL-SWCNT composites with varying SWNCT concentrations. The samples were prepared by dissolving them in HFIP/chloroform mixture before PTA. The SWCNT mass determined experimentally by integrating the entire area of the oxidizing phase in Figure 2.7 is notably lower than the expected value (shown as theoretical line, 10 mg x (sample concentration in %) x 0.01 (mass of SWCNT/mass of PCL-SWCNT composites)), although a very linear response of SWCNT with R^2 value 0.99 is observed, like in the case of MWCNT (Figure 2.4). Triplicate measurements of the 1% PCLSWCNT sample showed 29.7, 30.6 and 31.0 mg with a relative standard deviation of 1.8%. The PTA method is absolute relative to carbon as it measures the amount of carbon and does not include the metal impurities. Therefore, a systematic bias exists: the quantified CNT value is relative to carbon only and does not account for the mass contributed by 30% non-carbon metal impurities. If the measured CNT mass is corrected for the metal content (calculated by "quantified value"/ (1 - the fraction of metal impurities, 0.3 in this case)), the resulting values are closer to the expected concentrations (Figure 2.7) and are similar to the results obtained for the MWCNTs. This indicates that the quantification value is valid in terms of carbon, when the peaks appearing at lower temperature under inert condition are included. Therefore, this technique is also applicable to CNTs with metal impurities, although the amount of metal impurities must be known to determine the carbon mass.

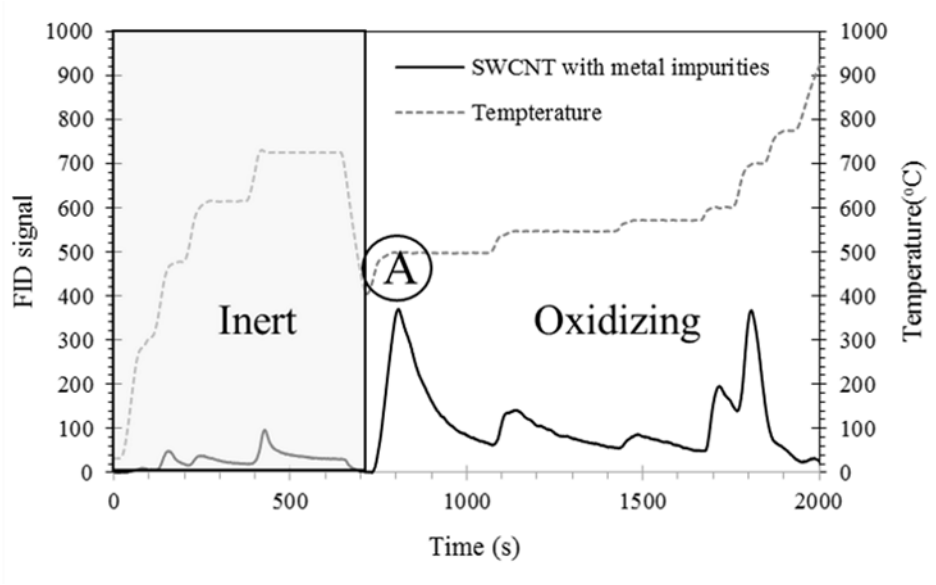

Figure 2.5 Thermogram of SWCNT with metal impurities. Peak Ⓐ indicates the thermal stability of the SWCNT decreased because CNTs generally do not combust below 500 °C.

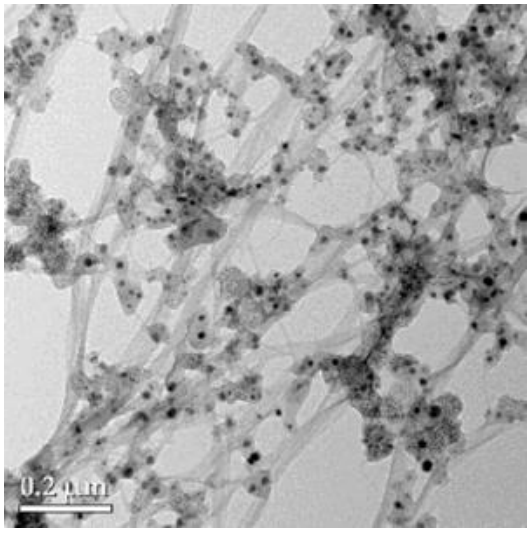

Figure 2.6 TEM image of SWCNT, dark dots are representing the metal catalysts.

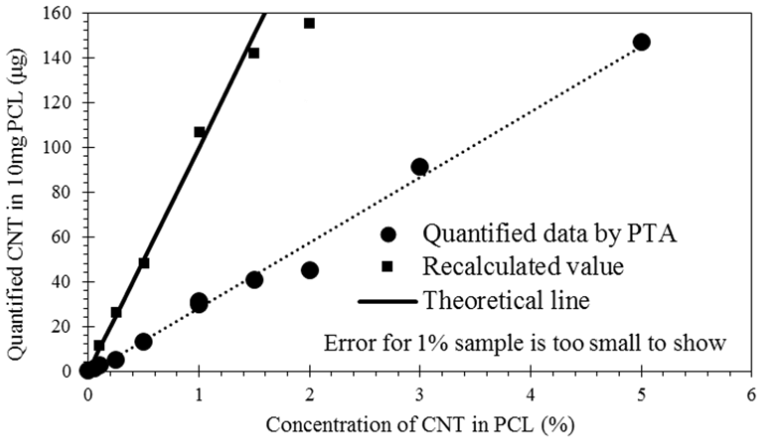

Figure 2.7 Quantified CNT mass in 10 mg PCL-SWCNT composites with different CNT concentrations. Solid line, squares and dots indicate expected value based on the concentration, recalculated values considering metal concentration of 30 wt% and peaks at 500 °C and the PTA results, respectively.

2.3.6 Quantification by ICP-MS

Although PTA is applicable to both SWCNT and MWCNT regardless the existence of metal impurities, there are some limitations. For example, the metal impurity content needs to be known because PTA measures only the amount of carbon and hence does not give access to a mass of CNT. Also, the quantified value could be off if CNTs are largely functionalized with elements that are not carbon. Therefore, as an alternative and conformational quantification method, ICP-MS was evaluated to quantify SWCNTs with metal impurities. First, a standard curve of the SWCNT concentration relative to an impurity (here yttrium) was obtained. The SWCNT concentration in PCL was then determined using the yttrium/SWCNT relationship obtained. Figure 2.8 shows the data points are along the 1 : 1 line that indicates theoretical values. Given these results, ICP-MS is an alternative quantification method for CNTs with high metal impurities. PTA is

preferred because it is easier to carry out than the ICP-MS method, which requires a digestion step with concentrated acids, but ICP-MS is beneficial when CNT samples contain metal catalysts that can be detected by ICP-MS with very little possibility of contamination.

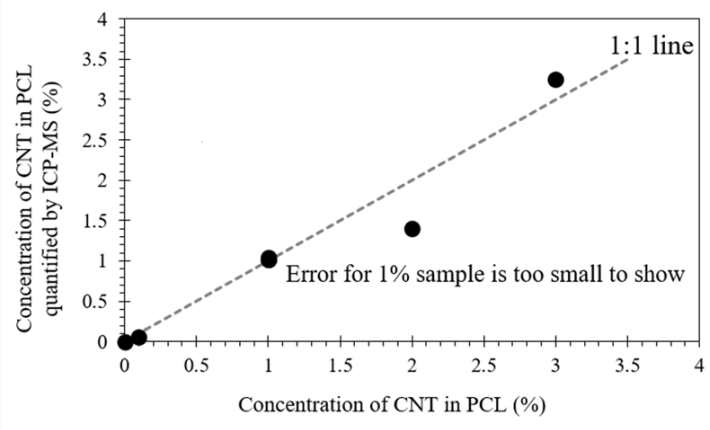

Figure 2.8 SWCNT concentrations as determined by ICP-MS using Y impurities.

2.4 Conclusions

An analytical method for determining CNTs embedded in polymers was presented. The method consists of a solvent dissolution and filtration step followed by PTA to quantify CNT mass in terms of carbon. The analytical method can achieve low detection limits at an absolute amount of 0.2 µg (0.2 ppm (m m^{-1}) for a 1 g sample) at a high reproducibility (<20% standard deviation) for MWCNTs. Lower detection limits can be obtained by using larger sample sizes. SWCNTs were also amenable to the analytical method but presented some challenges because of their lower thermal stability compared to MWCNTs and resulting potential for artefact formation in PTA. Certain metal catalysts typically contained in SWCNTs can enhance the SWCNT combustion at lower temperatures during PTA and hence exacerbate the PTA quantification issues. These challenges can be overcome through the dissolution process, which removes excess

carbon and reduces organic carbon signal production, and by correcting the measured carbon content to account for metal impurities. While the PTA method only quantifies carbon, the measurement can be corrected to SWCNT mass if metal and other impurities are determined (e.g. following isolation after dissolution).

The proposed two-step dissolution-PTA method is applicable to a wide variety of polymers as demonstrated in dissolution tests with the proposed HFIP/chloroform solvent mixture. The proposed methodology is likely amenable to other carbonaceous nanomaterials as PTA has already been successfully used with graphene materials. A quantification method that uses digestion followed by ICP-MS based on SWCNT impurities is also a viable option but requires CNT characterization or, at a minimum, information on the CNT impurities, which is not as straightforward as the solvent dissolution-PTA approach.

CHAPTER 3

FLAME RETARDANT PERFORMANCE OF CARBONACEOUS NANOMATERIALS ON POLYESTER FABRIC

3.1 Introduction

Flame retardants (FRs) play an important role in fire prevention and are applied to consumer products such as textiles (clothing, draperies, furniture upholstery) and electronics [86-88]. FRs slow or prevent fire ignition or growth by chemical/physical mechanisms such as radical quenching, endothermic degradation and thermal shielding[89]. Halogenated FRs such as brominated FRs and chlorinated FRs were commonly used due to their high compatibility with polymers and high efficacy resulting in low required dosage (0.3 to 4 wt%) [5]. However, a majority of halogenated FR chemicals were found to be persistent in the environment [17, 90], to bioaccumulate and potentially be toxic to humans resulting in regulations and many of these species, such as polybrominated diphenyl ethers (PBDEs), have been banned [16, 91].

Besides halogenated FRs, there are inorganic FRs, organophosphorus FRs and nitrogen-containing FRs that are commonly used. Inorganic FRs such as aluminum oxide hydrate and magnesium hydroxide raise fewer toxicity concerns than halogenated FRs. However, inorganic FRs require high mass loading (20-60 wt% [21, 22]) to achieve a similar flame retardancy as halogenated FRs at a fraction of the mass loading (0.3-4 wt%)[86, 92]. High mass loadings may not be suitable for certain applications like clothing. Organophosphorus FRs (e.g., triphenyl phosphate (TPHP), tricresyl phosphate (TCP)) are also applied to consumer products. These species exhibit comparable flame retardancy to halogenated FRs. The disadvantage of organophosphorus FRs is however their poor

durability resulting in volatilization and leaching [26, 27]. Organophosphorus FRs can also be easily washed off by contact with water and thus ultimately leading to high indoor exposure. Moreover, the health and environmental impacts of their exposure are not thoroughly understood [93].

Therefore, alternative FR materials that can potentially substitute halogenated FRs without compromising the performance are desired. Recently, various types of nanoparticles have also been proposed as potential new FRs. Silica nanoparticles were coated on cotton and showed high flame retardant performance [28, 29]. Carbonaceous nanomaterials (CNMs) such as carbon nanotubes and graphene are already applied to variety of products due to their unique properties such as high heat conductivity [33, 34] and thermal stability [35]. Some researchers hypothesized the potential of CNM-polymer nanocomposites as effective flame retardants because CNMs are capable of forming a continuous network structured protective layer which leads to a reduction in heat release rate [94, 95] and other investigators developed coating methods on fabric using CNMs as flame retardants [96, 97]. There is even a flame retardant coating product, containing carbon nanotubes (CNTs), that is commercially available [98]. Despite this interest in CNMs as flame retardants, little is known on the mechanisms of flame retardancy, on the chemical properties of the flame retardants or even the relationship between the dosage and flame retardancy.

This study evaluates the flame retardant performance of different CNMs. Given the common use of FRs on textiles, polyester fabric was chosen as model substrate onto which different FRs were coated. Coatings with carbon black (CB) were also evaluated as a carbonaceous material that is not “nano-sized” to contrast with nano-sized CNMs.

Effects of CNMs loading on flame retardancy was quantified using a standardize burning test that measures both ignition and remaining sample lengths. Flame retardant performance was related to the amount of CNMs applied in the coatings. A unique analytical approach, programmed thermal analysis (PTA), was used to quantify CNM loading on textiles. The relationship between the flame retardancy and CNMs loading of each material including CNMs and conventional FRs was discussed.

3.2 Experimental and Analytical Methods

3.2.1 Materials

MWCNTs, amine functionalized multi-walled carbon nanotubes (NH_2-MWCNT, from 2 different companies), oxidized MWCNTs (O-MWCNT), graphene oxide (GO) and a commercial flame retardant coating containing MWCNTs (Thermocyl™) were used. One type of NH_2-MWCNTs was purchased from Cheap Tubes (NH_2-MWCNT (C), Cambridgeport, USA) and the other NH_2-MWCNTs (NH_2-MWCNT (N)) and MWCNTs were purchased from NanoLab (Waltham, USA). GO, Thermocyl and CB (EMPEROR 2000 and VULCAN 9A32) were purchased from TW-Nano Materials (Garden Grove, USA), Nanocyl (Sambreville, Belgium) and Cabot Corporation (Boston, USA) respectively. Detailed information on the CNMs provided by the manufacturers is shown in Appendix A.

A polyester textile (athletic shirt, Asics (Kobe, Japan)) was used as base fabric. Dimethylformamide (DMF, Sigma Aldrich, St. Louis, USA) was used to suspend NH_2-MWCNTs. Chloroform (Sigma Aldrich, St. Louis, USA) and hexafluoroisopropanol (HFIP, CovaChem, Loves Park, USA) were used to dissolve polyester samples as the part of sample preparation for thermal analysis. Ammonium polyphosphate (APP, Hangzhou

JLS Flame Retardants Chemical Co., Ltd., Pomona, USA) was applied as part of the layer by layer (LBL) coating. Polyacrylamide (PAM) was purchased from Sigma Aldrich for one of GO LBL coatings.

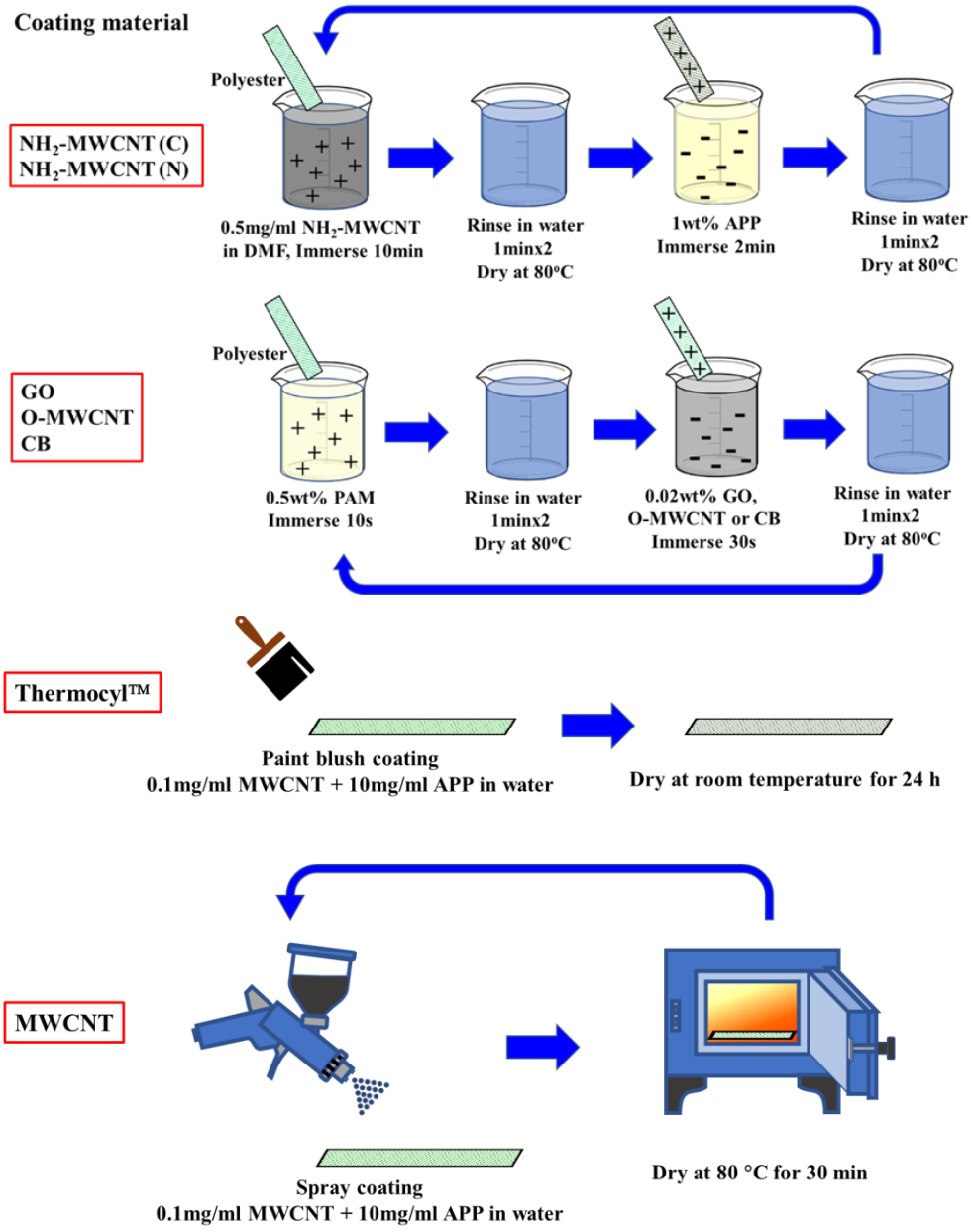

Figure 3.1 CNMs coating procedures on polyester. From the top, LBL coating (NH_2-MWCNT (C), NH_2-MWCNT (N), GO, O-MWCNT, CB1, CB2, paint blush coating (Thermocyl), and spray coating (MWCNT).

3.2.2 Textile Sample preparation

Coating procedures used in this study (Layer by layer (LBL) coating, paint brush coating and spray coating) are illustrated in Figure 3.1. All coatings were aimed to be around 1% by mass as previous research has shown that ~1% of CNT addition to polymer composites provided flame retardancy[99, 100].

NH_2-MWCNTs were applied by pairing negatively charged polymer layers since NH_2-MWCNT is charged positively [96]. In brief, 50 mg of NH_2-MWCNT (C) was suspended in 100 mL of DMF followed by bath sonication for 30 min. 1 wt% of APP solution was prepared by adding 1 g of APP into 100 mL Mill-Q water (≥18.2 MΩ-cm). The pH of the APP solution was adjusted to 10 by adding NaOH and HCl solution. Polyester fabric (110 mm x 65 mm) was immersed into the NH_2-MWCNT (C) solution for 10 min, then rinsed with water twice each for 1 min. It was dried in an oven for 10 min at 80 °C and soaked in the APP solution for 2 min, then rinsed with water twice each for 1 min then dried for 10 min at 80 °C. This process for creating one bilayer was repeated 10 times in this study. A control sample which contained only APP layers was prepared by the same process except using Mill-Q water instead of a NH_2-MWCNT solution.

NH_2-MWCNTs (N) were coated using the same process as outlined above, but water was used to disperse NH_2-MWCNTs instead of DMF because of their high hydrophilicity. GO, O-MWCNT and CB coatings were applied to the fabric using the LBL method paired with positively charged polyacrylamide (PAM) [101]. A 0.5 wt% PAM solution and a 0.02 wt% GO (or 0.05 wt% CB) solution were prepared in 100 mL Mill-Q water. Polyester fabric (110 mm x 65 mm) was first dipped into the PAM solution for 10

seconds and rinsed with water for 10 seconds, then dipped into the GO solution for 30 seconds and rinsed with water for 10 seconds. This process was repeated 10 times.

For O-MWCNT coating, MWCNTs were first oxidized by a nitric acid treatment [102]. 100 mg of MWCNTs were added to 200 mL of 70 % HNO_3 (in a 500 mL round bottom flask) and sonicated in a Branson Sonicator (70W) for one hour. This mixture was then heated to 140 °C, under reflux, for 90 minutes. The mixture was allowed to cool and settle overnight. The excess acid was then siphoned off the top, leaving the oxidized MWCNTs collected in the bottom of the flask. The remaining MWCNTs were then rinsed with water and centrifuged for 5 cycles. The MWCNTs were then rinsed and centrifuged for 5 cycles with 4 M NaOH, and this was repeated with 4 M HCl. The CNTs were then rinsed and centrifuged with Milli-Q water until the resistance of the supernatant was above 0.5 MΩ cm. The CNTs were then dried on a clean glass slide, removed, ground, and stored for use. Then 5 mg of O-MWCNT was dispersed in 100 mL Mill-Q water by bath sonication for 30 min. The remainder of the coating procedure was the same as for the GO coating.

One commercialized coating product (Thermocyl™) was applied using manufacturer instructions for comparison. The main component is a silicone-based polymer solution with MWCNTs. This solution was mixed with a curing agent then applied to polyester (110 mm x 65 mm) using a paint brush. The coating was dried at room temperature overnight.

One sample with MWCNT was prepared by spray coating (HVLP Gravity Feed Air Spray Gun, Harbor Freight Tools) as a more commercially viable method that requires shorter time. The coating solution was produced by adding 10 mg of MWCNT

and 1 g of APP in 100 mL Mill-Q water and sonicating for 10 min. Sonication was reapplied as necessary as the dispersion of MWCNT was steady for short period of time. 2.5 mL of the solution was sprayed on the polyester fabric, then the fabric was dried at 80 °C for 30 min. This process was repeated one more time to obtain the desired mass loading of MWCNTs.

3.2.3 CNM mass loading

The mass of CNMs coated on the sample was determined by PTA with a commercial carbon analyzer from Sunset Laboratory, Inc. This technique quantifies the mass of elemental carbon by combusting sample in a furnace under controlled atmosphere and following a specific temperature protocol[67]. Organic solvents were used to dissolve polyester as pretreatment. The procedure was followed by the CNT quantification method on CNT-polymer composite as previously described in Chapter 2[103]. In brief, a small piece of each sample (0.5 cm x 0.5 cm) was dissolved in 5 mL hexafluoroisopropanol (HFIP) and 10 mL chloroform to eliminate polyester. The solid components that are mainly CNMs were collected on quartz fiber filter (QFF, 1 x 1.5 cm) by means of a metal syringe filter. The QFF was inserted to sample chamber and analyzed by PTA.

3.2.4 Flame retardancy test

Flame retardancy tests were conducted in a similar manner to NFPA705 [104] to evaluate the performance as FR while the sample is exposed to a flame. CNM coated polyester samples were cut to 12mm x 110 mm each, then hung by a metal stand. A wooden match was used as flame source and located right under the edge of sample. For the samples that do not ignite, the morphology of the region the flame reaches was

monitored. The flame was removed once the sample ignited and burning behavior was observed. The remaining length of each sample was measured and the time to burn out was recorded for the samples which supported combustion.

3.2.5 Scanning Electron Microscopy (SEM)

Surface morphology of polyester fabric with MWCNT+APP coating was observed by SEM. SEM samples were prepared by cutting the fabric coated with MWCNT+APP into 0.5 mm x 0.5 mm size and taped on a SEM stub. Another sample with the fabric without coating was also prepared as a reference. Both samples were analyzed by FEG XL30 ESEM (FEI company, Hillsboro, USA) with energy dispersive spectroscopy (EDS) system and surface images of each sample with elemental composition data at specific spots were obtained.

3.2.6 X-ray Photoelectron Spectroscopy (XPS)

XPS was conducted on CNMs to determine the oxygen content. XPS was performed using a PHI 5600 Kα X-ray (1253.6 eV, Physical Electronics, Chanhassen, USA). Prior to analysis, CNM samples were dried overnight in a desiccator. Approximately 1 mg of a given sample was pressed down onto a double-sided copper tape that was then affixed to a sample stub. Survey scans were collected to ensure sample purity and a quantitative analysis of the carbon (C(1s)) and oxygen (O(1s)) regions was completed with a pass energy of 58.7eV and a step size of 0.125eV. XPS data analysis was performed with CasaXPS (CasaXPS LTD, Teignmouth, UK).

3.2.7 Raman spectroscopy

To investigate the degree of defects of CNMs such as intrinsic vacancies and disorders caused by functionalization, Raman spectroscopy was conducted. Raman

spectroscopy was performed using custom built Raman spectrometer. The instrument was equipped with a 150 mW Coherent Sapphire SF laser with a 532 nm laser wavelength and the data were collected using an Acton 300i spectrograph and a back thinned Princeton Instruments liquid nitrogen cooled CCD detector.

3.3 Results and discussion

3.3.1 Mass loading

The mass loading of each CNM was quantified (Table 3.1) and later used to examine relationships against the flame retardancy. Mass loadings ranged from 0.14 to 0.35 g/m^2. Poor dispersion of the NH_2-MWCNT (C) coating solution due to its low polarity may have affected the mass loading to a lower value and possibly the uniformity of the coating.

Table 3.1 Flame retardancy (compared to polyester without coating and with APP coating), mass loading quantified by PTA and oxygen % of each coating material.

	Flame retardancy test			PTA	XPS
Coating material	Remaining length (%)	Time to burn out (s)	Classification	Coated mass (g/m^2)	Oxygen %
Polyester	47	-	III		
APP	76	-	II		
GO	0	12.8	IV	0.29±0.02	30
O-MWCNT	0	13.1	IV	0.24±0.01	7.8
Thermocyl™	0	53	IV	N/A	N/A
CB1	21	-	III	0.14±0.01	5.0
CB2	53	-	III	0.26±0.02	0.2
NH_2-MWCNT (N)	54	-	III	0.35±0.02	9.9
NH_2-MWCNT (C)	93	-	I	0.2±0.01	0.9
MWCNT (spray)	91	-	I	0.31±0.02	0

3.3.2 Flame retardancy tests

Figure 3.2 shows pictures of each sample when exposed to a flame. Samples are a) polyester without coating, b) APP coated, c) NH_2-MWCNT (N) coated, d) NH_2-MWCNT (C) coated, e) GO coated, f) O-MWCNT coated, g) CB1 coated, h) CB2 coated, i) Thermocyl™ and j) MWCNT. Using the non-coated fabric a) as benchmark, samples with b) APP, d) NH_2-MWCNT (C) and j) MWCNT showed distinctly improved flame retardancy, preventing the samples from ignition. On the other hand, samples with e) GO, f) O-MWCNT and i) Thermocyl™ performed worse with intensified flame and ultimately burned the fabric out.

NFPA705 acknowledges that a specimen to have "passed" the test when it is not burned out after 12 seconds of flame exposure. Samples that ignited under flame exposure, which was majority of samples tested here, ended up with burning out after 12 seconds, meaning they "failed". However, there were distinct differences among the "failed" samples. To describe the variations in efficacy caused by individual coated materials, a more nuanced classification scheme was proposed in this research rather than "pass/fail".

Here, flame retardancy is categorized into 4 different classifications (Figure 3.3). First category is "no ignition and drip" (I), this type of sample does not ignite and melt while it is exposed to the flame. NH_2-MWCNT (C) and MWCNT fall into this category. When the flame was introduced to the bottom of the sample, the edge of the sample got shrunk and turned to black. The sample remained the same once the edge turned black. This black product is presumably a mixture of char created by exposing flame source to polyester and concentrated CNT. The char and concentrated CNT help the sample not to

catch fire as both are thermally stable. This classification is equivalent to “pass” for NFPA705. Second is “no ignition with drip” (II), indicating the sample does not ignite but it melts and causes some drip. APP falls into this category and the APP coating sample showed consistent result with the flame retardant property of APP[105] described in the literature. The third is “ignition with self-extinguishing” (III), this type of sample ignites with some drip, but eventually the flame extinguishes by itself. Uncoated polyester, NH_2-MWCNT (N) and CBs are in this category. The fourth is “continuous burning” (IV). This type of sample burns thoroughly once it ignites. Samples in this category added negative effect on the polyester in terms of flame retardancy. O-MWCNT, GO and Thermocyl™ showed this tendency. Categories II, III and IV would all be classified as “fail” in NFPA705.

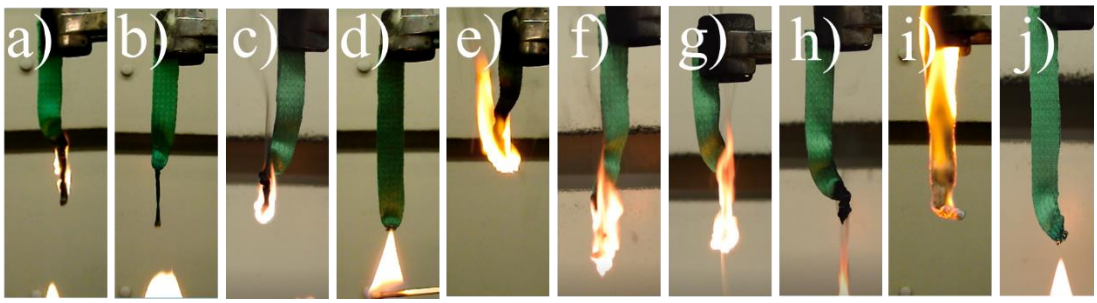

Figure 3.2 Images of burning test on a) polyester, b) APP coated, c) NH_2-MWCNT (N) coated, d) NH_2-MWCNT (C) coated, e) GO coated, f) O-MWCNT coated, g) CB1 coated, h) CB2 coated i) commercialized CNT product coated and j) MWCNT.

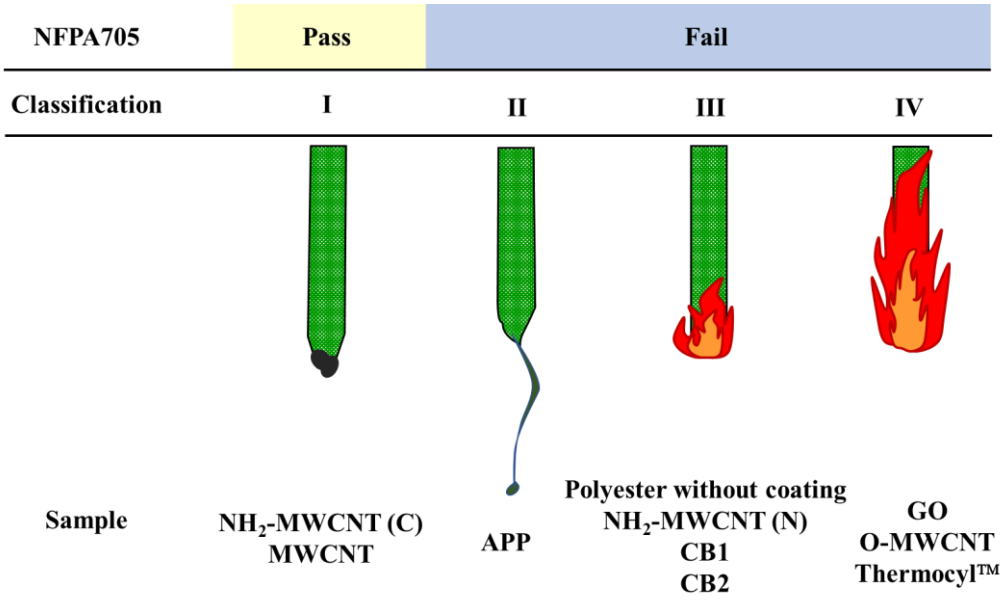

Figure 3.3 Visualized classifications of flame retardancy and samples fall into each category.

Table 3.1 includes the remaining, unburned, length of each sample after it is exposed to the flame, the time to burn out for samples that did not extinguish by itself and flame retardancy classification. Samples listed as classification I and II kept over 70 % of original sample length while the rest lost 50 % or more. Between 2 types of CBs, g) CB2 took longer time to extinguish the flame resulting in only 21 % of the sample length left. The sample with commercial coating product took longer time to burn completely compared to O-MWCNT and GO coating. This may be because its thicker coating, consisting of CNT and silicone, prolongs the time to complete burning by physically protecting the fabric until the coating was completely burned out.

3.3.3 Surface morphology

Figure 3.4 shows the SEM images of polyester fabric without coating and with MWCNT+APP coating. MWCNT+APP coating was chosen as an example of sample with high flame retardancy. Compared to the fabric itself (top left), clearly the fabric was covered by the coating extensively (top right). The existence of both APP and MWCNT were confirmed by EDS (bottom left and right). There are multiple factors that are considered to contribute to MWCNT's flame retardancy. First, MWCNT is known to have high thermal conductivity and high heat absorption coefficient [106]. Both properties improve the flame retardancy by delaying/inhibiting the heat reaching the fabric for continuous burning. High heat absorption lets MWCNT absorb the heat energy from the flame rapidly and the heat is distributed over the coated fabric due to high thermal conductivity. Another factor is char-forming ability, which is similar to APP itself as intumescence flame retardant. The surface of the polyester is induced to transform to char along with the coating itself turning into char, and the char layer acts as an insulation layer. The distinct difference between MWCNT and APP is APP's melting tendency, causing the quicker sample loss without ignition. Lastly, studies have shown that CNTs have a free radical scavenging effect [37]. Reactive free radicals such as hydroxyl radicals are one of the major driving forces for continuous burning, and quenching those radicals assists in delaying/disrupting flame extension.

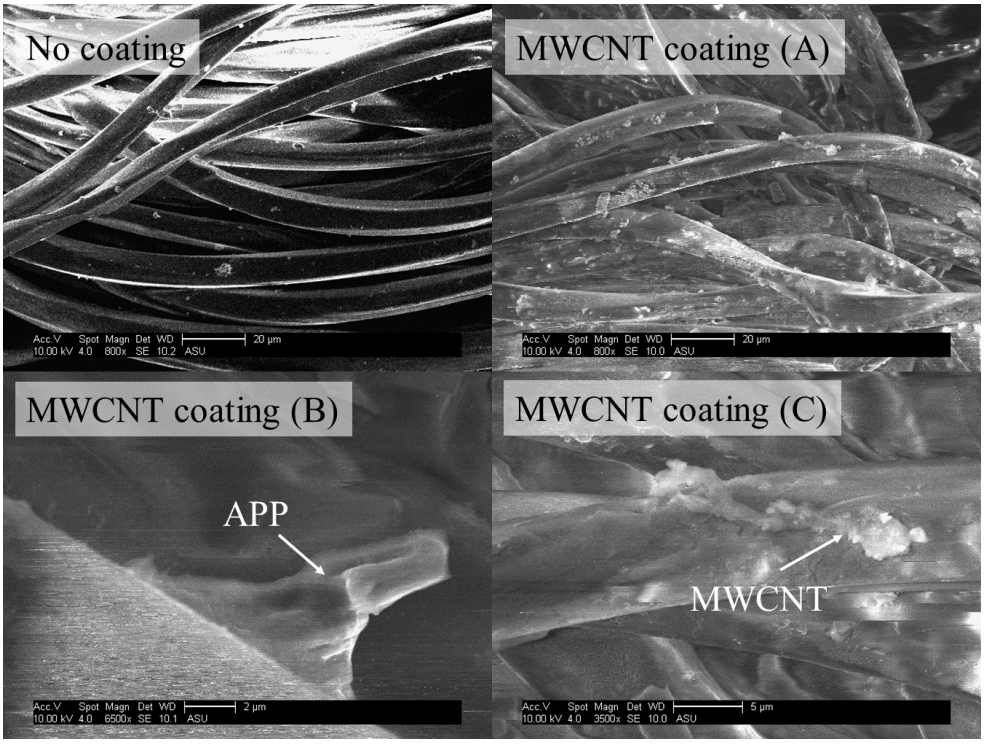

Figure 3.4 SEM images of polyester without coating (top left) and polyester with MWCNT+APP coating (low magnification (A), high magnification focused on APP (B) and high magnification focused on MWCNT (C))

3.3.4 Oxygen content

I hypothesize that samples with higher oxygen contents perform poorly as flame retardant since oxygen facilitates oxidation and hence combustion. Figure 3.5 shows the relationship between the oxygen contents of coating materials analyzed by XPS (original XPS spectra is shown in Appendix B) and the flame retardancy. The only two samples that showed classification I efficacy contained less than 1 % oxygen while other parameters like CNT diameter were comparable. Additional data supports the hypothesis, GO and O-MWCNT contain high oxygen contents, 30 % and 7.8 % respectively and those two burned intensely and the flame kept going until the entire sample turned to ash (classification IV). NH_2-MWCNT (N) contained more oxygen than NH_2-MWCNT (C),

this explains why NH_2-MWCNT (C) performed better during flame retardancy test. Moreover, the nitrogen contents of NH_2-MWCNT (C) and NH_2-MWCNT (N) analyzed by XPS were 0.3 % and 7.4 % respectively. This indicates that NH_2-MWCNT (C) had very few amine group attached and possibly NH_2-MWCNT (N) contained mainly amide group rather than amine group (higher O content). The same trend seems to apply to CBs as CB1 had higher oxygen content than CB2 and burned longer resulting in less remaining fabric (Table 3.1).

Further analysis of the data (Figure 3.5) suggests that the structure difference between CNMs and CBs could contribute to differences in flame retardancy as CB2 contains 0.2 % oxygen and still falls into classification III, despite the low content. Carbon black has an amorphous structure. It therefore can be hypothesized that that the higher thermal stability stems from CNM's crystalline structure led to the efficacy improvement than CB with amorphous structure.

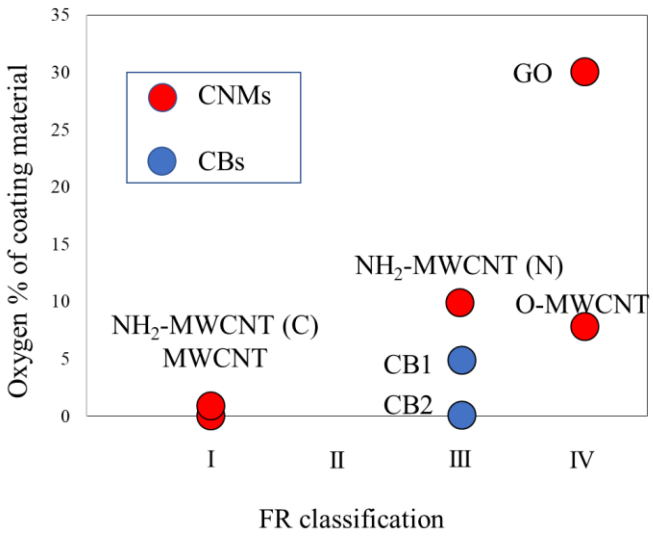

Figure 3.5 Flame retardancy classification vs. oxygen content. Red dots represent CNMs and blue dots are CBs.

3.3.5 Structural defects

The degree of structural defects on CNMs was shown to lower their thermal stability [67]. Raman spectroscopy was conducted to investigate the impact of defects on flame retardancy. Figure 3.6 shows Raman spectra of MWCNT, NH_2-MWCNT (C) and NH_2-MWCNT (N). Peaks observed at 1340 cm^{-1} and 1580 cm^{-1} correspond to D band and G band respectively. The intensity ratio of D band and G band (I_D/I_G) indicates the degree of structural defect as D band originates from the defects. The best performing MWCNTs, in flame retardancy classification I, showed significantly lower I_D/I_G values compared to the other two, implying fewer defects. However, NH_2-MWCNT (C) is also categorized as classification I although the I_D/I_G value was the highest out of 3 while NH_2-MWCNT (N) showed classification III efficacy. Therefore, it is concluded that the structural defect of CNMs is not the critical parameter for flame retardancy.

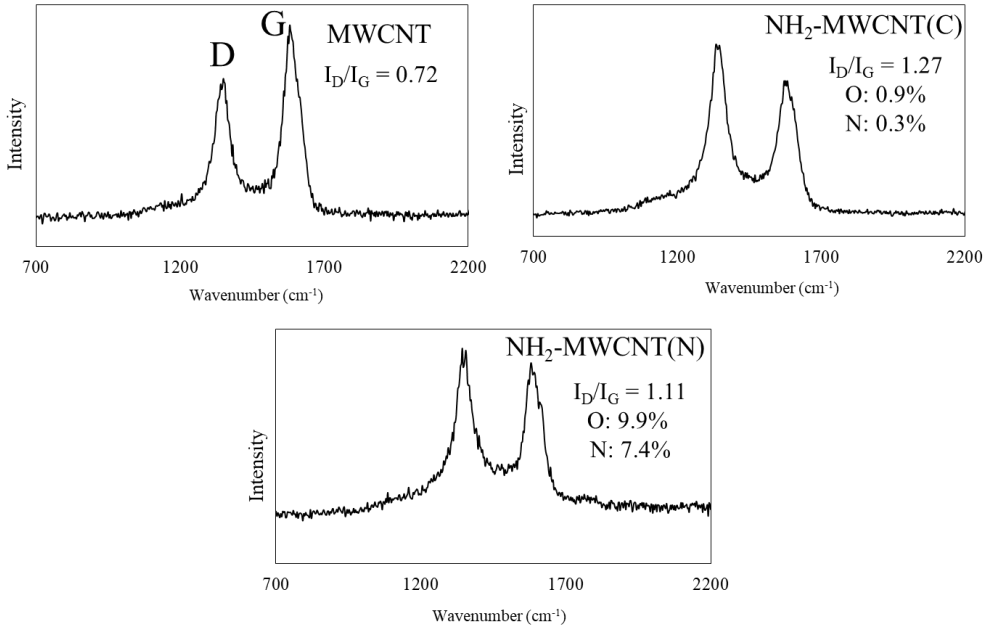

Figure 3.6 Raman spectra of MWCNT, NH_2-MWCNT (C), and NH_2-MWCNT (N) with the intensity ratio of D and G band (I_D/I_G)

3.3.6 Summary diagram for FRs

Figure 3.7 summarizes the information on 1) type of flame retardant coating, 2) mass loading, 3) oxygen content and 4) flame retardancy in one conceptual diagram. The best flame retardant materials are those that achieve high flame retardancy (higher along y axis) but at low mass loading (left along x axis). Traditional flame retardant materials, such as inorganic FR and halogenated FR, shown in orange in Figure 3.7 achieve high flame retardant characteristics but also require high mass loadings, especially the inorganic FRs. On the other hand, NH_2-MWCNT (C) and MWCNT achieve a same level of efficacy with 10 to 100 times smaller mass loading compared to traditional FRs. This suggests that these emerging nanomaterials are promising alternatives to existing FRs.

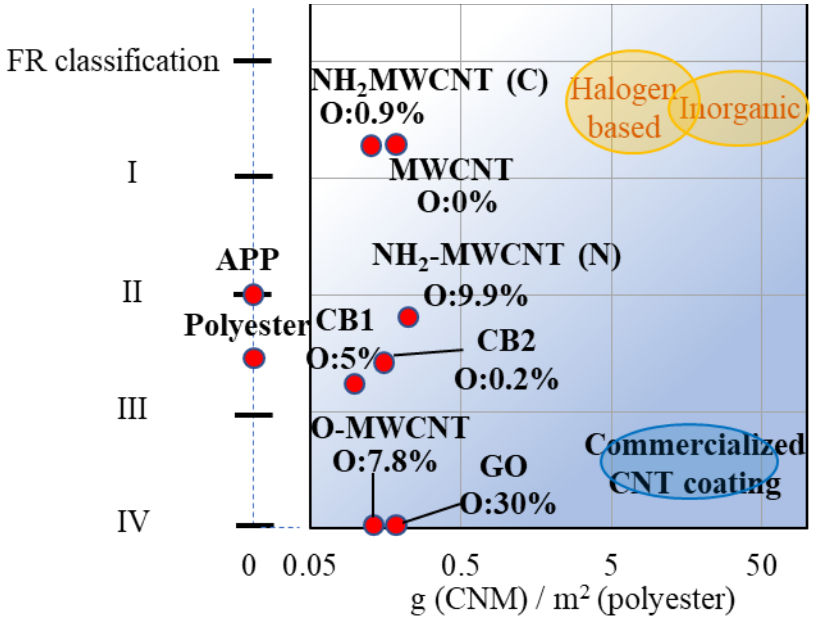

Figure 3.7 Summary diagram of CNM type, mass loading and flame retardancy

NH_2-MWCNT (N) showed lower efficacy compared to NH_2-MWCNT (C). The difference between NH_2-MWCNT (N) and NH_2-MWCNT (C) is a 10x higher oxygen

content in the former. The oxygen content of NH_2-MWCNT (N) determined by XPS was similar to that of O-MWCNT which showed poor flame retardancy. This indicates that the flame retardancy of APP was compromised by NH_2-MWCNT (N) hence the flame retardancy was found between APP coating and polyester without coating.

Rather than using a nanosized carbonaceous material, an alternative could be larger sized, widely available carbon black (CB). However, both CB1 and CB2 coating does not appear to provide any substantial added benefit in terms of flame retardant properties. The poor flame retardancy of CB1 coating is speculated to be resulting from the higher % oxygen. Considering the mass loading and % oxygen between CB1 and NH_2-MWCNT (C) are comparable, one can conclude that CNM's chemically stable crystal structure induces high flame retardancy. As discussed in Figure 3.5, it was found that the oxygen contents appeared to be the key for the efficacy as the only CNMs performed classification I efficacy was NH_2-MWCNT(C) and MWCNT which contained negligible oxygen contents. It has been reported that some functional groups such as carboxyl group attached to CNTs get decomposed at high temperature. This supports the hypothesis that the oxygen contained in CNMs as functional groups facilitates combustion when exposed to flame. This study suggests that CNMs with low oxygen contents could be a good alternative FR material requires smaller coating mass compared to traditional FRs.

3.4 Conclusions

CNMs were coated on polyester fabric using a layer-by-layer approach, paint coating and spray coating, and the resulting flame retardancy of these coatings was evaluated. CNMs containing minimal amounts of oxygen (< 1%) displayed a high flame retardancy (classification I), forming an agglomeration of char around the area where

exposed to the flame. In contrast, samples coated with oxygen rich CNMs such as GO and O-MWCNT resulted in sustained burning once they were ignited (classification IV). Oxygen content of CNMs emerged as a critical determinant for their efficacy as flame retardant. Potentially, oxygen supplied from CNMs facilitates the production of reactive radicals such as hydroxyl radical, driving and sustaining the burning processes. The nano-sized crystalline structure of CNMs was also found to improve the flame retardancy as CB did not display the same flame retardancy as NH_2-MWCNT(C) and MWCNT while their oxygen contents and the mass loading were comparable. Raman spectroscopy concluded that structural defects on CNMs were not critical parameter in regard to flame retardancy as NH_2-MWCNT(C) which contained the highest defects showed classification I while NH_2-MWCNT(N) with less defects performed classification III. Conventional FRs require typically 0.3-4 wt% for halogenated FRs and 20-60 wt% for inorganic FRs, the CNMs tested achieved similar flame retardant efficacy but at smaller material use (0.09-0.25 wt%). This study demonstrates the benefits of CNMs use as FR offering high flame retardancy at low mass loading. Future studies are addressing the durability of CNM coatings to evaluate their viability as replacements for conventional FRs.

CHAPTER 4

DEVELOPMENT OF CNT COATING ON FABRIC

4.1 Introduction

In Chapter 3, the promising potential of CNTs as flame retardants was demonstrated. A core challenge of the application is their dispersion in solution to allow for coating processes such as layer by layer approaches as used in Chapter 3. Dispersing CNTs in either aqueous or organic solution is known to be challenging [107]. Both chemical and physical CNT modification methods have been proposed to improve the dispersion behavior. Physical modifications include the addition of a surfactant which works by different mechanisms depending on the type of surfactant[108]. "Wrapping", for example, is one mechanism by which a linear polymer wraps around CNTs to eliminate the hydrophobic interface between the CNTs and the aqueous medium[109], which prevents CNTs from aggregating. Sodium dodecyl sulfate (SDS), Tween 20 and Triton-X are commonly used surfactants[110]. The most common chemical modification to facilitate dispersion are oxidations using strong, oxidizing acids such as nitric acid [45]. This treatment introduces polar functional groups such as −C=O, −COOH and −OH to the sidewall of CNTs[107] and increases the electrostatic repulsion between the CNTs[111, 112]. However, the significant finding in Chapter 3 was that oxygen content in CNMs might play a critical role in terms of the flame retardancy. In fact, CNMs with high amounts (several %) of oxygen may not provide any flame retardant benefit and might actually favor thermal decomposition by supplying oxygen. Both types of physical/chemical modification result in adding oxygen to CNTs and hence may counteract the flame

retardant properties, which are aimed for. Therefore, these approaches do not let themselves to flame retardant applications.

The results from the previous chapter suggest that functionalization of CNT to convey them a surface charge without introducing oxygen could be a viable approach. In fact, I have shown that a coating with amine functionalized nanotubes (NH_2-MWCNT) purchased from Cheap Tubes (NH_2-MWCNT(C)) had the potential as alternative FR material as it showed comparable FR efficacy to traditional FR at a lower mass loading. It is expected that the mechanism of CNTs as FR is the mixture of that of organophosphorus FRs and halogen based FRs. By contrast, the coating with the other NH_2-MWCNT product, purchased from NanoLab (NH_2-MWCNT(N)) Inc., appeared to show poor efficacy. Although both are claimed to be NH_2-MWCNT, there are differences in functional groups. NH_2-MWCNT(N) is a derivative of COOH functionalized MWCNT, therefore it contains amide group (-C(=O)-NH-) between MWCNT and the amine group on the edge (CNT-C(=O)-NH-CH_2-CH_2-NH_2)). XPS conducted on NH_2-MWCNT(N) confirmed 7.4% nitrogen and 9.9% oxygen. NH_2-MWCNT(C), on the other hand, contained only 0.3% nitrogen and 0.9% oxygen. This difference agrees with their dispersibility in water, NH_2-MWCNT(N) was easily dispersed with bath sonication while dispersing NH_2-MWCNT(C) was challenging as typically having polar functional groups improves the material's hydrophilicity[111, 113, 114]. Hence there is no commercially available chemically modified CNTs that can be easily dispersed in water and does not contain oxygen. Although there are "amine functionalized CNTs" available, they generally contain oxygen as part of functionalized group like NH_2-MWCNT(N) tested in Chapter 3.

The goal of this chapter is to obtain uniformly coated CNTs flame retardant on polyester without compromising its flame retardancy. Two approaches were pursued, amine functionalization on CNTs then coating by LBL method, and spray coating with short term dispersion using dimethylformamide (DMF) or ammonium polyphosphate (APP). The first approach that has been attempted, was functionalization with amine group to add hydrophilicity to CNTs. A few functionalizing approaches[16, 115, 116] including gas phase and liquid phase reactions were selected, and each outcome was discussed. Following the functionalization, the dispersibility was evaluated, then chemical characterizations such as FTIR were conducted. Lastly, the functionalized CNTs were coated on polyester by LBL method and the flame retardancy was tested. As alternative approach, short term CNTs dispersed solutions were developed using DMF and APP. These solutions were paired with spray coating to produce uniform coatings on the polyester. The flame retardancy of the coatings were evaluated the same way as the samples with functionalized CNTs.

4.2 Experimental and Analytical Methods

4.2.1 Materials

Both SWCNT (diameter ~1.5 nm, length 1-5 μm) and MWCNT (OD 15 ± 5 nm, length 5-20 μm) used in this study were purchased from NanoLab (Waltham, USA). Sodium nitrate, ethylenediamine, sulfuric acid, hexadecylamine and sodium dodecylsulfate were purchased from Sigma Aldrich (St. Louis, USA) and used for amine functionalization. Dimethylformamide (Fisher Scientific, Hampton, USA) was used for rinsing CNTs after functionalization and as a solvent for spray coating. Ammonium

polyphosphate (APP, Hangzhou JLS Flame Retardants Chemical Co., Ltd., Pomona, USA) was used in one of the bi-layers of LBL coating as well as in the solution for spray coating. Athletic polyester T-shirts were purchased from Asics (Kobe, Japan) and used as base fabric for coatings. Chloroform (Sigma Aldrich, St. Louis, USA) and hexafluoroisopropanol (HFIP, CovaChem, Loves Park, USA) were used to dissolve polyester samples as a part of sample preparation for thermal analysis.

4.2.2 Amine functionalization

Three amine functionalization methods were tested in this Chapter based on published work. [16, 115, 116] The common concept of the reactions is to attach a polar amine group on the surface of the CNTs to improve their dispersion in water.

Reaction 1[115]

In a first reaction scheme (Figure 4.1), ethylenediamine was used as reactant for functionalization. SWCNTs (70 mg) were mixed with $NaNO_2$ (93 mg) and ethylenediamine (85 mg) in a 100 ml round bottom flask, then sulfuric acid (0.061 ml) was added to the flask and the mixture was heated at 60 °C for 1 hour. After it was cooled to room temperature, DMF was added and centrifuged to remove unreacted reagents. The washing process was repeated a few times and Milli-Q water was used at the end.

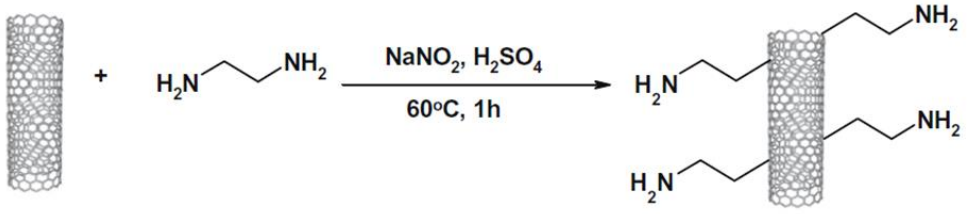

Figure 4.1 Scheme of reaction 1, referenced from the article[115]

Reaction 2[116]

In the second approach, SWCNTs were functionalized with hexadecylamine at high temperature. SWCNTs (200 mg) were mixed with 1 g hexadecylamine (HDA) in a 100 ml round bottom flask and heated at 180 °C for 15 hours. The sample was washed with ethanol to remove any excess HDA and the solid component was collected by filtration through a nylon membrane. The collected sample was dried at 110 °C overnight.

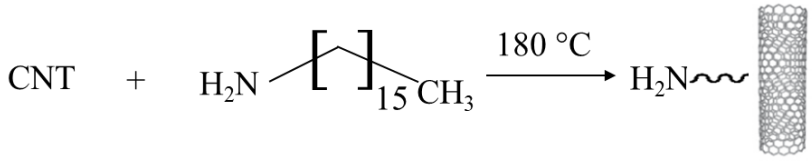

Figure 4.2 Scheme of reaction 2.

Reaction 3A[16]*-C*

In the third approach, MWCNTs were dispersed with a surfactant before being reacted with hydrazine (Figure 4.3). 5 mg of MWCNT was dispersed in 10 mL Milli-Q water with 72 mg sodium dodecylsulfate (SDS) in a glass vial by bath sonication for 1 hour at room temperature. 1.5 mL of hydrazine hydrate (50 % in water) was added to the vial and the mixture was stirred for 48 hours at room temperature. As an alternative trial (reaction 3B), the same procedure was conducted at 80 °C for 6 hours. The solution was diluted with DMF and filtered through PTFE membrane filter. The filtered MWCNTs were rinsed with ethanol and Milli-Q water twice each.

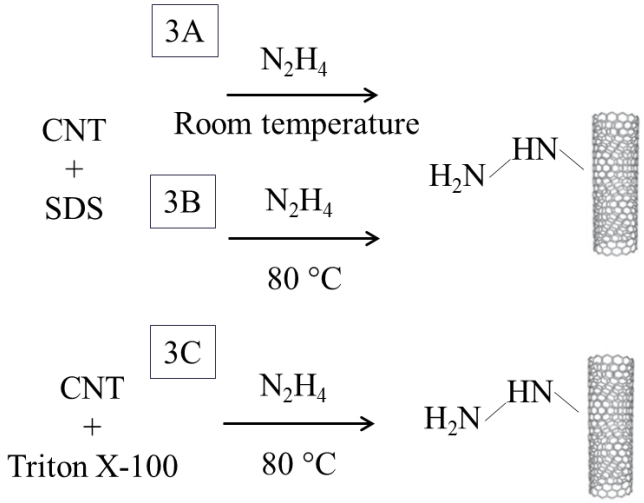

Figure 4.3 Scheme of reaction 3.

In a similar manner, Triton X-100 was used as a surfactant in place of SDS (reaction 3C). 1 mg of MWCNT and 0.1 g of Triton X-100 were added to 10 mL Milli-Q water in a glass vial, then the solution was pre-dispersed by sonication for 3 hours. 1.5 mL of hydrazine hydrate was added to the vial and heated at 80 °C with magnetic stirring for 6 hours. The solution was allowed to cool and undergone ultrafiltration with 50 mL Amicon Ultra-15 Centrifugal Filter (10 K NMWL, MilliporeSigma, Darmstadt, Germany). 10 mL of NH_2-MWCNT and 5 mL of Milli-Q water were added to an ultrafiltration filter unit and it was centrifuged at 3408 x g for 5 min. The solution passed through the filter was removed, then another 5 mL of Milli-Q water was added to the top of the filter unit for 2nd round of centrifugation at the same rate. This filtration process was repeated 5 times.

4.2.3 Coating

LBL coating

Amine-functionalized MWCNT (NH_2-MWCNT) processed by method 3 described above was coated by LBL coating method. NH_2-MWCNT was applied by pairing negatively charged polymer layers since NH_2-MWCNT is charged positively [96]. 1 wt% of APP solution was prepared by adding 1 g of APP into 100 mL Mill-Q water (≥18.2 MΩ-cm). The pH of APP solution was adjusted to 10 by adding NaOH and HCl solution. Polyester fabric (110 mm x 65 mm) was immersed into NH_2-MWCNT solution for 10 min, then rinsed with water twice each for 1 min. It was dried in an oven for 10 min at 80 °C and soaked in APP solution for 2 min, then rinsed with water twice each for 1 min then dried for 10 min at 80 °C. This process for creating one bilayer was repeated 10 times in this study.

Spray coating

For spray coating, the dispersion needs to be stable for only a short amount of time (approximately 3 min) as each spray process can be done quickly. Two types of MWCNTs solution were prepared for the spray coating using APP and DMF. Those were chosen because both were capable of dispersing MWCNTs in a short term readily by bath sonication, and APP was proven to improve the flame retardancy in a previous study and DMF could be removed by evaporation at the boiling point. The first solution (APP-MWCNT) was prepared by mixing 1 mg of MWCNTs and 100 mg of APP in 10 mL Milli-Q water, then sonicated for 20 min. The latter (DMF-MWCNT) was prepared by adding 1 mg of MWCNT in 10 mL DMF and sonicating for 20 min. Sonication was reapplied as needed as both solutions are stable only for limited amount of time (up to 30

min). An air spray gun (Central Pneumatic®) was used for spray coating. 2.5 mL of MWCNT solution was spray coated on polyester (1.2 cmx 10.8 cm) then dried in the oven at 100°C for 10 min. This process was repeated one more time to achieve desired amount of coating (0.2 - 0.3 g/m^2). After the coating was completed, the sample was dried in the oven overnight at 100°C for APP-MWCNT and 154°C for DMF-MWCNT. Additionally, a set of APP-MWCNT samples with different mass loading controlled by total sprayed volume (2mL ~ 7mL) was prepared to investigate the minimal mass loading of MWCNTs to obtain the desired efficacy.

4.2.4 Characterization

FTIR

To evaluate the outcome of the amine functionalization on MWCNTs, FTIR was conducted using a Bruker IFS66V/S (diamond ATR, Bruker, Billerica, USA). A sample with the same concentration of Triton X-100 and hydrazine as functionalized MWCNTs was prepared to obtain the background signals. A few drops of sample were deposited on a liquid sample cell for each measurement.

Flame retardancy test

Flame retardancy tests were conducted in a similar manner to NFPA705 to evaluate the performance as FR while the sample is exposed to flame. CNMs coated polyester samples were cut to 12mm x 110 mm each, then hung by a metal stand. A wooden match was used as flame source and located right under the edge of sample for 10 seconds. For the samples that do not ignite, morphology of the region the flame reaches were monitored. The flame was removed once the sample ignited and burning

behavior was observed. The remaining length of each sample was measured and the time to burn out was recorded for the samples supported combustion.

MWCNT mass loading

To evaluate the MWCNTs mass loading on fabric, programmed thermal analysis (PTA) was conducted. Triplicate samples (0.66 cm^2) were cut out from spray coated MWCNTs dispersed in water with APP. Each piece was dissolved in a mixture of 5 mL HFIP and 10 mL chloroform in a beaker for 5 min. The solid component in the solution was collected by glass syringe filtration on quartz fiber filter (QFF, 1 x 1.5 cm, WhatmanTMQM-A, Fisher Scientific, Hampton, USA). The filter was loaded into the PTA instrument and the temperature program established in Chapter 2 was used.

4.3 Results and discussion

4.3.1 Improvement of dispersion by amine functionalization

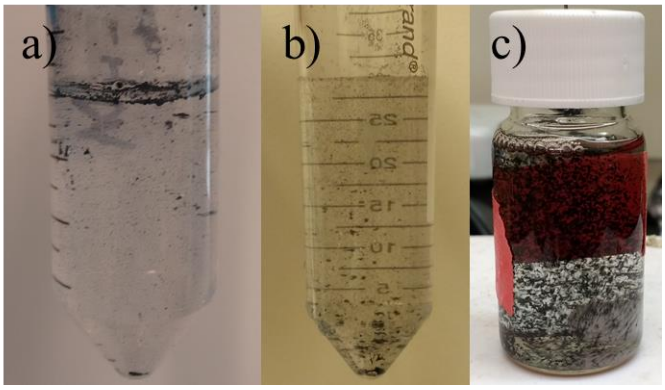

Figure 4.4 Images of CNTs resuspended in water after functionalization method 1 (a, gas phase reaction with $NaNO_2$ and ethylenediamine), 2 (b, gas phase reaction with HDA), and 3B with SDS (c, liquid phase reaction with hydrazine hydrate).

As shown in Figure 4.4, the CNTs processed by functionalization methods 1 and 2 did not improve the dispersibility of SWCNTs in water. Likewise, the MWCNTs sample with SDS by method 3B showed poor dispersibility. These results led us to the conclusion that methods 1, 2 and 3B were not successful in improving the CNTs dispersibility. These approaches were not further pursued and the products were not further characterized.

The pictures of MWCNTs prepared by method 3C are shown in Figure 4.5. MWCNTs before (a) and after (b) the thermal treatment with Triton X-100 were compared. Three vials in the images are “MWCNT only”, “MWCNT + Triton X-100 + hydrazine” and “MWCNT + Triton X” from the left. Prior to the thermal treatment, all vials were sonicated with bath sonicator for 3 hours. The vial without Triton X-100 (left in the image) kept all MWCNTs precipitated on the bottom of the vial as aggregation, showing MWCNT’s strong hydrophobicity. Both vials contain Triton X-100 (middle and right in the image) appeared to be darker, which indicates the MWCNTs dispersion. However, letting them stand for 9 hours after the thermal treatment broke the dispersion of the sample without hydrazine while the dispersion of the sample with hydrazine was retained. This proved that the functionalizing reaction 3B successfully improved the dispersity of MWCNTs.

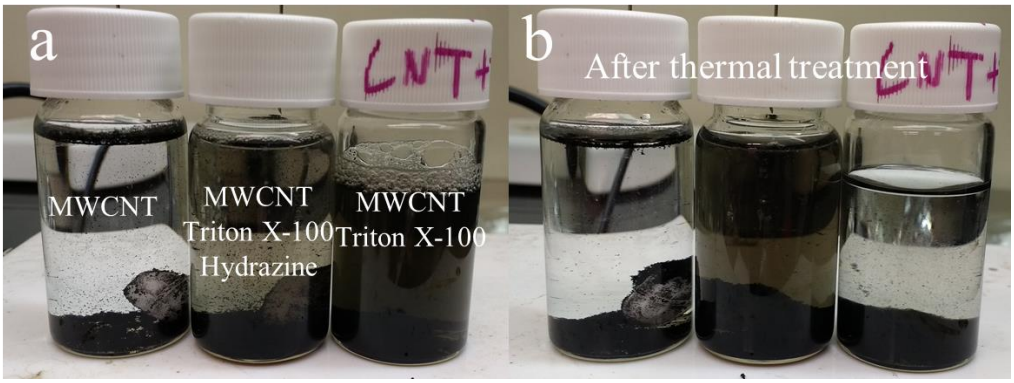

Figure 4.5 Images of MWCNT + 1 % Triton X-100 solution with 3 hours sonication (a) before and (b) 9 hours after thermal treatment with hydrazine at 80 °C for 2 hours. In each image, MWCNT only (left), MWCNT with Triton X-100 and hydrazine (middle), MWCNT with Triton X-100 (right).

FTIR

Subsequently, the sample with hydrazine after the thermal treatment was characterized with liquid FTIR to verify that indeed the amine functionalization was successful. Figure 4.6 shows the FTIR results of samples contain "Triton X-100 and hydrazine" and "Triton X-100, hydrazine and MWCNT" after thermal treatment. The signal of Triton X-100 was subtracted from both spectra. It was confirmed that some unreacted hydrazine remained in the samples as the peak at 3263 cm^{-1} which is unique to the N-H group appeared on both spectrums. Considering the pristine MWCNTs do not show any FTIR signal, any variance would be regarded as the outcome of the thermal treatment with hydrazine. There are three small peaks on the spectrum (b) distinct from the spectrum (a) around 1568 cm^{-1}, 1442 cm^{-1} and 1261 cm^{-1}. Two peaks at 1568 cm^{-1} and 1442 cm^{-1} and 1261 cm^{-1} peak are believed to be N-H bond and C-N bond

respectively, indicating the attachment of nitrogen to MWCNTs. One can conclude that these new bonds created by the thermal treatment contributed to the improvement of dispersion by introducing hydrophilic amine groups.

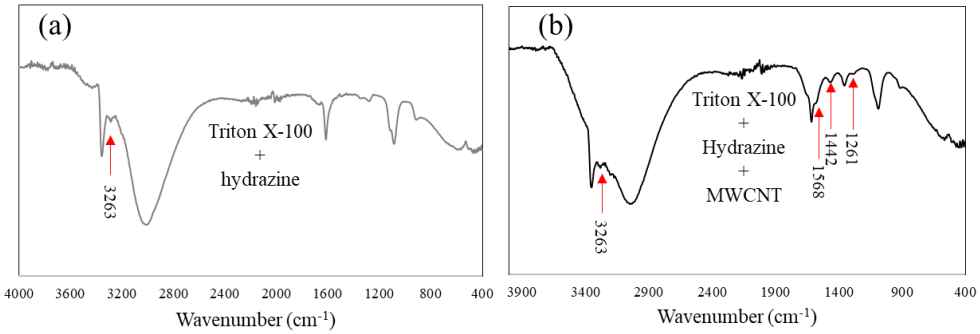

Figure 4.6 FTIR spectrums of the sample with (a) Triton X-100 + hydrazine and (b) Triton X-100 + hydrazine + MWCNT after the thermal treatment.

Flame retardancy

Following the improvement of the dispersibility by functionalization, the functionalized MWCNTs were coated on polyester fabric and the resulting flame retardancy was evaluated. Flame retardancy is categorized into 4 different classifications previously in this research (Chapter 3). First category is “no ignition and drip” (I), this type of sample does not ignite and melt while it is exposed to the flame. CNTs without any functional groups are categorized in this classification. Second is “no ignition with drip” (II), indicating the sample does not ignite but it melts to cause some drip. The third is “ignition with self-extinguishing” (III), this type of sample ignites with some drip, but eventually the flame extinguishes by itself. Uncoated polyester falls into this category. The fourth is “continuous burning” (IV). This type of sample burns thoroughly once it ignites. Samples in this category added negative effect on the polyester in terms of flame

retardancy. Oxygen rich materials like O-MWCNT and graphene oxide have such tendency.

The solution was presumed to negatively impact the flame retardancy because the solution contained Triton X-100. Although Triton X-100 is not particularly flammable, one can assume it may contribute to continuous combustion due to its high oxygen content. In Figure 4.7, the image of the flame retardancy test on the fabric coated with NH_2-MWCNT produced. Signature images of each flame retardancy classification from Chapter 3 were also shown as references. As expected, the coating showed poor flame retardancy, comparable to polyester without coating (III in Figure 4.7) or slightly worse considering the remained length of the fabric. This is the similar case to NH_2-MWCNT (N) purchased from NanoLab, Inc. in Chapter 3, which was also categorized as classification III, that the flame retardancy of MWCNT was compromised due to the oxygen contained in the coating material/solution.

To diminish the negative effect of Triton X-100, ultracentrifugation was conducted. This process removed majority of Triton X-100 and unreacted hydrazine. However, the flame retardancy appeared to be the same as the sample with MWCNT solution without ultracentrifugation (Figure 4.8). This indicates that the remaining Triton X-100 was not completely removed from the solution, and the fact that repeating the ultracentrifugation process eventually started breaking the dispersion resulting in us concluding that this method is not be the appropriate approach for MWCNT flame retardant coating.

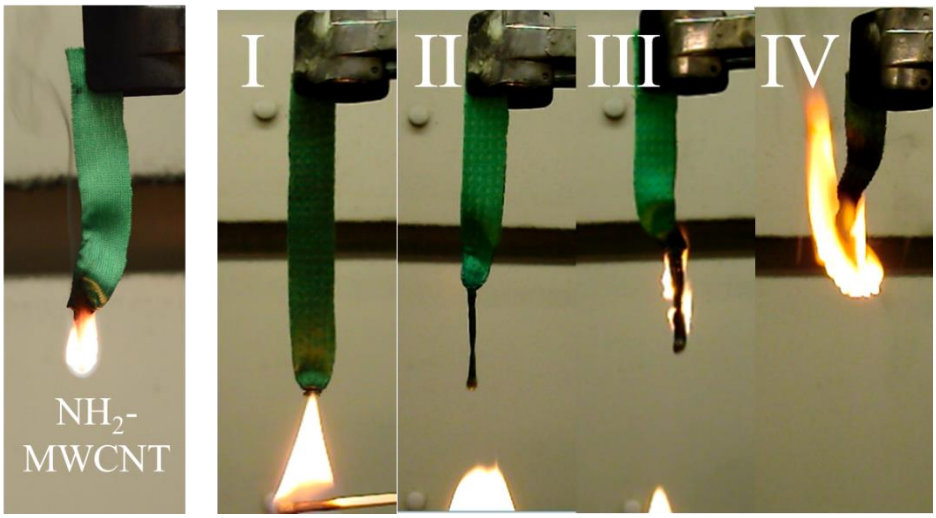

Figure 4.7 Image of efficacy test on NH_2-MWCNT coating with reference images of each flame retardancy classification I-IV.

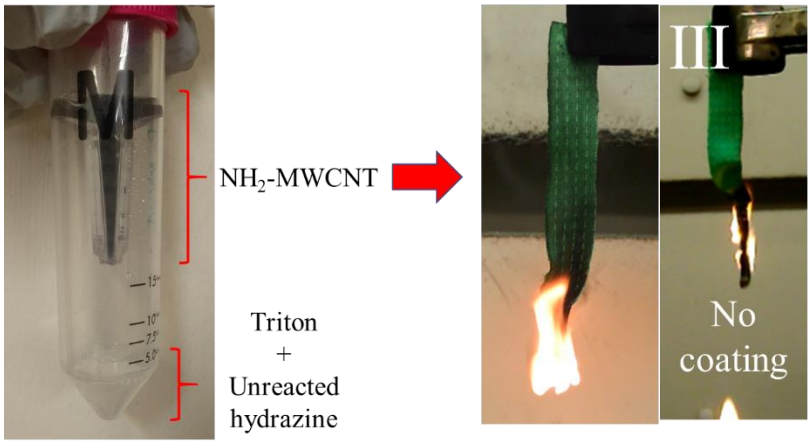

Figure 4.8 Images of NH_2-MWCNT after ultracentrifugation and the flame retardancy test applied on polyester fabric with a reference sample (fabric without coating).

4.3.2 Spray coating

Dispersion in DMF

Dimethylformamide allowed for the dispersion of raw MWCNT from NanoLab (Figure 4.9) and the dispersions remained stable for over 24 hours, while the same

MWCNT in water was poorly dispersed. Two samples were prepared by spray coating with MWCNTs in DMF at different drying temperatures, room temperature and 154 °C which is the boiling point of DMF. The sample dried at room temperature was anticipated to show poor flame retardancy as DMF is considered as flammable liquid and contains oxygen. As predicted, the sample continuously burned once it ignited and burned out completely. This is categorized as classification IV, the same as samples coated with high oxygen content materials in Chapter 3. In contrast, the sample dried at 154 °C demonstrated classification I flame retardancy which represents no ignition with melting the area where exposed to the flame source. Hence, it was confirmed that the drying process at 154 °C successfully evaporated the DMF.

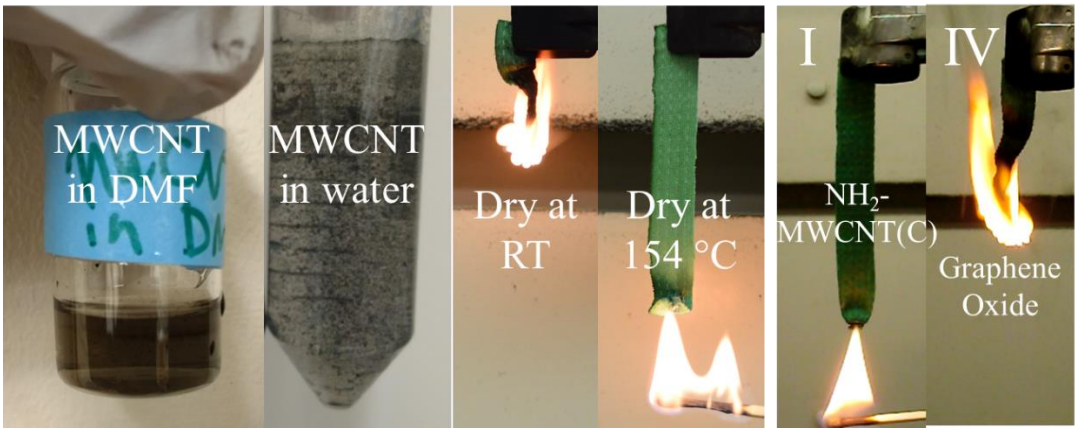

Figure 4.9 Images of MWCNT dispersed in DMF and water after 3 bath sonication and the flame retardancy test on the coating with MWCNT in DMF dried at room temperature and 154 °C after spray coating with reference images of NH_2-MWCNT (C) from Cheap Tubes (classification I) and graphene oxide (classification IV).

Dispersed in APP

MWCNT was successfully dispersed in water with APP after bath sonication (Figure 4.10). In comparison with MWCNTs dispersed in DMF, however, the dispersion duration was shorter, requiring bath sonication before each spraying process. As shown in Figure 4.10, the flame retardancy of this coating was categorized as classification I, indicating the sample did not ignite nor melt while the flame source was reached to the edge of the sample. The MWCNT mass loading was determined to be 0.31 g/m^2 by PTA. The surface concentration is comparable to the values observed in Chapter 3.

Both samples spray coated with MWCNTs in DMF and water with APP showed high efficacy (classification I) as flame retardant. This study suggests that this MWCNTs spray coating method using DMF or APP could be a practical technique for MWCNTs flame retardant coating application on fabric. With the limitation MWCNTs in DMF requiring high drying temperature at 154 °C, the solution using APP may be considered as more appropriate method.

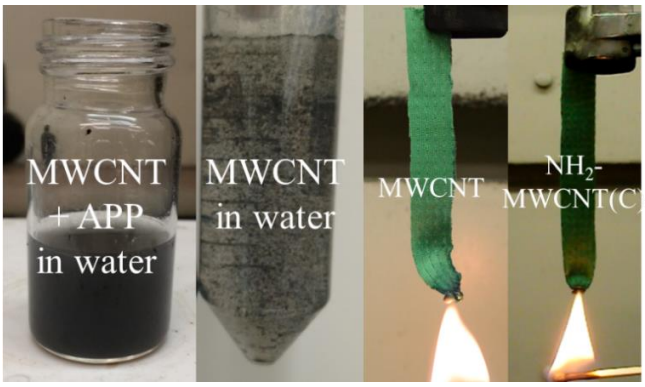

Figure 4.10 Images of MWCNTs dispersed with and without APP in water and the flame retardancy test on the sample spray coated on polyester fabric with reference image of NH_2-MWCNT(C) coating as classification I.

Finally, the minimal mass loading of MWCNT required to show the classification I efficacy (and passing NFPA705 test) was investigated by testing the flame retardancy and the mass loading of samples coated with different surface concentration. The flame retardancy of five samples contain various surface concentration (0.067 g/m^2 ~ 0.18 g/m^2) were tested (Figure 4.11). The highest mass loading sample (0.18 g/m^2) showed the classification I efficacy while the rest appeared to be classification III with ignition. The scale of ignited flame got smaller as the mass loading increased (right to left in Figure 4.11), indicating the improvement of efficacy caused by MWCNT added. As seen in Figure 4.11, there is a fine line between the sample performed as classification I and III, especially the sample with 0.16 g/m^2 only got minimal ignition. Therefore, it can be concluded that the minimal mass loading required to perform classification I efficacy is 0.18 g/m^2.

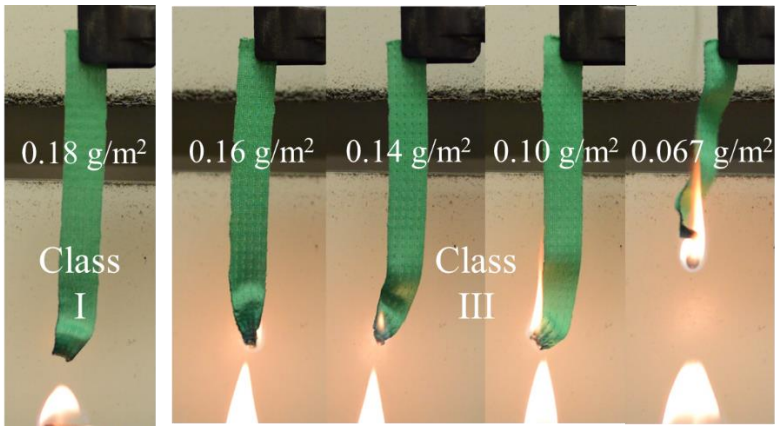

Figure 4.11 Flame retardancy test results on samples coated with MWCNT-APP with different surface concentration

4.4 Summary and Conclusions

Amine functionalization of CNTs was attempted by 3 reaction pathways to attach polar functional groups to the surface of CNTs. A synthesis (Route 3B) using hydrazine

and the surfactant Triton X-100 successfully improved the dispersity of MWCNTs and stabilized the dispersion for over 24 hours. However, the required surfactant (Triton X-100) could not be completely eliminated after different clean-up steps and its residual negated the flame retardant properties of the CNTs.

Alternatively, two types of short-term dispersions of MWCNT were obtained by bath sonication, one in solution in DMF and a second one in a water/APP solution. The short-term dispersions proved to be of sufficient persistence to allow for spray coating of fabric. The resulting coating of the MWCNT in DMF showed the desired efficacy (classification I) when the sample was dried at high temperature (154 °C). The MWCNTs applied by spray-coating of the water/APP solution achieved the same performance. Requiring high drying temperatures may be an issue with certain applications as textiles are typically not thermally stable. Therefore, the dispersion using APP would be a more accessible method although both coatings showed the desired efficacy. It was found that the minimal mass loading of MWCNTs required to show classification I efficacy was 0.18 g/m^2. Considering that the mass loading of halogen based FR that is one of the most efficient traditional FRs is 0.42 g/m^2 ~ 56 g/m^2, the combination of this coating solution and spray coating is a promising method for an alternative FR coating.

CHAPTER 5

RELEASE OF MWCNTS DURING USE PHASE OF FABRIC: IMPACT ON MWCNT EXPOSURE POTENTIAL AND FLAME RETARDANT EFFICACY

5.1 Introduction

In Chapter 3, I demonstrated that select CNM materials such as MWCNTs and NH_2-MWCNTs can act as efficient flame retardants, showing comparable efficacy to classical flame retardant materials at an approximately 10 times lower mass loading. In Chapter 4, I showed that spray coating of MWCNTs with APP allows for obtaining highly efficient flame retardant coatings with a process that has commercial application potential.

Investigating the release of the MWCNTs as well as testing changes in efficacy during the use phase of the material is critical for practical application. Especially, inspecting the coating on fabric material is crucial as common applications of FR coating are upholstery and clothing that have high probability of physical abrasion and contact with water during usage. Former wide use FRs have resulted in exposure and toxicity concern either by the chemical itself or by its degradation products[6, 7], therefore it is crucial to evaluate any potential replacement FRs in terms of potential toxicity and the exposure. In fact, a common FR family aimed at replacing halogenated FRs, the organophosphorus compounds, have poor durability resulting in FR release to the air and the potential to be washed off readily[26, 27].

Nanomaterials are increasingly used in coatings including silver nanoparticles[117, 118], titanium dioxide nanoparticles[119] and CNTs[48], and investigating their potential release is critical to assess in particular as the hazard and resulting environmental risk, impact

and toxicity are not well understood. Silver nanoparticles, for example, have been applied to consumer products due to their antibacterial properties[117, 118]. Some studies were focused on the release and effects on the efficacy of silver nanoparticles contained in fabric during use phase[120, 121]. However, besides the nanoparticle release estimated by a modeling study[122], there is not enough data on potential CNTs release from textiles during use phase such as mechanical abrasion on draperies and leaching from clothing. A major limitation to any exposure and release studies is the lack of suitable techniques to quantify CNTs in low concentrations in a variety of complex matrices. In Chapter 2, an extended technique of CNTs quantification with Programmed Thermal Analysis (PTA) was developed specifically for polymer-CNT samples[103], which allows the CNTs released from the textile samples to be monitored. This Chapter is focused on understanding the efficacy and the potential exposure of CNM FR material coated on fabric during use phase. The mass of CNM coating was monitored as well as the flame retardancy and the relationship between was assessed. This leads to a better understanding of CNM surface concentration required to perform as FR and the durability of the coatings.

First, the mass loading of MWCNTs coated on fabric was quantified by PTA. Samples were prepared by following spray coating method developed in Chapter 4. This provided a quantification of initial mass loading. Second, the release of CNM during use phase was monitored by simulating friction following ASTM standard [123] by abraser along with leaching test simulating laundry wash.

5.2 Experimental and Analytical Methods

5.2.1 Sample preparation

Samples for both mechanical abrasion and wash test were prepared by a spray coating method using a spray gun (HVLP Gravity Feed Air Spray Gun, Harbor Freight Tools). Polyester fabric (athletic shirt, Asics (Kobe, Japan)) was cut into circular (13 cm diameter) or rectangular pieces (4.8 cm x 11 cm) for mechanical abrasion and wash test respectively. The spray coating solution was prepared by adding 10 mg of MWCNTs (NanoLab (Waltham, USA)) and 1 g of APP (Hangzhou JLS Flame Retardants Chemical Co., Ltd., Pomona, USA) in 100 mL Milli-Q water under 10 min bath sonication. 10 mL of this solution was then spray coated to the circle-shaped fabric uniformly, then the fabric sample was dried at 80 °C for 30 min. A small part of the fabric (2 cm from the edge) was covered during the spray coating as the outer region was used to hold the sample down for abrasion test. This process was repeated 5 times to achieve desired mass loadings. The targeted mass loading was around 0.2-0.3 g/m^2 as the efficacy was achieved in the range in Chapter 3. For wash test samples, the same process was done to the rectangular fabrics with 4 ml of MWCNT-APP solution.

5.2.2 Mechanical abrasion

A taber abraser (Taber Industries, North Tonawanda, USA) was used for mechanical abrasion tests on polyester fabric samples coated with MWCNT-APP. The operating conditions were set up based on "AS 2001.2.28—1992"[123]. In brief, a round shape sample was mounted on the abraser and 2 sets of 250 g loadings and rubber wheels (CS-0) were set (Figure 5.1). The abrasion test was conducted for 500 rotations with 72

rpm. This test condition was chosen as it was found the polyester fabric started to be worn at heavier loading than 250 g, or more than 500 rotations during preliminary test.

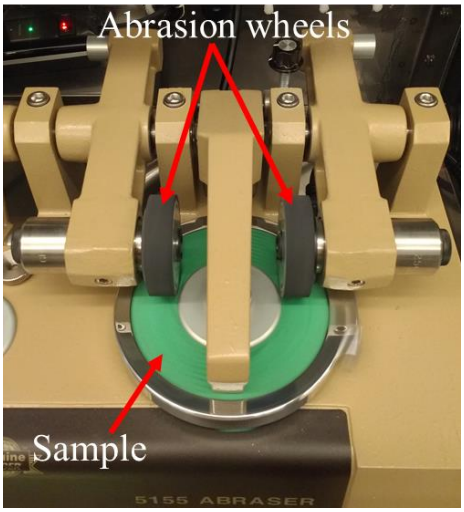

Figure 5.1 Mechanical abrasion setup, two rubber abrasion wheels are set on the polyester fabric sample with MWCNT-APP coating.

Triplicate pieces (0.66 cm^2) of both abraded (yellow colored) and not abraded area (orange colored) were cut out as PTA sample to monitor the amount of MWCNTs lost after the abrasion (Figure 5.2). To account for potential non-uniformity of the coating, triplicate pieces were taken from different areas for both, the abraded and the non abraded area. For the flame retardancy efficacy test, both abraded and non-abraded area were cut out after PTA samples were prepared (Figure 5.3).

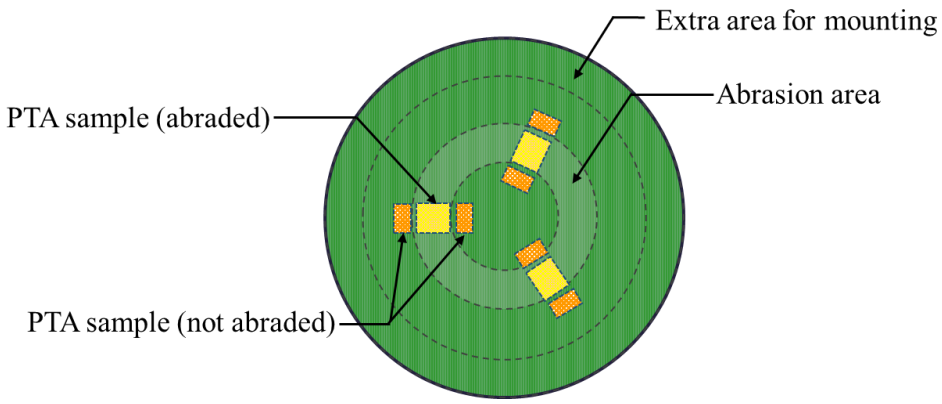

Figure 5.2 Sample for PTA after mechanical abrasion, triplicate samples for both abraded (yellow) and not abraded area (orange) at different spots.

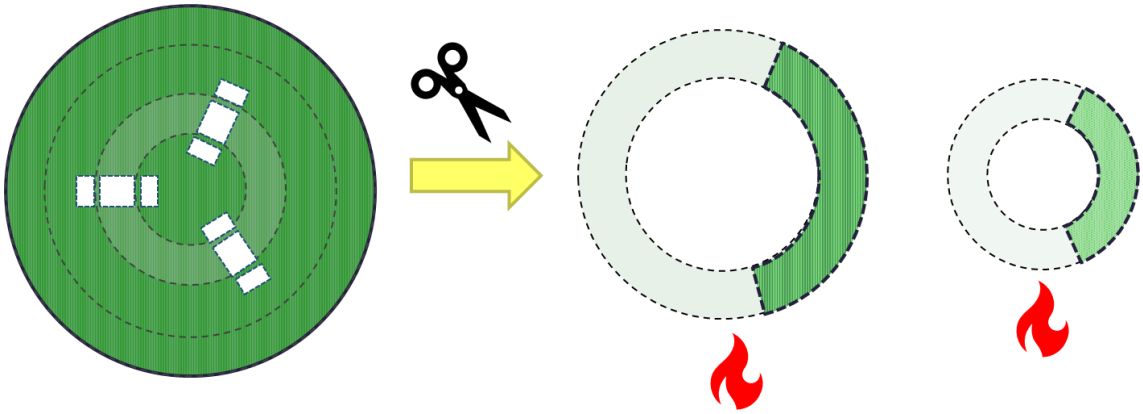

Figure 5.3. Flame retardant efficacy test samples after mechanical abrasion, non-abraded area (middle) and abraded area (right).

5.2.3 Wash test

The rectangular samples prepared by spray coating were cut to 4 pieces (Figure 5.4). Each piece went through 0, 1, 5 and 10 washing cycles. The washing process was conducted following a protocol used for silver nanoparticle release from fabric[120]. In brief, each sample was immersed in a plastic vial with 50 mL DI water and 5 glass beads (8 mm). The vial was placed in a rotating mixer and mixed at 40 rpm for 30 min. The sample was removed from the vial and immersed into another vial with DI water and glass beads for the next washing cycle. Once the washing process was completed, samples were dried at room temperature for 24 hours. All DI water used during the washing cycle was collected, pooled and subject to PTA analysis, like the corresponding fabric samples.

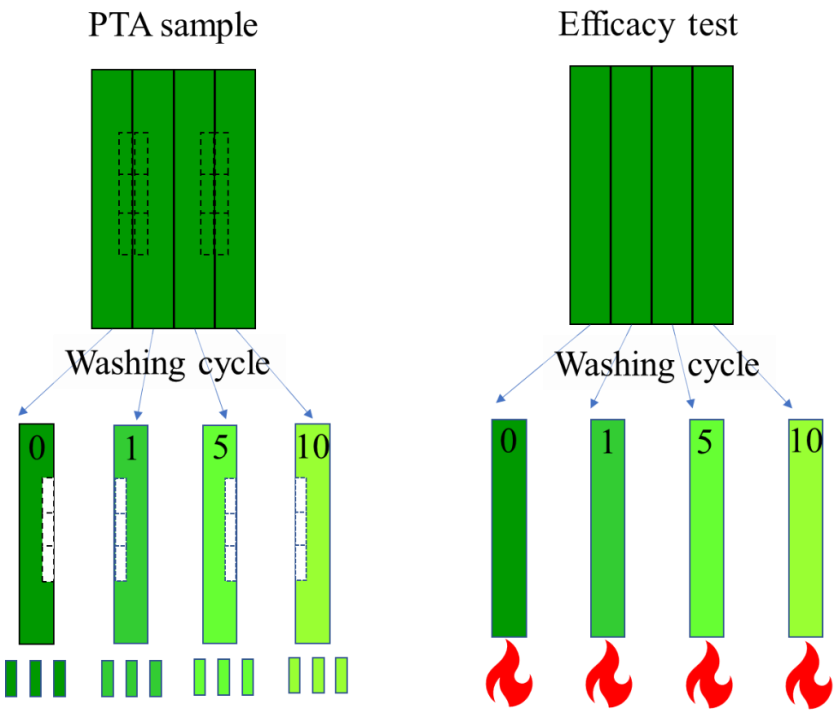

Figure 5.4 Samples for PTA (left, triplicate for each sample) and efficacy test (right) after wash test.

5.2.4 Programmed Thermal Analysis (PTA) on fabric

The amount of MWCNTs released by mechanical abrasion/wash test was determined by difference of MWCNTs mass loading between worn/washed and a control sample using the PTA technique developed in Chapter 2. In brief, following the abrasion process and wash test, triplicate samples (0.66 cm^2) for PTA were taken from all abraded samples along with control samples. Each piece was dissolved in a mixture of 5 mL hexafluoroisopropanol (HFIP, CovaChem, Loves Park, USA) and 10 mL chloroform in a beaker for 5 min. The solid component in the solution was collected by glass syringe filtration on quartz fiber filter (QFF, 1 x 1.5 cm, WhatmanTMQM-A, Fisher Scientific, Hampton, USA). The filter was loaded into the PTA instrument (Sunset Laboratories, Tigard, USA) and the temperature program established previously (Chapter 2) was applied. For the wash water samples collected after the washing process, the MWCNTs were collected on a QFF with direct syringe filtration.

5.2.5 Flame retardant efficacy test

The flame retardant efficacy of the coatings after the use tests was evaluated by the same flame retardancy test described in previous Chapters (3 and 4). In brief, samples were hung by a metal stand and observed while an ignited wooden match was placed right under. The flame was removed once the sample ignited and burning behavior was observed, and the remaining length of samples was measured afterward as well as the time to extinguish the flame for the strips which ignited.

5.3 Results and discussion

5.3.1 MWCNT mass release

First, the amount of MWCNTs released from the fabric during the mechanical abrasion was determined by PTA. The PTA results of abraded area and non-abraded area were compared in Figure 5.5. The triplicate samples of both abraded and non-abraded area showed 15 % relative standard deviation, indicating the spray coating was uniform. The mechanical abrasion resulted in 50 % of MWCNTs coating lost after 500 rotations. The pictures shown in Figure 5.6 support the results as the area the abrasion wheel contacted appeared lighter color after the abrasion process.

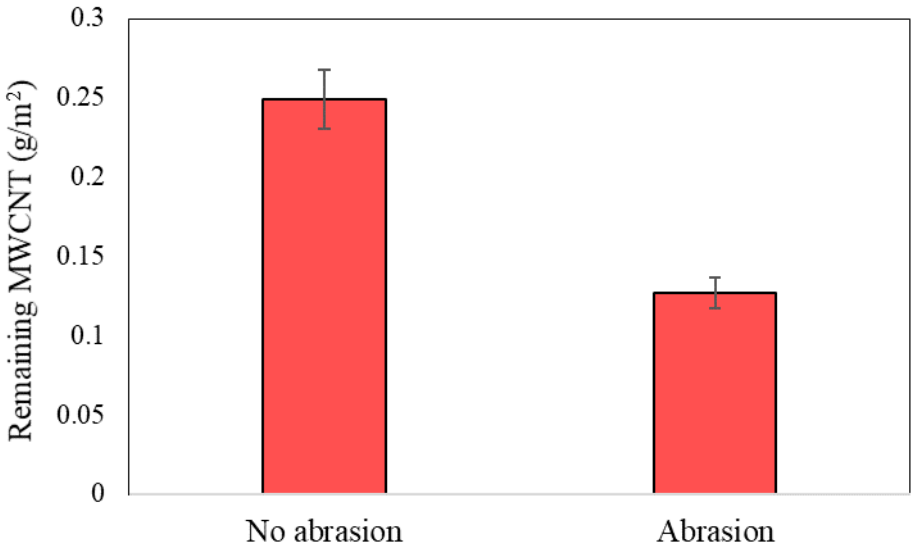

Figure 5.5 Comparison of MWCNT mass detected on fabric between areas with and without mechanical abrasion.

Figure 5.6 Pictures of MWCNT-APP coated polyester fabrics before (left) and after (right) the mechanical abrasion.

Subsequently, MWCNT mass release after washing was determined using PTA (Table 5.1 and Figure 5.7). As with mechanical abrasion samples, the uniformity of the coating was confirmed by the low relative standard deviation (9 %~31 %). The higher relative standard deviation coming from samples after 5 and 10 wash cycles could be due to inhomogeneous release from the process, which is independent of the uniformity of the coating. The first washing process removed approximately 40 % of MWCNTs compared to the sample without washing. MWCNTs was removed continuously as the washing process proceeded, leaving only 15 % of MWCNTs on the sample after 10 wash cycles. The amount of MWCNTs mass detected in the wash water is shown in Figure 5.8. It was found that 60-70 % of MWCNTs lost from the fabric samples was detected in the wash water. Considering that the standard deviation of detected MWCNTs mass was 9%-31%, and the possibility the MWCNTs getting stuck on the vial the wash water was stored, this data justifies that the MWCNTs on the fabric was transferred to the wash water.

Both mechanical abrasion and wash test, resulted in a significant decrease (approximately 50 % by 500 mechanical abrasion rotations and 80 % by 5 washing cycles) of MWCNTs coating from the fabric. One can speculate that the main reason of the large % coating loss is because most of the coating materials was on the surface of the fabric, held with weak Van Der Waals forces, therefore the coating was easily removed when the samples were experiencing mechanical abrasion/washing process.

A conclusion of these use tests is that the coating method used will result in environmental release during the use phase with exposure of consumers or organisms to CNMs by CNTs release to air through physical contacts and water. Consequently, the proposed coating technique needs to be improved to increase durability and prevent release. Approaches like introducing another protective layer (e.g. Teflon based coating) over the MWCNTs coating may be addressed for practical application. Hereafter we will investigate if MWCNTs loss will impact flame retardant efficacy of the coating.

Table 5.1 Quantified MWCNT mass per 0.66 cm^2 piece on the samples after wash test and surface concentration calculated.

Sample	Quantified mass (0.66 cm^2)	g/m^2
MWCNT-APP No wash	19.7 μg	0.3
MWCNT-APP 1 wash	12.3 μg	0.19
MWCNT-APP 5 wash	4.3 μg	0.07
MWCNT-APP 10 wash	3.0 μg	0.05

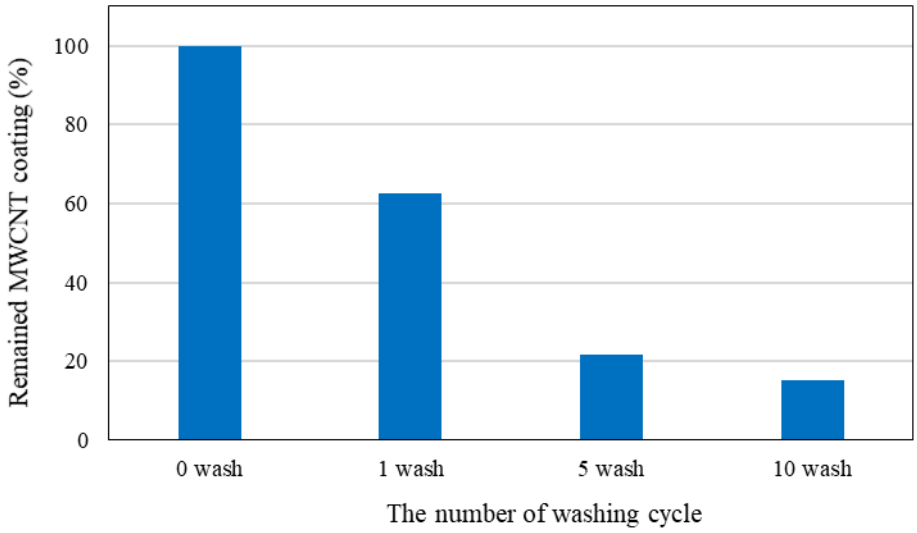

Figure 5.7. The fraction of MWCNT mass remained after multiple washing tests.

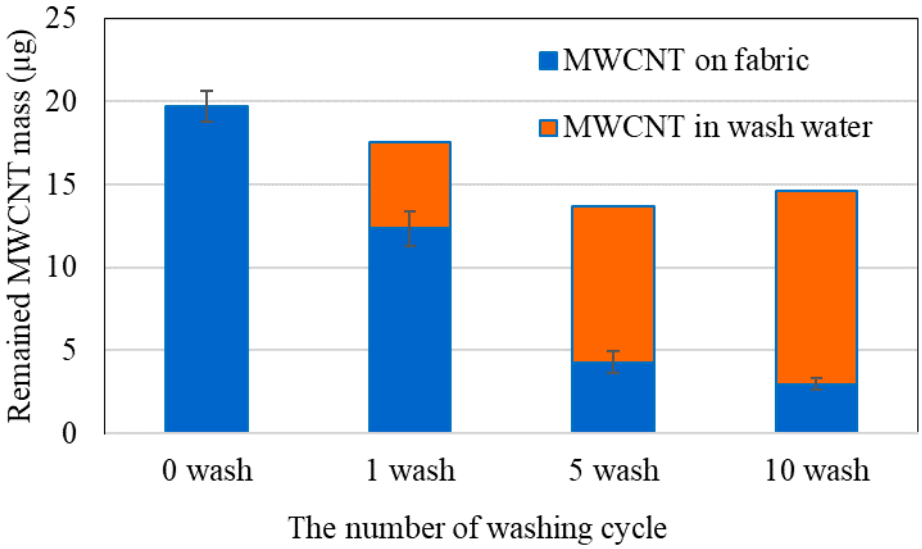

Figure 5.8. Detected MWCNT mass on the fabric (blue) and in the wash water (orange) following wash test.

5.3.2 Flame retardancy

In order to investigate the impact of the use test by abrasion on efficacy, flame retardancy tests were performed and the results are shown in Figure 5.9. The sample after the mechanical abrasion continuously burned once it was ignited. This was in sharp contrast to the sample cut from a non-abraded area, which did not ignite with slight melting on the edge, performance expected (cf Chapter 3). Considering that approximately 50 % of MWCNT was lost confirmed by PTA, this result is not surprising as the surface concentration of the material (0.12 g/m^2) was significantly lower than that of the sample (0.2 g/m^2) showed desired efficacy observed in Chapter 3.

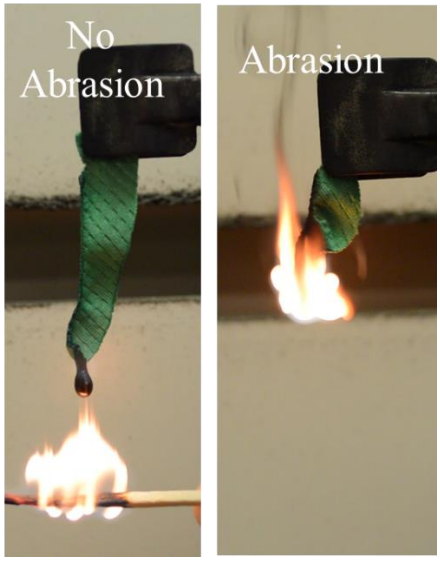

Figure 5.9 Flame retardant test results on MWCNT-APP coated polyester samples after mechanical abrasion, non-abraded area (left) and abraded area (right, approximately 50 % of MWCNT was released, confirmed with PTA).

Figure 5.10 shows the pictures of samples after wash tests during the efficacy test and polyester without coating as reference. The sample without any washing cycle (left in Figure 5.10) performed as expected (classification I) in the flame retardancy test, showing no ignition and drip. The edge of the sample turned black once the flame approached and stayed steady afterward. The remaining, after washing, 3 samples behaved like classification III which is “ignition with self-extinguishing”. At the beginning they acted similarly to the sample without washing as turning the edge black, however they ignited within a few seconds. This agreed with the PTA results showing that about 40 % of MWCNTs coating was removed after the first washing process. The polyester fabric itself was also considered as classification III as discussed in Chapter 3, therefore after 1 washing cycle, the flame retardant benefit had all but disappeared.

Although the samples after wash test were categorized in the same FR category as polyester without coating, there were still some differences among the fabric without coating and MWCNT-APP coated samples with wash test. For example, the period between the fire ignition and the extinguishment was shorter with less washing cycles. Also, given the fact that the remaining length of the fabric after the test shown in Table 5.2 was longer with less washing process and the sample after 10 washing cycles still held slightly more fabric, one can assume that the addition of coating contributed to the flame retardancy improvement.

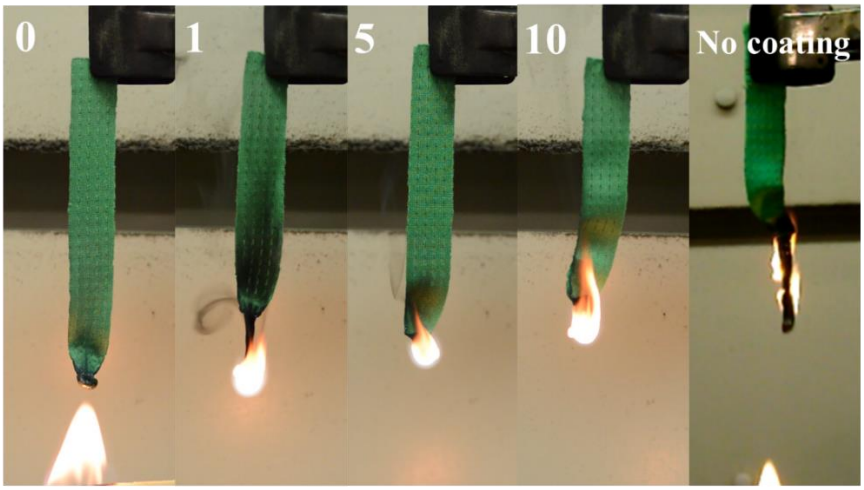

Figure 5.10 Flame retardant test results on MWCNT-APP coated polyester samples after wash test and polyester without coating as reference (0, 1, 5, 10 washing cycles and the reference from left to right).

Table 5.2 Results of flame retardancy test (FR) classification and remaining length of samples) after the washing test.

	Flame retardancy test		**PTA**
Sample	Remaining length (%)	Classification	Coated mass (g/m^2)
Polyester	47	III	0
APP	76	II	0.02
MWCNT-APP No wash	78	I	0.30
MWCNT-APP 1 wash	67	III	0.19
MWCNT-APP 5 wash	62	III	0.07
MWCNT-APP 10 wash	53	III	0.05

5.4 Conclusions

Polyester fabric samples coated with MWCNT and APP were prepared by spray a coating method as a potential alternative to existing flame retardant products. The MWCNT release, flame retardant efficacy and the relationship between during use phase were investigated by conducting mechanical abrasion and wash test. A significant amount of MWCNTs was lost by both tests (approximately 50 % after the mechanical abrasion test and 40 % after 1 wash). The efficacy was compromised after the release tests, showing a comparable efficacy to the fabric without coating (classification III). It was concluded that both simulating the material release by physical contact and leaching when exposed to water causes significant amount of the material loss, and it critically diminishes the efficacy. This coating technique tested leads to a high risk of exposure to air by physical contact and water/aquatic organisms by release of the wash water. Additional work focused on improving the durability can be beneficial to realistic flame retardant application using CNMs.

CHAPTER 6

THE USE OF PTA FOR VARIETY OF CARBONACEOUS MATERIALS AND MATRICES

6.1 Introduction

Carbonaceous nano and micro size materials are widely used, and the applications are emerging for novel nanosized allotropic carbon. The applications range from flame retardant materials such as those discussed here to polymer composites, membranes, electronics and food products. Therefore, quantitative analysis for all kinds of carbon such as 0D (fullerenes), 1D (single SWCNT and multi walled nanotubes MWCNT), 2D (graphene) and 3D (e.g. carbon black) is warranted (Figure 6.1), for quality control applications in manufacturing as well as environmental monitoring or toxicity studies.

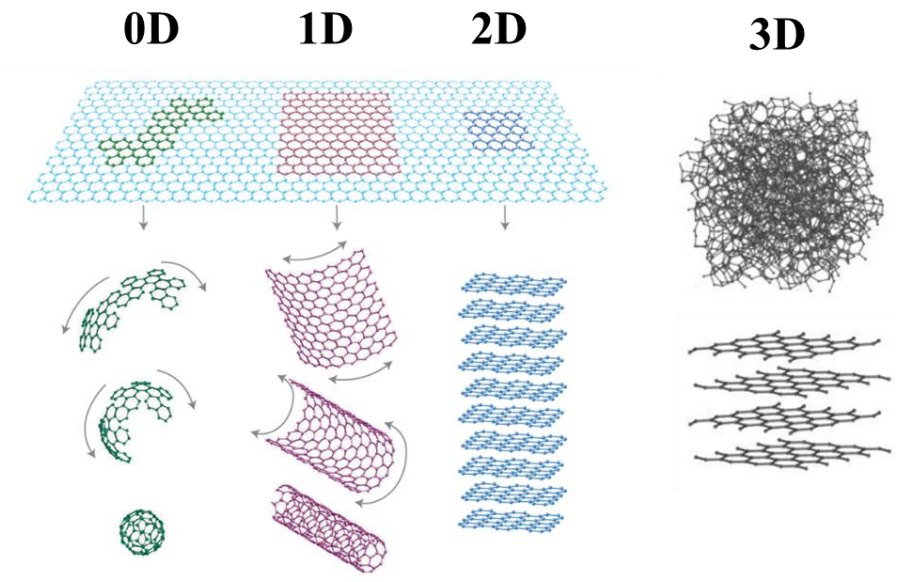

Figure 6.1 Structure of carbonaceous materials. Fullerene (0D), carbon nanotube (1D), graphene (2D)[38] and amorphous carbon/graphite (3D)[124].

Quantitative analysis of carbon materials is challenging as the materials, with the exception of fullerenes, are not amenable to mass spectrometry because of their large and variable size. In addition, frequently applications embed these species in organic matrices or require their detection in biological materials and hence the carbon from the material needs to be quantified in a background of carbonaceous material. Programmed Thermal Analysis (PTA) has emerged as a technique able to analyze carbonaceous nanomaterials. It was originally developed for airborne carbonaceous particles and to differentiate between soot and other (organic) carbon[77]. A commercial instrument is available from Sunset Laboratory, Inc[125]. Some researchers proposed this technique for carbonaceous nanomaterials[68] and then researchers at ASU explored the applicability over a wide range of nanotubes in biological materials[67]. Samples are analyzed by combusting the carbon portion at high temperature and transforming the evolved gases to carbon dioxide in an oxidizing oven. The carbon dioxide is converted to methane by a methanator that is set beside the oxidizing oven, and the carbon mass is determined with a flame ionization detector (FID) whose signal was calibrated with a methane standard.

During my PhD research, I supported research at ASU on carbonaceous nanomaterials by adapting the analytical parameters to extend the range of nanomaterials amenable to PTA analysis to a larger variety of carbonaceous materials including 1D (functionalized CNTs, commercial products), 2D and 3D (carbon black, activated carbon). I also adapted the sample preparation methodologies as well as modified temperature protocols to accommodate novel, more challenging matrices. This resulted in 2 co-authorship manuscripts as well as acknowledgements in manuscripts and several projects are still ongoing[43, 126, 127]. In this Chapter, I will summarize the overall

applicability of PTA to the characterization of carbonaceous materials in general and emphasize on my contributions in this area.

6.2 Experimental and Analytical Methods

Table 6.1 shows the list of all carbonaceous materials tested in this study as well as their manufacturer. In brief, samples for PTA were prepared by placing the materials onto a 1 x1.5 cm quartz fiber filter (WhatmanTMQM-A, Fisher Scientific, Hampton, USA) with mass loading targeted in the 10-200 µg range. The filter was set in the PTA sample chamber with specific temperature program selected. The temperature program can be modified accommodating to types of material. Initially, the basic temperature program was set to test the thermal stability and applicability. Two temperature programs (basic and extended) were mainly used for this research. The thermogram and the actual program file of both basic and extended are shown in Figure 6.2 and Appendix C respectively.

Table 6.1 Carbonaceous materials tested in this study with the applicability to PTA.

	Materials	Manufacturer	Pretreatment	Applicability
0D	C_{60}	MER Corp	N/A	No
1D	SWCNT	Sigma Aldrich	N/A	Yes
	SWCNT	Carbon Solutions, Inc	N/A	Yes
	MWCNT	Alfa Aesar	N/A	Yes
	MWCNT	Sigma Aldrich	N/A	Yes
	MWCNT	NanoLab	N/A	Yes
	NC7000™	Nanocyl	N/A	Yes
	NH_2-MWCNT	NanoLab	N/A	Yes
	NH_2-MWCNT	Cheap Tubes	N/A	Yes
2D	FLG (few layer graphene)	Angstron Materials	N/A	Yes
	GO	TW-Nano Materials	$NaBH_4$	Yes
3D	CB (Vulcan V9A32)	Cabot Corporation	N/A	Yes
	CB (Monarch 800)	Cabot Corporation	N/A	Yes
	CB (Emperor 2000)	Cabot Corporation	N/A	Yes
	Bamboo charcoal	Charcoal House LLC	N/A	Yes
	Carbon material	Hualong fertilizer technology	N/A	Yes
	SPAC	Standard Purification	N/A	Yes

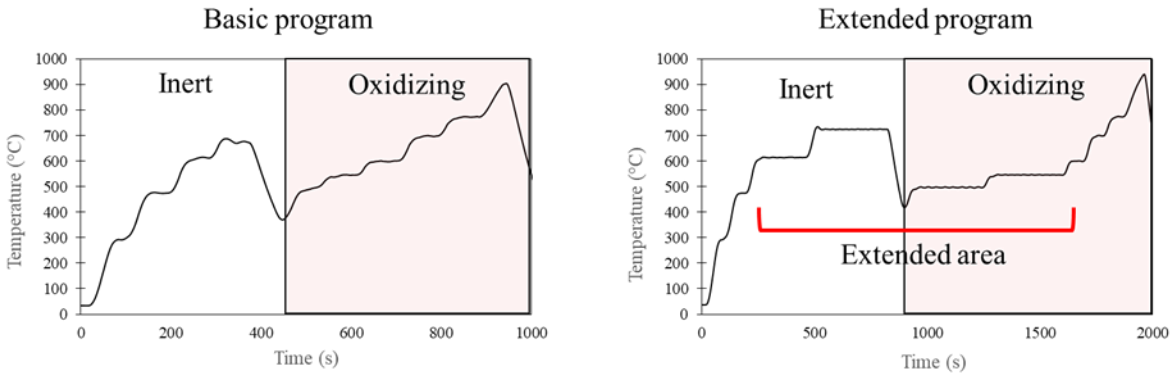

Figure 6.2 Basic temperature program (left) and extended program (right) used for polymer/fabric samples.

6.3 Results and discussion

6.3.1 0D materials

0D materials such as fullerenes and fullerols have been attempted in PTA (Figure 6.3, courtesy Dr. Troy Benn[128]) but their relatively low thermal stability makes them combust under inert condition (no oxygen) like most carbonaceous material. Therefore, it is not feasible to differentiate C_{60} from any matrices containing organic carbon and PTA technique is not appropriate for C_{60} quantification. It is noteworthy though that 0D materials, as they are molecular in nature, are amenable to mass spectrometry and other molecular characterization techniques[129-131]

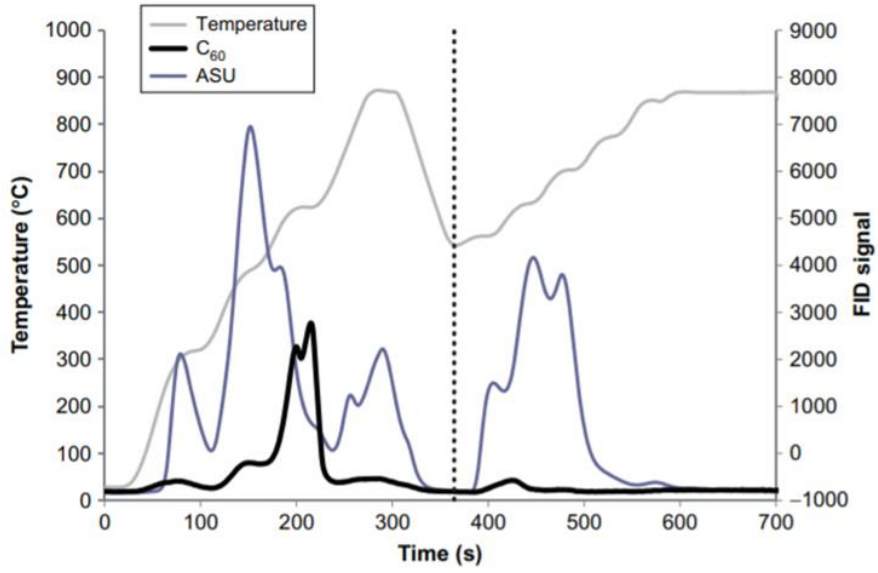

Figure 6.3 Thermogram example showing an example of an ambient aerosol sample (ASU) as well as of a C_{60} standard. The C_{60} standard evolves in the first portion of the thermogram, corresponding to the atmospheric organic carbon fraction.[128]

6.3.2 1D materials: Carbon nanotubes (CNTs)

6.3.2.1 Neat materials

Original work by Doudrick et al demonstrated that PTA is applicable to a wide variety of single and multiwalled carbon nanomaterials as long as the species are highly refractory (i.e. have high thermal stability)[67]. In this study I extended the range of CNTs to all the species shown in Table 6.1. The thermal stability of CNTs differs with variety of factors. For example, it is known that CNTs with more defect sites including oxygen rich CNTs tend to have lower thermal stability as they are chemically more reactive[132, 133]. Also, the presence of metals such as nickel in substantial quantities reduces CNT's thermal stability by catalyzing the oxidation[63]. However, the oxidizing temperature of all CNTs tested was high enough to differentiate from other form of carbon. Therefore, all CNTs I tested including industrial MWCNT (NC7000™), and even functionalized ones and ones with high metal impurities were amenable to analysis by PTA as neat compounds.

6.3.2.2 Applications to the analysis of 1D materials

Previously, pretreatment for rat lung tissue containing CNTs was developed for toxicity studies[70] as potentially the biological tissue can interfere the signal from the CNTs. Solvable, alkaline chemical product was adopted as reagent to extract CNTs from rat lung sample.

In my thesis, I focused on polymer composites as target samples as this is an emerging application involving 1D materials. CNTs are embedded in polymer products as thermal packaging, or to enhance the product durability due to their high mechanical properties and thermal conductivity. Those polymer products contain large amount of

organic carbon which is problematic for PTA as signals stem from the organic carbon may interfere the signal from CNTs and the accuracy of quantified value is compromised. Chapter 2 in this dissertation was focused on the method development of PTA for specifically polymer samples[103]. The critical point is to separate CNTs from organic carbon. Therefore, organic solvents were used to dissolve the polymer part completely, then the solid components which is mostly CNTs were collected by syringe filtration. This technique was applied to MWCNTs coated on polyester fabric (Chapter 3). The quantification analysis was critical for this dissertation as it was essential for release study and investigating the relationship between the mass loading and efficacy in Chapter 5.

As another application example containing CNTs, membrane products (Figure 6.4) made of MWCNT (three types, just MWCNT, MWCNT with 10% polyurethane binder and MWCNT with polyvinyl alcohol (PVA) and the 10% binder) were tested. These particular products were made for removal of different kinds of metals with certain voltage applied from waste stream[134]. The object of this project is to evaluate the durability of the membrane by monitoring the amount of CNTs released to the effluent water. Essentially, this type of application does not involve large amount of organic carbon like polymer composites, hence no additional pretreatment was needed. PTA was conducted on both the membrane itself and the effluent water after passing the membrane and collected by syringe filter, and there was no issue observed. The results confirmed high durability of the membranes as only negligible amount of MWCNTs (0.3 - 0.4 μg) was detected in the effluent water.

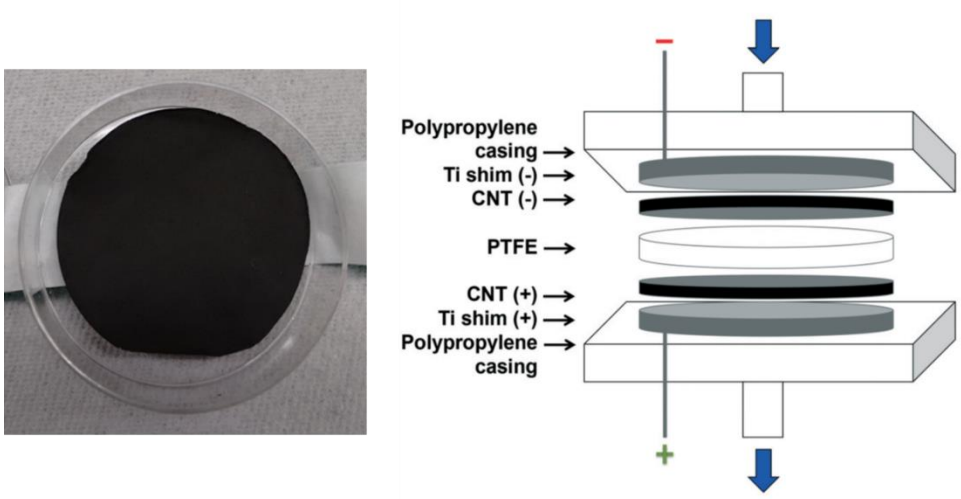

Figure 6.4 Images of CNT membrane and diagram of electrochemical filtration system[134].

6.3.3 2D materials: Graphene, Graphene oxide (GO)

6.3.3.1. Neat materials

Graphene can be quantified by PTA using the same temperature program as that of CNTs without functionalization as the thermal stability of graphene is comparable to CNTs. In contrast, the thermal stability of GO is much lower than that of CNTs and graphene due to its high oxygen content, and the peaks observed from GO may overlap with any potential organic carbon signal. A reduction reaction using sodium borohydride ($NaBH_4$) was developed as pretreatment to improve the thermal stability. As shown in Figure 6.6, the signal from the reduced GO (RGO) was shifted to the right (higher temperature area, compared to pristine GO, indicating the improvement of its thermal stability.

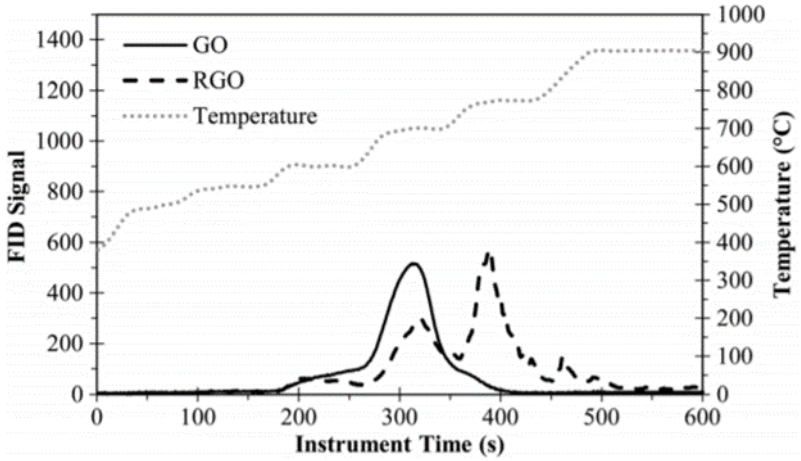

Figure 6.5 PTA thermograms (oxidizing phase) for RGO reduced with 2% $NaBH_4$ in water.[126]

6.3.3.2 Applications to the analysis of 2D materials

Similar to CNTs, there are a variety of proposed applications using 2D materials, especially in the electronics markets. Some studies were done on detection of those materials in wastewater biomass to determining exposure concentrations and assessing the fate and transport routes[43, 126]. The same technique developed for biological tissue samples with CNTs was applied to those samples. Solvable decomposed most biomass and the graphene/GO were successfully separated from the organic portion. For GO samples, $NaBH_4$ was added for reduction during the biomass decomposition process with Solvable. Figure 6.6 shows that there was no interference from biomass for GO quantification with Solvable&$NaBH_4$ treatment. Dr. Kyle Doudrick and I worked on this project on neat GO (section 6.3.3.1) and GO in biomass (section 6.3.3.2) quantification and publish the work[126]. Additionally, I worked on another study utilizing the technique to quantify few-layer graphene (FLG) in wastewater biomass as collaboration research with Dr. Yu Yang[43].

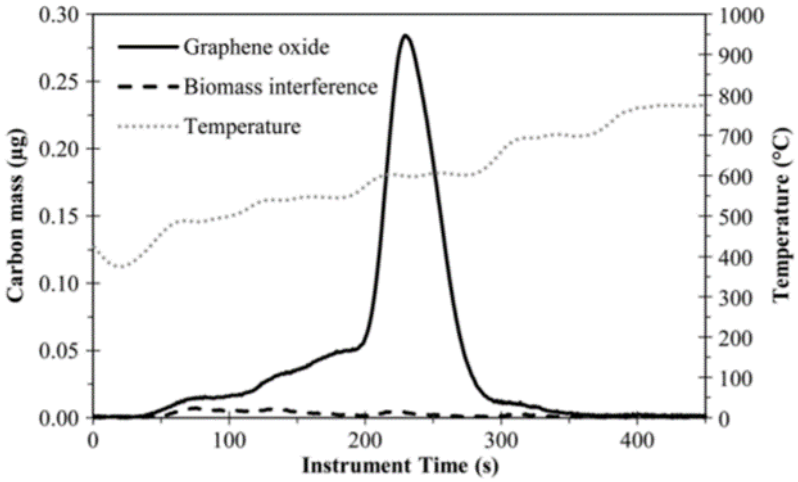

Figure 6.6 PTA thermogram showing biomass interference for GO in wastewater biosolids. Solvable and 2% $NaBH_4$ treatment[126].

6.3.4 3D materials: Activated Carbon, Carbon black, bamboo charcoal

6.3.4.1 Neat materials

Different kind of 3D carbonaceous materials exist, partly nano-sized and sometimes larger. The 3D materials I worked on analyzing using PTA include carbon black, superfine powdered activated carbon (SPAC), charcoal, and carbon particles added to fertilizer. As pure, neat materials, all the 3D materials tested (Table 6.1) were amenable to PTA quantification just like 1D and 2D materials.

Within a set of materials there can be differences in thermal stability which might require optimization of the temperature program. As an example, 3 different carbon black materials were tested (Figure 6.7), two were very thermally table while 1 burned at much lower temperature. XPS results on the carbon black samples showed the oxygen concentration for each type was 0.3 %, 0.6 % and 5 % for Vulcan V9A32, Monarch 800 and Emperor 2000 respectively, suggesting that the higher oxygen content material has lower thermal stability, consistent with all other materials tested in my research. In case

of even weaker thermal stability, a process like reduction treatment developed for GO quantification could be developed to solve the issue.

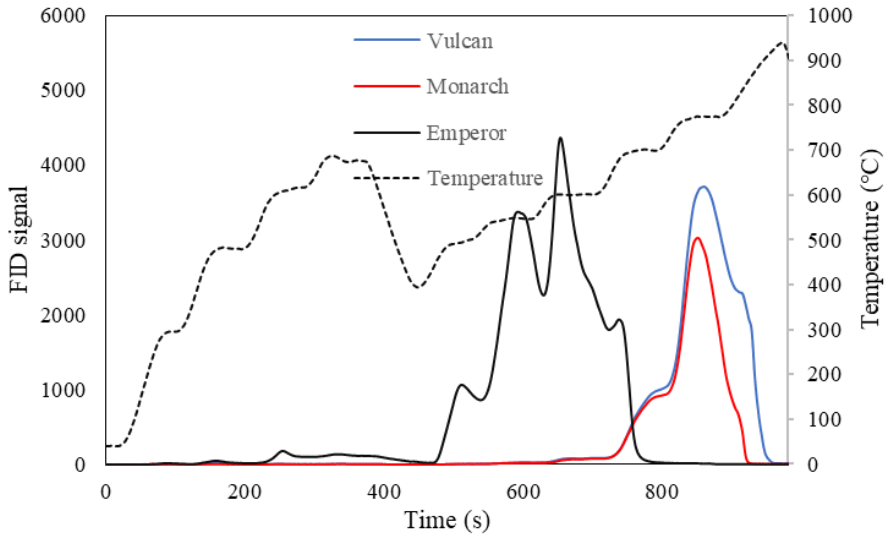

Figure 6.7 Thermograms of Vulcan V9A32, Monarch 800 and Emperor 2000.

6.3.4.2 Applications to the analysis of 2D materials

There are variety of applications contain 3D materials such as food products and rubber products. As discussed in Chapter 2, accurate quantification can be achieved when the organic carbon component in the matrix is separated from the carbon materials.

In this work I collaborated with researchers who added SPAC to electrospun polystyrene fibers [127] for use in water treatment. After verifying that SPAC was amenable to PTA, I developed a sample preparation protocol, similar to the HFIP/chloroform treatment (Chapter 2). In this case only chloroform was chosen as polystyrene fibers were readily dissolved without adding any other solvent. The development of the method allowed these researchers to confirm the SPAC content in the fibers for the product development.

On the other hand, some matrices are challenging to extract the carbon materials from. Carbon particles purchased from Huanlong fertilizer technology, for example, were used for an agricultural study. The object for this sample was to trace and quantify the carbon particles originally added to the soil as the plants grow. For samples containing soil and/or plant, the dissolving technique with organic solvent developed was not applicable. For this type of matrix, another approach like microwave digestion needs to be applied. One concern with the method is the possibility to lose the carbon material itself during the digestion process.

Food coloring is another challenging case. E153, a food additive used for black color, is used in baked goods and gummy candy. I worked on this sample to evaluate the applicability of PTA to food products. It was difficult to extract from thick polymer ingredient such as glycerol and gelatin. Centrifuging combined with dilution technique was attempted, however E153 was not successfully separated.

6.4 Summary and conclusion

The increasing use of carbonaceous nanomaterials lead to an increasing need for a general analytical method that can quantify these materials in a wide range of matrices for quality control, exposure and toxicity studies. Programmed thermal analysis (PTA) can be applied to quantify variety of carbon materials. During my PhD work I demonstrated the use of PTA on a variety of materials and developed for my and other research projects analytical protocols to quantify carbonaceous nanomaterials n research and commercial products. PTA proved to be applicable to a wider range of 1D, 2D and 3D carbonaceous materials but failed on 0D materials (fullerenes) of lower thermal stability. Pretreatments such as reduction processes may be required for samples with

high oxygen contents such as graphene oxide. Due to the variability in thermal stability, the temperature program during analysis needed to be adapted to the target material, the matrix involved and to minimize instrument run time. Sometimes the thermal combustion phases needed to be extended such as in the case of polymer composite samples, where an extended time was required to eliminate the risk of overlap between the evolution of carbon from residual organic carbon and the actual carbonaceous nanomaterial.

In most cases a specialized pretreatment needed to be developed to separate the nanomaterial from, at least the interfering, carbonaceous background. Organic solvents like HFIP and chloroform are appropriate for wide range of polymer-based samples. Solvable, on the other hand, is effective to remove biological samples like biomass. Finally, all applications tested in this study was summarized in Table 6.2.

Table 6.2 Summary of carbonaceous material applications tested with analysis information.

Dimension	Material	Matrix	Pretreatment	Applicability	Program
1D	MWCNT	Rat lung tissue	Solvable	Yes	Basic
	MWCNT filter	Water containing metals	N/A	Yes	Basic
	MWCNT	Polycaprolactone	HFIP&chloroform	Yes	Extended
	MWCNT	Polyester	HFIP&chloroform	Yes	Extended
	NH_2-MWCNT	Polyester	HFIP&chloroform	Yes	Extended
2D	FLG (few layer graphene)	Biomass	Solvable	Yes	Basic
	GO	Biomass	Solvable&$NaBH_4$	Yes	Basic
3D	SPAC	PS fiber	Chloroform	Yes	Basic
	CB (Emperor 2000)	CB-SiO_2	N/A	Yes	Basic
	THERMOCYL™X1	Polyester	N/A	No	–
	Carbon material	Plant, Soil	N/A	No	–
	E153 food coloring	Food (gummy etc.)	N/A	No	–

CHAPTER 7

SUMMARY AND OUTLOOK

7.1 Summary

This dissertation focused on the use of carbonaceous nanomaterials (CNMs) in flame retardant coatings on fabric. This research investigated the potential of CNMs to act as flame retardants (FRs) by testing different CNM materials and coating methods, quantifying the CNM mass loadings on the fabric, testing the FR efficacy of the CNMs coatings and finally their durability in mechanical abrasion and washing processes.

A major challenge to CNMs product studies is the quantification of carbonaceous nanomaterials in a carbonaceous sample matrix including polymer composites or textiles. Therefore, we first addressed the question "**Are CNMs in polymers amenable to quantification using Programmed Thermal Analysis (PTA)?"** In Chapter 2, a two-step CNMs quantification method was developed to minimize the carbonaceous background signal and allow for accurate quantification by PTA. The first dissolution step using a mixture of organic solvents (hexafluoroisopropanol (HFIP) and chloroform) managed to remove the CNTs from polymer components for the following PTA process. This method can detect and quantify as little as an absolute amount of 0.2 µg of CNTs with a high reproducibility (< 20 % standard deviation). The method was shown to be applicable to a variety of polymers such as polyester and polystyrene.

Once an analytical technique was available, different kinds of CNMs were coated on polyester fabric and the efficacy of the coatings as flame retardant was evaluated in Chapter 3. The overarching question was "**Do CNM coatings show flame retardancy comparable to existing FR coatings?"** The work showed that we were able to coat

successfully MWCNT, functionalized MWCNTs (NH_2-MWCNT (C) and NH_2-MWCNT (N) purchased from two manufacturers and O-MWCNT) and graphene oxide (GO) in the target mass loading range using layer by layer techniques. CNMs with minimal amount of oxygen (< 1 %) such as MWCNT and NH_2-MWCNT (C) showed the highest flame retardancy. In contrast, the efficacy of oxygen rich CNMs like O-MWCNT and GO appeared to be worse than the polyester without any coating. It was concluded that oxygen content in CNMs is a critical factor for the flame retardancy, indicating high oxygen content impacts the flame retardancy negatively. Comparable efficacy to classical flame retardant materials was observed with MWCNT and NH_2-MWCNT(C) at an approximately 3-33 times lower mass loading.

A major challenge to creating CNT coatings is to achieve stable coating dispersions to allow uniform coating. Chemical/physical modifications of MWCNTs were tested to improve their dispersibility in Chapter 4. A first question was **"Can amine functionalization of CNT add hydrophilicity to CNTs and achieve stable coating dispersions?"** It was concluded that amine functionalization to append hydrophilicity was challenging due to the difficulty to functionalize with amine group heavily. Considering that commonly used functionalization process often involves oxygen attachment, chemical modification may not be the appropriate approach to improve the dispersibility. On the other hand, a different approach aimed for dispersion of short duration presented promising outcome. As an alternative we asked the questions **"Can dispersions of short duration be used in conjunction with spray coating as a viable alternative to layer by layer techniques to generate homogeneous coatings?"**. Using dimethylformamide (DMF) instead of water, short term dispersions of MWCNTs were

easily obtained by bath sonication. Similarly, ammonium polyphosphate (APP) acted as surfactant and assisted MWCNT disperse in water. Both solutions held stable dispersion for desired period of time (~5 min) for spray coating. Coatings formed with the dispersions of short duration by spray coating method showed comparable efficacy to the traditional frame retardants.

In Chapter 5, we addressed the potential of the use phase of the FR coatings to lead to a CNM release and consequent exposure as well as impacting the FR properties. The research question can hence be summarized into **"Are spray coated CNM FR coatings durable, maintain their efficacy and do not release CNMs in the environment?".** In order to evaluate the durability of spray coated MWCNTs (generated in Chapter 4), samples were subjected to mechanical abrasion and washing processes. Approximately 50 % of MWCNT by 1 set of mechanical abrasion, 40 % of MWCNT by 1 washing cycle was lost. The efficacy was diminished after the abrasion test/washing test to the same level as pure polyester without coating (FR classification III). It was found that the mass loading range required to show great FR efficacy (classification I) is 0.19 ~ 0.3 g/m^2.

In Chapter 6, I summarized all the work on PTA analysis on different carbonaceous materials conducted for various projects outside of the CNM flame retardant study. The main research question here is **"Can PTA be applied to other carbonaceous materials in various matrices?"**. PTA was proven to work on not only CNTs, but also wide range of carbonaceous materials such as 2D materials like GO and 3D materials like carbon black and activated carbon. A reduction process using sodium borohydride as pretreatment for PTA was developed for materials with lower thermal

stability like GO. Dissolution processes were introduced to separate the target carbonaceous nanomaterials from a carbon containing matrix. Solvable, for example, was used for samples with biological compounds and HFIP/chloroform mixture was chosen for polyester and several other polymer samples. Modified temperature programs were developed and optimized for each individual application.

As a conclusion, it was found that CNTs are viable alternative material as flame retardant. Among various types of CNTs, non-functionalized MWCNT with a mass loading of 0.18 g/m^2 is the most promising kind according to the findings in Chapter 3 and 4. Further study is necessary for practical application mostly due to the poor durability observed in Chapter 5. Realistic application with CNT requiring less mass loading compared to the traditional flame retardants would be achieved if the durability of the coating and the optimization of the mass loading are met.

7.2 Outlook

Additional work can be beneficial to develop realistic flame retardant applications using CNMs. As observed in Chapter 5, 40-50 % of coating was released within one set of mechanical abrasion or one single wash test. Durability is a crucial property for consumer products and here the poor durability performance of the coatings would clearly need to be improved. One option is to use finishing methods to improve the durability of FRs by creating cross-linking bonds. Tetrakis(hydroxymethyl)phosphonium chloride (THPC), which is one of phosphorus based FRs, for example, is applied with urea to a piece of fabric, resulting polymetric matrix due to cross-linking chemical reaction. The final product can be retained within the fabric structure mechanically. However, CNMs, especially CNTs without functionalization are extremely chemically

stable. Therefore, improvement of durability by using chemical reactions can be challenging.

As a comparable approach, silicone based spray can be applied on top of CNMs coatings as a protective layer. This results in an enhancement of adhesion to the fabric due to polymerization in a similar manner to THPC. One of the potential issues is a compromised air permeability, which potentially limits the type of application. Similarly, CNMs can be incorporated in non-flammable polymers like silicone and applied on the fabric as the polymer cures. It leads to mass accretion of final product along with poor air permeability issue. Another alternative approach would be applying Teflon based coating. Polytetrafluoroethylene (PTFE) based coating adds the hydrophobicity to the sample as well as resistance to physical friction, which prevents CNMs from detaching by both mechanical abrasion and washing process. This approach allows the fabric to retain the air permeability.

As a different approach from surface coating methods to improve the durability, incorporating CNMs into fabric can be investigated. Technique like electrospinning touched in Chapter 6 for polystyrene containing fabric superfine powdered activated carbon will improve the durability. It is possible the mass loading required for the desired efficacy may be higher as the CNMs will be distributed to the entire fabric instead of CNMs being concentrated on the surface. Therefore, the relationship between the mass loading and efficacy is an important point to be studied.

An extended use phase study may be beneficial to obtain better understandings of the coating. Chapter 5 focused on indoor use phase situations. Additional study regarding chemical alternation of the FR coating such as highly oxidizing conditions like UV

irradiation and exposing to different humidity/temperature will provide further insights on the realism of an application of CNMs as flame retardants.

Finally, carbonaceous material analysis using PTA has more room to develop. First, expanding the CNM extraction technique would help the applicability of PTA to wider range of products. Polypropylene, for example, that is commonly used for variety of polymer product such as plastic packaging and nonwoven fabric does not get dissolved by HFIP/chloroform mixture suggested in Chapter 2. Moreover, there are some challenges for extracting materials from food products and plants (Chapter 6). Customized sample preparation processes depending on the target matrix would enhance the usability of PTA. For example, samples mainly consist of polymers can be prepared for PTA by introducing different solvents to dissolve a target polymer. For samples like food products that solvents are not effective to, microwave digestion can be applied to remove the carbon component in the matrix.

Second, it is beneficial to investigate the impact different metal may add to the combustion temperature during PTA. Certain types of metal like nickel can catalyze oxidation of CNMs as discussed in Chapter 2, which causes a shift of peak position due to the lower combustion temperature and potentially harms the accuracy of quantified data. Most CNMs used in this dissertation were purified (i.e. very little metal catalyst left), however, a lot of commercial CNM products available still contain metal catalysts such as iron, molybdenum and cobalt. It is critical to understand how each metal affects the combustion temperature of CNMs and the minimum concentration of each metal to start influence. This study would prevent inaccurate measurements caused by the metal impurities.

REFERENCES

1. *Technical Bulletin 117_2013*
Requirements, Test Procedure and Apparatus for Testing the Smolder Resistance of Materials Used in Upholstered Furniture, S.o. California and D.o.C. Affairs, Editors. 2013.

2. *Furniture and Furnishings (Fire Safety) Regulations*. 1988.

3. Alexander B. Morgan, *ABM FR Chem 093009*, NIST, Editor. 2009.

4. Alexander B. Morgan Charles A. Wilkie, *Fire Retardancy of Polymeric Materials, Second Edition*. 2009.

5. F. Rahman, K. H. Langford, M. D Scrimshaw, and J. N. Lester, Sci. Total Environ., 2001. **275**: p. 1-17.

6. P. Darnerud, Environment International, 2003. **29**(6): p. 841-853.

7. E. Roze, L. Meijer, A. Bakker, K. N. Van Braeckel, P. J. Sauer, et al., Environ Health Perspect, 2009. **117**(12): p. 1953-8.

8. United States Environemental Protection Agency, *Furniture Flame Retardancy Partnership Environmental Profiles of Chemical Flame-Retardant Alternatives for Low-Density Polyurethane Foam Volume 1*. 2005.

9. United States Environmental Protection Agency, *Furniture Flame Retardancy Partnership Environmental Profiles of Chemical Flame-Retardant Alternatives for Low-Density Polyurethane Foam Volume 2*. 2005.

10. A. Blum and B. Ames, Science, 1977. **195**(4273): p. 17-23.

11. A. T. McDonald, Chemosphere, 2002. **46**: p. 745-755.

12. R. J. Fowles, A Fairbrother, L Baecher-Steppan, and I. N Kerkvliet, Toxicology, 1993. **86**: p. 49-61.

13. S. Hallgren and O. P. Darnerud, Toxicology, 2002. **177**: p. 227-243.

14. P. Eriksson, H. Viberg, E. Jakobsson, U. Orn, and A. Fredriksson, Toxicol. Sci, 2002. **67**: p. 98-103.

15. S. N. Kuriyama, C. E. Talsness, K. Grote, and I. Chahoud, Environmental Health Perspectives, 2004. **113**(2): p. 149-154.

16. L. M. Pasquini, S. M. Hashmi, T. J. Sommer, M. Elimelech, and J. B. Zimmerman, Environ Sci Technol, 2012. **46**(11): p. 6297-305.

17. L. S. Birnbaum and D. F. Staskal, Environmental Health Perspectives, 2004. **112**(1): p. 9-17.

18. *Or. Rev. Stat. § 453.085(16)*. 2015.

19. *Md. Code. Ann., Health-Gen. § 24-306* S.o. Maryland, Editor. 2014.

20. *Fire-Retardant/Fire-Resistive Coatings*, in *Coatings Materials and Surface Coatings*, A.A. Tracton, Editor. 2006, CRC Press.

21. *Polymer Green Flame Retardant*, ed. C.D. Papaspyrides and P. Kiliaris. 2014.

22. Alenka Bunderšek, Boštjan Japelj, Branka Mušič, Nevenka Rajnar, Sašo Gyergyek, et al., Polymer Composites, 2016. **37**(6): p. 1659-1666.

23. B. Schartel, Materials (Basel), 2010. **3**(10): p. 4710-4745.

24. S. Boryniec and W. Przygocki, Progress in Rubber, Plastics and Recycling Technology, 2001. **17**(2): p. 127-148.

25. A. W. Schwartz, Philos Trans R Soc Lond B Biol Sci, 2006. **361**(1474): p. 1743-9; discussion 1749.

26. H. Carlsson, U. Nilsson, G. Becker, and C. Ostman, Environ. Sci. Technol., 1997. **31**: p. 2931-2936.

27. A. A. Younis, Egyptian Journal of Petroleum, 2016. **25**(2): p. 161-169.

28. G. Laufer, F. Carosio, R. Martinez, G. Camino, and J. C. Grunlan, J Colloid Interface Sci, 2011. **356**(1): p. 69-77.

29. F. Carosio, G. Laufer, J. Alongi, G. Camino, and J. C. Grunlan, Polymer Degradation and Stability, 2011. **96**(5): p. 745-750.

30. H. W. Kroto, J. R. Heath, S. C. O'Brian, R. F. Curl, and R. E. Smalley, Nature, 1985. **318**: p. 162-163.

31. S. Iijima, Nature, 1991. **354**: p. 56-58.

32. K. S. Novoselov, A. K. Geim, S. V. Morozov, D. Jiang, Y. Zhang, et al., Science, 2004. **306**: p. 666-669.

33. S. Berber, YK. Kwon, and D. Tománek, Phys. Rev. Lett., 2000. **84**(20): p. 4613-4616.

34. A. V. Savin, B. Hu, and Y. S. Kivshar, Physical Review B, 2009. **80**(19).

35. A. Mahajan, A. Kingon, Á. Kukovecz, Z. Konya, and P. M. Vilarinho, Materials Letters, 2013. **90**: p. 165-168.

36. A Galano, J. Phys. Chem. C, 2008. **112**: p. 8922–8927.

37. I. Fenoglio, M. Tomatis, D. Lison, J. Muller, A. Fonseca, et al., Free Radic Biol Med, 2006. **40**(7): p. 1227-33.

38. A. K. Geim and K. S. Novoselov, Nature, 2007. **6**: p. 183-191.

39. Uniterd States Environmental Protection Agency, *Nanomaterial Case Study A Comparison of Multiwalled Carbon Nanotube and Decabromodiphenyl Ether Flame-Retardant Coatings Applied to Upholstery Textiles*. 2013.

40. N. C. Mueller and B. Nowack, Environ. Sci. Technol., 2008. **42**: p. 4447-4453.

41. K. Doudrick, T. Nosaka, P. Herckes, and P. Westerhoff, Environ. Sci.: Nano, 2015. **2**(1): p. 60-67.

42. K. Doudrick, N. Corson, G. Oberdo¨ rster, A. Eder C, P. Herckes, et al., ACS Nano, 2013. **7**(10): p. 8849-8856.

43. Y. Yang, Z. Yu, T. Nosaka, K. Doudrick, K. Hristovski, et al., Frontiers of Environmental Science & Engineering, 2015. **9**(5): p. 823-831.

44. J. D. Saxby, S. P. Chatfield, A. J. Palmisano, A. M. Vassallo, M. A. Wilson, et al., J. Phys. Chem., 1992. **96**(1): p. 17-18.

45. V. Datsyuk, M. Kalyva, K. Papagelis, J. Parthenios, D. Tasis, et al., Carbon, 2008. **46**(6): p. 833-840.

46. H. M. Stapleton, S. Klosterhaus, S Eagle, J Fuh, D. J Meeker, et al., Environ. Sci. Technol. , 2009. **43**: p. 7490–7495.

47. R. Baughman H, A. Zakhidov A, and W. de Heer A, Science, 2002. **297**(5582): p. 787-792.

48. M. De Volder F. L., S. Tawfick H, R. Baughman H, and A. Hart J, Science, 2013. **339**: p. 535-539.

49. A. Montazeri, J. Javadpour, A. Khavandi, A. Tcharkhtchi, and A. Mohajeri, Materials & Design, 2010. **31**(9): p. 4202-4208.

50. *Carbon Nanotube Composited Fabric*. [cited 2017; Available from: http://www.bulletproof-it.com/_p/prd12/1904991565/product/carbon-nanotube-composited-fabric.

51. E. J. Petersen, D. X. Flores-Cervantes, T. D. Bucheli, L. C. Elliott, J. A. Fagan, et al., Environ Sci Technol, 2016. **50**(9): p. 4587-605.

52. P-C. Ma, N. A. Siddiqui, G. Marom, and J-K. Kim, Composites Part A: Applied Science and Manufacturing, 2010. **41**(10): p. 1345-1367.

53. D. Qian, E. C. Dickey, R. Andrews, and T. Rantell, Applied Physics Letters, 2000. **76**(20): p. 2868.

54. M. J. Biercuk, M. C. Llaguno, M. Radosavljevic, J. K. Hyun, A. T. Johnson, et al., Applied Physics Letters, 2002. **80**(15): p. 2767.

55. P. Cherukuri, M. S. Bachilo, H. S. Litovsky, and B. R. Weisman, J. Am. Chem. Soc., 2004. **126**: p. 15638-15639.

56. N. T. Mattison, D. M. O'Carroll, R. Kerry Rowe, and E. J. Petersen, Environ Sci Technol, 2011. **45**(22): p. 9765-75.

57. F. Hennrich, R. Krupke, S. Lebedkin, K. Arnold, R. Fischer, et al., J. Phys. Chem. B, 2005. **109**: p. 10567-10573.

58. S. Attal, R. Thiruvengadathan, and O. Revev, Anal. Chem., 2006. **78**(23): p. 8098-8104.

59. A. E. Porter, M. Gass, K. Muller, J. N. Skepper, P. A. Midgley, et al., Nat Nanotechnol, 2007. **2**(11): p. 713-7.

60. E. Mansfield, A. Kar, and S. A. Hooker, Anal Bioanal Chem, 2010. **396**(3): p. 1071-7.

61. F. Irin, B. Shrestha, J. E. Cañas, M. A. Saed, and M. J. Green, Carbon, 2012. **50**(12): p. 4441-4449.

62. Y. He, S. R. Al-Abed, and D. D. Dionysiou, Sci Total Environ, 2017. **580**: p. 509-517.

63. D. L. Plata, C. M. Reddy, and P. M. Gschwend, Environ Sci Technol, 2012. **46**(22): p. 12254-61.

64. R. B. Reed, D. G. Goodwin, K. L. Marsh, S. S. Capracotta, C. P. Higgins, et al., Environ. Sci.: Processes Impacts, 2013. **15**(1): p. 204-213.

65. C. Cerrillo, G. Barandika, A. Igartua, O. Areitioaurtena, A. Marcaide, et al., Environ Toxicol Chem, 2015. **34**(8): p. 1854-62.

66. A. Schierz, A. N. Parks, K. M. Washburn, G. T. Chandler, and P. L. Ferguson, Environ Sci Technol, 2012. **46**(22): p. 12262-71.

67. K. Doudrick, P. Herckes, and P. Westerhoff, Environ Sci Technol, 2012. **46**(22): p. 12246-53.

68. H. Hyung, D. J Fortner, B. J. Hughes, and J. H Kim, Environ. Sci. Technol., 2007. **41**: p. 179-184.

69. *Methodology: Sample Analysis Method for Organic and Elemental Carbon Aerosols.* [cited 2017 July]; Available from: http://www.sunlab.com/about-us/methodology/.

70. K. Doudrick, N. Corson, G. Oberdo¨ rster, A. Eder C, P. Herckes, et al., ACS Nano, 2013. **7**(10).

71. *Carbon Nanotubes (CNT) Market Analysis By Product (Single Walled Carbon Nanotubes (SWCNT), Multi Walled Carbon Nanotubes (MWCNT)), By Application (Polymers, Energy, Electrical & Electronics) And Segment Forecasts To 2022.* [cited 2017 July]; Available from: http://www.grandviewresearch.com/industry-analysis/carbon-nanotubes-cnt-market.

72. R. S. Lankone, J. Wang, J. F. Ranville, and D. H. Fairbrother, Environmental Science: Nano, 2017. **4**(4): p. 967-982.

73. A. Yamamori, J. Kasukami, and T Mutou, Central Customs Laboratory Report, (47): p. 99-102.

74. T. Myojo, T. Oyabu, K. Nishi, C. Kadoya, I. Tanaka, et al., Journal of Nanoparticle Research, 2008. **11**(1): p. 91-99.

75. National Institute for Occupational Safety and Health, *Elemental Carbon (Diesel Particulate): Method 5040*, in *NIOSH Manual of Analytical Methods*. 2003.

76. J. Wang, R. S. Lankone, R. B. Reed, D. H. Fairbrother, and J. F. Ranville, NanoImpact, 2016. **1**: p. 65-72.

77. M. E. Birch and R. A. Cary, Aerosol Science and Technology, 1996. **25**(3): p. 221-241.

78. C. I. Czimczik, C. M. Preston, M. W. I. Schmidt, R. A. Werner, and E.-D. Schulze, Organic Geochemistry, 2002. **33**.

79. H. Y. Kweon, M. K. Yoo, I. K Park, T. H. Kim, H. C. Lee, et al., Biomaterials, 2003. **24**: p. 801-808.

80. A. Taghizadeh and B. D. Favis, Carbohydr Polym, 2013. **98**(1): p. 189-98.

81. Monica Mattioli-Belmonte, Giovanni Vozzi, Yudan Whulanza, Maurizia Seggiani, Valentina Fantauzzi, et al., Materials Science and Engineering: C, 2012. **32**(2): p. 152-159.

82. L. Pan, X. Pei, R. He, Q. Wan, and J. Wang, Colloids Surf B Biointerfaces, 2012. **93**: p. 226-34.

83. K. Saeed and S-Y. Park, Journal of Applied Polymer Science, 2007. **104**(3): p. 1957-1963.

84. A. Moisala, A. G. Nasibulin, and E. I. Kauppinen, J. Phys. Condens. Matter, 2003. **15**: p. 3011-3035.

85. C-W. Lam, J. T. James, R. McCluskey, S. Arepalli, and R. L. Hunter, Critical Reviews in Toxicology, 2008. **36**(3): p. 189-217.

86. H. M. Stapleton, S. Klosterhaus, A. Keller, P. L. Ferguson, S. van Bergen, et al., Environ Sci Technol, 2011. **45**(12): p. 5323-31.

87. H. M. Stapleton, S. Sharma, G. Getzinger, P. L. Ferguson, M. Gabriel, et al., Environ Sci Technol, 2012. **46**(24): p. 13432-9.

88. M. Alaee, Environment International, 2003. **29**(6): p. 683-689.

89. G. Camino, L. Costa, and M. P. Luda di Cortemiglia, Polymer Degradation and Stability, 1991. **33**: p. 131-154.

90. O. Segev, A. Kushmaro, and A. Brenner, Int J Environ Res Public Health, 2009. **6**(2): p. 478-91.

91. R. E. Dodson, L. J. Perovich, A. Covaci, N. Van den Eede, A. C. Ionas, et al., Environ Sci Technol, 2012. **46**(24): p. 13056-66.

92. H. M. Stapleton, S. Klosterhaus, S. Eagle, J. Fuh, J. D. Meeker, et al., Environ Sci Technol, 2009. **43**(19): p. 7490-7495.

93. K. Hoffman, S. Garantziotis, L. S. Birnbaum, and H. M. Stapleton, Environ Health Perspect, 2015. **123**(2): p. 160-5.

94. T. Kashiwagi, F. Du, J. F. Douglas, K. I. Winey, R. H. Harris, Jr., et al., Nat Mater, 2005. **4**(12): p. 928-33.

95. S. Peeterbroeck, F. Laoutid, J. M. Taulemesse, F. Monteverde, J. M. Lopez-Cuesta, et al., Advanced Functional Materials, 2007. **17**(15): p. 2787-2791.

96. T. Zhang, H. Yan, M. Peng, L. Wang, H. Ding, et al., Nanoscale, 2013. **5**(7): p. 3013-21.

97. A. G. Gonçalves, B. Jarrais, C. Pereira, J. Morgado, C. Freire, et al., Journal of Materials Science, 2012. **47**(13): p. 5263-5275.

98. *THERMOCYL™ X1*. Available from: http://www.nanocyl.com/product/thermocyl-x1/.

99. T. Kashiwagi, F. Du, K. I. Winey, K. M. Groth, J. R. Shields, et al., Polymer, 2005. **46**(2): p. 471-481.

100. K. Grzybowski, *Potential application of Carbon Nanotubes (CNTs) as a flame retardant additive - technical and market analysis*. 2009.

101. G. Huang, J. Yang, J. Gao, and X. Wang, Industrial & Engineering Chemistry Research, 2012: p. 120913163620003.

102. K. A. Wepasnick, B. A. Smith, K. E. Schrote, H. K. Wilson, S. R. Diegelmann, et al., Carbon, 2011. **49**(1): p. 24-36.

103. T. Nosaka, R. S. Lankone, Y. Bi, D. H. Fairbrother, P. Westerhoff, et al., Analytical Methods, 2018. **10**(9): p. 1032-1037.

104. National Fire Protection Association, *NFPA 705*, in *Recommended Practice for a Field Flame Test for Textiles and Films*. 2018.

105. A. Richard Horrocks, D. Price, and Knovel (Firm), *Fire retardant materials*. 2001.

106. B. Dittrich, K.-A. Wartig, D. Hofmann, R. Mülhaupt, and B. Schartel, Polymer Degradation and Stability, 2013. **98**(8): p. 1495-1505.

107. J. Hilding, E. A. Grulke, Z. G. Zhang, and F. Lockwood, J. Dispersion Sci. Technol., 2003. **24**(1): p. 1-41.

108. L. Vaisman, H. D. Wagner, and G. Marom, Adv Colloid Interface Sci, 2006. **128-130**: p. 37-46.

109. M. J. O'Connell, B. Poul, L. M. Ericson, C. Huffman, Y. Wang, et al., Chem. Phys. Lett., 2001. **342**: p. 265-271.

110. R. Rastogi, R. Kaushal, S. K. Tripathi, A. L. Sharma, I. Kaur, et al., J Colloid Interface Sci, 2008. **328**(2): p. 421-8.

111. P. S. Goh, A. F. Ismail, M. Aziz, Mohamad Rusop, and Tetsuo Soga, 2009: p. 224-228.

112. S. Kim, Y-I. Lee, D-H. Kim, K-J. Lee, B-S. Kim, et al., Carbon, 2013. **51**: p. 346-354.

113. Y-P. Sun, K. Fu, Y. Lin, and W. Huang, Acc. Chem. Res., 2002. **35**: p. 1096-1104.

114. E. Heister, C. Lamprecht, V. Neves, C. Tıˆlmaciu, L. Datas, et al., ACS Nano, 2010. **4**(5): p. 2615–2626.

115. W. Chidawanyika and T. Nyokong, Carbon, 2010. **48**(10): p. 2831-2838.

116. S. K. Pillai, J. Ramontja, and S. Sinha Ray, *Nanostructured Materials and Nanotechnology V: Ceramic Engineering and Science Proceedings, 1*. Amine Functionalization of Carbon Nanotubes for the Preparation of CNT Based Polylactide Composites ‐ A Comparative Study, ed. S. Mathur, et al. 2011.

117. H. Y. Ki, J. H. Kim, S. C. Kwon, and S. H. Jeong, Journal of Materials Science, 2007. **42**(19): p. 8020-8024.

118. B. Filipowska, E. Rybicki, A. Walawska, and E. Matyjas-Zgondek, Fibres Text. East. Eur., 2011. **87**: p. 124-128.

119. D. Hanigan, L. Truong, J. Schoepf, T. Nosaka, A. Mulchandani, et al., Water Res, 2018. **139**: p. 281-290.

120. R. B. Reed, T. Zaikova, A. Barber, M. Simonich, R. Lankone, et al., Environ Sci Technol, 2016. **50**(7): p. 4018-26.

121. C. Lorenz, L. Windler, N. von Goetz, R. P. Lehmann, M. Schuppler, et al., Chemosphere, 2012. **89**(7): p. 817-24.

122. N. C. Mueller and B. Nowack, Environ. Sci. Technol., 2008. **42**: p. 4447–4453.

123. ASTM, *Standard Guide for Abrasion Resistance of Textile Fabrics (Uniform Abrasion)*. 2016.

124. *Eight Allotropes of Carbon*. [cited 2018 April]; Available from: https://commons.wikimedia.org/wiki/File:Eight_Allotropes_of_Carbon.png.

125. *Lab OC-EC Aerosol Analyzer*. [cited 2018 April]; Available from: http://www.sunlab.com/lab-oc-ec-aerosol-analyzer/.

126. K. Doudrick, T. Nosaka, P. Herckes, and P. Westerhoff, Environmental Science: Nano, 2015. **2**(1): p. 60-67.

127. O. G. Apul, N. Hoogesteijn von Reitzenstein, J. Schoepf, D. Ladner, K. D. Hristovski, et al., Sci Total Environ, 2017. **592**: p. 458-464.

128. T. Benn, P. Herckes, and P. Westerhoff, 2012. **59**: p. 291-303.

129. Z. Chen, P. Westerhoff, and P. Herckes, Environmental Toxicology and Chemistry, 2008. **27**(9): p. 1852-1859.

130. B. F. Pycke, T. M. Benn, P. Herckes, P. Westerhoff, and R. U. Halden, Trends Analyt Chem, 2011. **30**(1): p. 44-57.

131. T. C. Chao, G. Song, N. Hansmeier, P. Westerhoff, P. Herckes, et al., Anal Chem, 2011. **83**(5): p. 1777-83.

132. D Bom, R. Andrews, D. Jacques, J Anthony, B. Chen, et al., Nano Lett., 2002. **2**(6): p. 615-619.

133. H. F. Bettinger, J. Phys. Chem. B, 2005. **109**(15): p. 6922-6924.

134. M. P. O'Connor, R. M. Coulthard, and D. L. Plata, Environmental Science: Water Research & Technology, 2018. **4**(1): p. 58-66.

APPENDIX A

CHAPTER 3 CARBONACEOUS NANOMATERIALS INFORMATION

Table A.1 CNMs information provided from the manufacturer

Material	Manufacturer	Purity	Outer diameter	Length
NH_2-MWCNT (C)	Cheap Tubes	> 99 %	< 20 nm	1-12 µm
NH_2-MWCNT (N)	NanoLab	> 95 %	15 ± 5 nm	5-20 µm
MWCNT	NanoLab	> 95%	15 ± 5 nm	5-20 µm
O-MWCNT	NanoLab*	> 95%	15 ± 5 nm	5-20 µm
Thermocyl	Nanocyl	N/A	N/A	N/A
Material	Manufacturer	Purity	Size	Area
GO	TW-Nano Materials	> 90 %	0.5–20 µm in x–y	>1200 $m^2 g^{-1}$

APPENDIX B

CHAPTER 3 XPS SPECTRA OF CARBON NANOTUBES

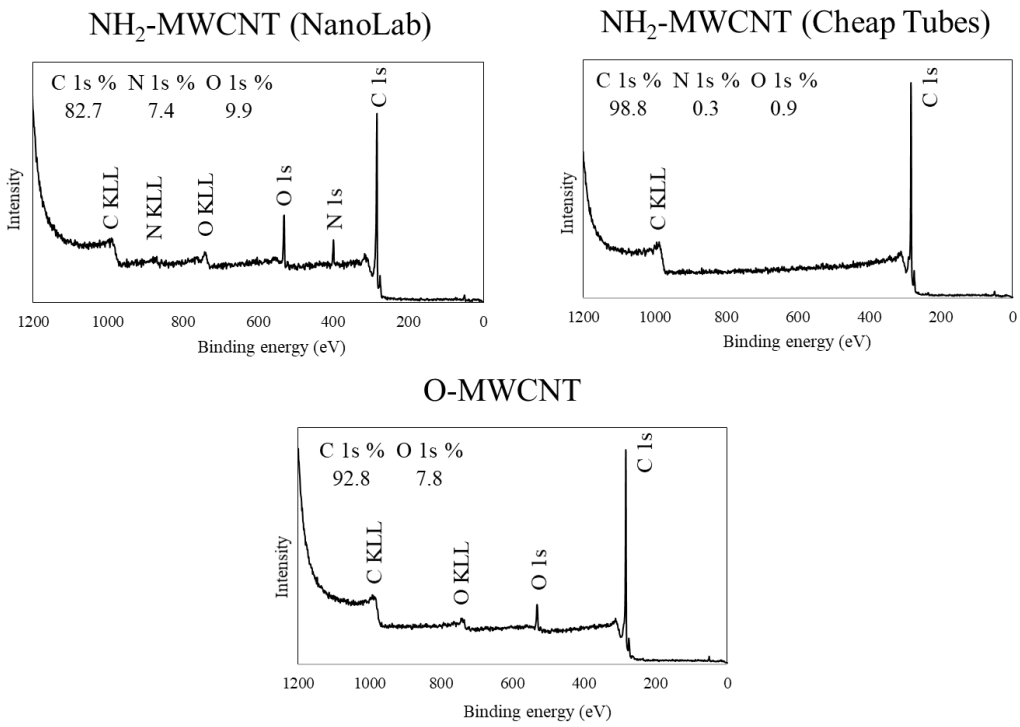

Appendix B. XPS spectra of functionalized MWCNTs (O-MWCNT and NH2-MWCNTs purchased from NanoLab and Cheap Tubes) used for flame retardant coating.

APPENDIX C

CHAPTER 6 PTA TEMPERATURE PROGRAM FILE INFORMATION

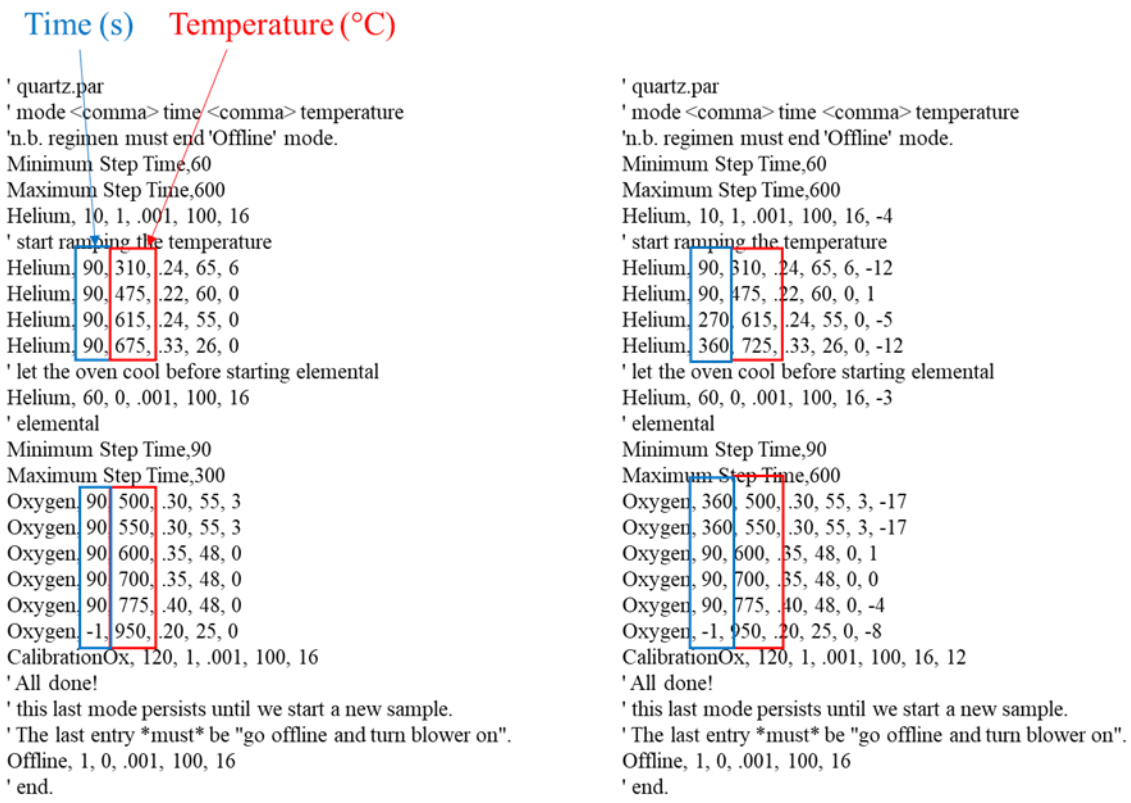

Appendix C. Temperature program files, numbers enclosed in blue shows time and red shows temperature, basic program (left) and extended program (right).